Analysis of the miRNA-mediated regulation of AP-1 in non-tumorigenic and tumorigenic HPV18-positive cell lines

INAUGURAL-DISSERTATION
zur
Erlangung der Doktorwürde
der
Naturwissenschaftlich-Mathematischen Gesamtfakultät
der
Ruprecht-Karls-Universität
Heidelberg

vorgelegt von
Apotheker
Matthias Sobel
geb. in Mainz

November 2009

Analysis of the miRNA-mediated regulation of AP-1 in non-tumorigenic and tumorigenic HPV18-positive cell lines

Die vorliegende Arbeit entstand im Zeitraum von Oktober 2006 to Oktober 2009 am Deutschen Krebsforschungszentrum (DKFZ) Heidelberg unter Anleitung von Prof. Dr. Frank Rösl.

Gutachter:

Prof. Dr. Elisabeth Schwarz

Deutsches Krebsforschungszentrum Heidelberg

Prof. Dr. Frank Rösl

Deutsches Krebsforschungszentrum Heidelberg

Tag der mündlichen Prüfung:

Eidesstattliche Versicherung

Ich erkläre hiermit, dass ich die vorgelegte Dissertation selbst verfasst und mich dabei keiner anderen als der von mir ausdrücklich bezeichneten Quellen und Hilfen bedient habe. Diese Dissertation wurde in dieser oder in anderer Form weder bereits als Prüfungsarbeit verwendet, noch einer anderen Fakultät als Dissertation vorgelegt. An keiner anderen Stelle ist ein Prüfungsverfahren beantragt.

Heidelberg, den 18.11.2009

Matthias Sobel

für meine Eltern

Table of contents

Summary

The transcription factor AP-1 is built up by dimerization of Jun and Fos family members and regulates major biological events like proliferation, invasion and apoptosis. The dimerization pattern of AP-1 changes when HPV-positive cells undergo malignant progression. While in HPV-positive non-malignant cells (“444”) AP-1 is composed of c-Jun/Fra-1, their malignant counterparts (“CGL3”) mainly express c-Jun/c-Fos heterodimers. Since microRNAs (miRNA), a potent group of post-transcriptional regulators, are often deregulated during malignant transformation, the regulation of AP-1 by miRNAs during cancer progression was analyzed.

For this purpose, Drosha and Dicer, the key processing proteins in miRNA biogenesis, were knocked down by siRNAs. Quantitative RT-PCRs and Western blots showed that Fra-1 was regulated by miRNAs in non-tumorigenic and tumorigenic hybrids, but not in parental tumorigenic HeLa cells. c-Jun is repressed by miRNAs only in 444 and HeLa cells, but not in CGL3 cells, which express only low amounts of c-Jun. Conversely, c-Fos is indirectly upregulated by miRNAs in HeLa cells. As analyzed by electro-mobility-shift / super shift-assays, the observed changes in protein expressions also resulted into modulations of AP-1 dimer composition that were also confirmed by AP-1 responsive Luciferase assays (TRE-Luc). Furthermore, reporter constructs harboring the 3’UTRs of c-Jun and Fra-1 showed direct regulation by miRNAs throughout the full-length 3’UTRs suggesting multiple miRNA binding sites and / or multiple regulatory miRNAs. Using an “Illumina” miRNA expression array, differentially expressed miRNAs in the non-tumorigenic and tumorigenic cell hybrids were detected and matched with miRNAs that were predicted to regulate c-Jun according to a bioinformatics analysis with PicTar, TargetScan, miRBase and DIANA microT. The data pointed towards miR-495 as one regulatory miRNA targeting c-Jun. Preliminary luciferase assays with overexpressed miR-495 did not reveal an interaction with a reporter construct harboring c-Jun 3’UTR. Other potential candidates were not tested.

These results show for the first time that c-Jun and Fra-1 are direct targets of miRNAs and that c-Fos is submitted to an indirect miRNA regulation, thereby expanding known miRNA-c-Fos regulatory circuits. Moreover, it is demonstrated that miRNAs can modulate AP-1 composition and transcriptional activity in cervical carcinoma cells with potential consequences on AP-1 target genes.

Zusammenfassung

Der Transkriptionsfaktorkomplex AP-1 entsteht durch Dimerisierung von Jun und Fos Proteinen und reguliert wichtige biologische Prozesse wie Proliferation, Invasion und Apoptose. Die AP-1 Zusammensetzung ändert sich während der malignen Transformation HPV-positiver Zellen. Während die AP-1 Dimere in HPV-positiven, nicht malignen Zellhybriden („444“) vor allem aus c-Jun/Fra-1 bestehen, exprimieren maligne Zellhybride („CGL3“) c-Jun/c-Fos Heterodimere. Da microRNAs (miRNA) eine bedeutende Rolle bei der post-transkriptionellen Regulation spielen und durch maligne Transformation oft dereguliert sind, wurde die Regulation von AP-1 durch miRNAs vor dem Hintergrund der Krebsentwicklung untersucht.

Für diesen Zweck wurden Drosha und Dicer, Schlüsselenzyme in der miRNA Biogenese, durch siRNAs supprimiert. Die anschließende Analyse mittels quantitativer RT-PCR und Western blots zeigte, dass Fra-1 in den nicht-tumorigenen und tumorigenen Zellhybriden reguliert ist, nicht aber in den parentalen, tumorigenen HeLa Zellen. c-Jun wird in 444 und HeLa Zellen durch miRNAs kontrolliert, während in CGL3 Zellen, die nur geringe Mengen c-Jun exprimieren, eine solche Regulation nicht gefunden wurde. Im Gegensatz dazu wurde gezeigt, dass c-Fos nur in HeLa Zellen indirekt durch miRNAs reguliert ist. Die Suppression der miRNAs führte zu stöchiometrischen Veränderungen von AP-1, was mittels „electro-mobility-shift/super shift-assays“ (EMSA) gezeigt werden konnte. Darüber hinaus wurde auch die transkriptionelle Aktivität von AP-1 moduliert, wie am Beispiel von AP-1 sensitiven Luciferase Experimenten (TRE-Luc) verdeutlicht wurde. Weiterhin zeigten Luciferase Experimente mit Reporterkonstrukten der 3’UTRs, dass c-Jun und Fra-1 direkt durch mehrere miRNA Bindestellen und / oder mehrere miRNAs inhibiert werden. Um die verantwortlichen miRNAs zu identifizieren, wurde ein miRNA Expressionsprofil der nicht-tumorigenen und tumorigenen Zellhybride erstellt. Der Abgleich unterschiedlich exprimierter miRNAs mit miRNAs, für die eine regulatorische Funktion durch *in-silico* Analysen (PicTar, TargetScan, miRBase and DIANA microT) vermutet wird, deutete auf miR-495 als verantwortliche miRNA für c-Jun hin. Jedoch zeigten vorläufige Luciferase Experimenten mit überexprimierter miR-495 keine Interaktion mit den c-Jun Reporterkonstrukten. Andere potentielle miRNAs wurden nicht getestet.

Diese Ergebnisse zeigen zum ersten Mal, dass c-Jun und Fra-1 direkt durch miRNAs reguliert werden, und dass c-Fos einer indirekten miRNA Regulation unterliegt, was die bisherigen Kenntnisse über die miRNA-c-Fos Regulation erweitert. Des Weiteren zeigt diese Arbeit, dass miRNAs die Zusammensetzung und die transkriptionelle Aktivität von AP-1 in Gebärmutterhalskrebs Zelllinien mit möglichen Auswirkungen auf AP-1 Zielgene modulieren können.

1. Introduction

1.1. Cervical cancer and human papillomaviruses

Cervical cancer is one of the most common cancers in women worldwide, with an estimated global incidence of 470,000 new cases and approximately 233,000 deaths per year (Parkin *et al.*, 2001; Bosch and de Sanjose, 2003). Among all cancer types, cervical cancer is the primary cause of death of women in many developing countries, where widespread screening by cervical cytology is still unavailable (Cronje, 2004). In developed countries, the incidence is lower as a consequence of cervical screening and ongoing active health education programs (Pecorelli *et al.*, 2003). In future, the incidence will hopefully further decrease due to large-scale vaccination programs started in 2007.

The development of cervical cancer is a multi-stage process lasting, from several years up to decades (zur Hausen, 1996; Hahn and Weinberg, 2002). This multi-stage development towards an infiltrative tumor is marked by progression of pre-cancerous lesions, also termed “cervical intraepithelial neoplasias” (CIN), which are classified according to their grade of malignancy: mild dysplasia (CIN I), moderate dysplasia (CIN II) and severe dysplasia (CIN III), which still needs years to decades to develop into an invasive tumor (zur Hausen, 2002). Precancerous stages often regress, so that only 10% of all cases develop into CIN III and maybe to cervical cancer in the long run (Katase *et al.*, 1995).

Epidemiological and functional studies link cervical carcinomas with the infection of high-risk HPVs (*human papillomavirus*). In addition, further factors contribute to the multi-stage carcinogenesis process, leaving HPV infection not as the only cause, but definitely as a requisite (zur Hausen, 2002). Human papillomaviruses constitute a heterogeneous group of more than 100 genotypes that belong to the family of *Papovaviridae* (de Villiers *et al.*, 2004). HPVs infect basal cells of the skin (cutaneous HPV types) or of the mucosa (mucosal HPV types).

Since only a subgroup of the mucosal HPVs is associated with the development of more than 90% of the cases of cervical cancer, they are called high-risk HPVs (Dürst *et al.*, 1983; Boshart *et al.*, 1984). This group is, amongst others, composed of HPV-16 (Dürst *et al.*, 1983), HPV-18 (Boshart *et al.*, 1984), HPV-31 (Goldsborough *et al.*, 1989), HPV-33 (Cole and Streeck, 1986) and HPV-35 (Lorincz *et al.*, 1987).

1.1.1. Genomic organization and replication of HPV

Human papillomaviruses are small, non-enveloped, icosahedral viruses containing circular genomic DNA of about 8 kbp (Favre *et al.*, 1975; Pfister and zur Hausen, 1978). The viral genome organization is highly conserved and can be divided in three different regions according to the function (Danos *et al.*, 1982).

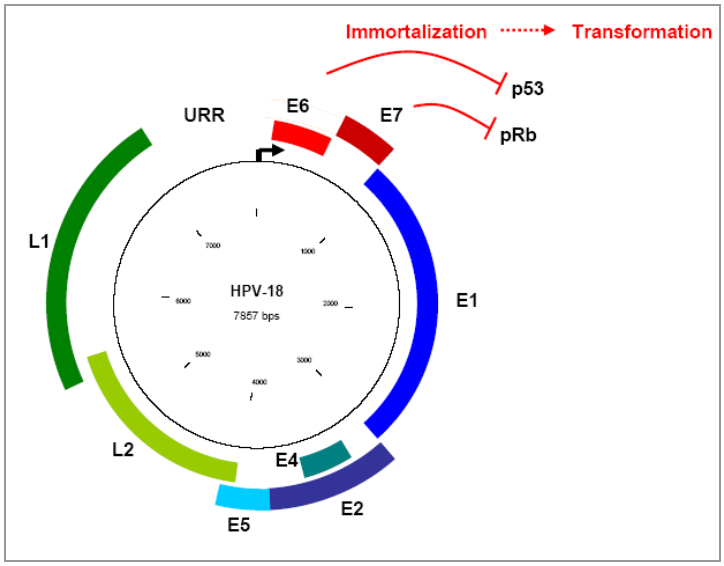

Figure 1-1: Genomic organization of human papillomaviruses, as exemplified by HPV-18

The circular genome contains open reading frames for the early genes E1-E7 and the late genes L1 and L2. The *cis*-regulatory elements like enhancer, promoter and the origin of replication are located in the URR. The interaction of the viral oncogenes E6 and E7 with the tumor suppressor proteins p53 and pRB is responsible for the immortalization of the host cell and represents an important step towards malignant transformation.

The URR (*upstream regulatory region*) contains the origin of DNA replication, the promoter elements driving gene expression and the epithelial-specific transcriptional enhancer. Only one of the viral transcription factors possesses a binding site herein. The viral protein E2 can either activate or repress transcription, depending on the DNA-status. All other regulators are of cellular origin, e.g. Oct-1, Sp-1, GR, KRF-1, YY-1 and AP-1, which is the key regulator of viral transcription (Butz and Hoppe-Seyler, 1993; Hoppe-Seyler and Butz, 1994).

The early region encodes non-structural proteins that are responsible for viral DNA replication (E1/E2) (Del Vecchio *et al.*, 1992), transcriptional self-regulation (E2) (Bouvard *et al.*, 1994), disruption of cellular cytokeratin network during productive infection (E4) (Doorbar *et al.*, 1991) and cellular transformation and immortalization (E5, E6 and E7) (Fehrmann and Laimins, 2003).

The late region codes for the structural proteins (major capsid protein L1 and minor capsid protein L2) that are required for capsid assembly (Zhou *et al.*, 1991).

The productive life-cycle of HPV depends on the degree of differentiation of the host cell. Through lesions of the outer layers, viruses infect undifferentiated, epithelial cells of the basal layer, where the early proteins are expressed (Iftner *et al.*, 1992). Vertical differentiation

of epithelial cells is paralleled by expression of late proteins, which finally results in assembly and release of new virus particles. Since virus production and cell lysis is restricted to more differentiated cells, viruses are able to persist in an episomal state in the nucleus of their host cells for years.

Additionally, viral DNA can integrate into the host genome. Prior to integration, virus DNA is linearized by disruption of the E2 ORF, which leaves L1 and L2 ORFs without promoter. Consequently, virus capsid production is abolished and the *trans*-repressory effect of E2 on the transcription of the viral oncogenes E6 and E7 is abrogated. This leads to an increase in E6 and E7 transcription (Cripe *et al.*, 1987) and subsequently enhances the proliferation rate (von Knebel Doeberitz *et al.*, 1991). Integration into the host genome is considered to be an early step towards carcinogenesis (zur Hausen, 2002).

1.1.2. Viral oncogenes E6 and E7

The viral oncogenes E6 and E7 are responsible for the transforming capability of high-risk HPV types, which is achieved through the interaction with cellular tumor suppressor genes (Munger and Howley, 2002).

Besides other proteins, E6 targets p53 that arrests the cell cycle in the event of DNA damages to allow DNA repair (Helton and Chen, 2007). High-risk HPV E6 binds to p53 and its ubiquitin protein ligase E6-AP, thus triggering degradation of the tumor suppressor protein by the proteasome (Werness *et al.*, 1990; Scheffner *et al.*, 1993). This results in an anti-apoptotic effect, an accumulation of mutations, chromosomal instability and aneuploidy (Duensing and Münger, 2003). Additionally, E6 activates telomerase activity, which contributes to the immortalization of the host cell (Klingelhutz *et al.*, 1996).

High-risk HPV E7 binds to pRb and p107 (Dyson *et al.*, 1989) that normally interact with the transcriptional regulator E2F and thus controls expression of growth regulatory genes (Goodrich and Lee, 1993). After E7 binding, pRb is degraded and E2F is released from the complex. Then, E2F activates its target genes, finally resulting in an increased proliferation rate (Bagchi *et al.*, 1990).

1.2. The transcription factor AP-1

The transcription factor AP-1 (*activator protein-1*) plays a mayor role in many crucial processes like proliferation, differentiation, apoptosis and neoplastic transformation (Angel and Karin, 1991; van Dam and Castellazzi, 2001; Eferl and Wagner, 2003). In addition, AP-1 positively or negatively controls the expression of oncogenes of most of the HPV-types, including high-risk types HPV-16 and HPV-18, making it an important factor for HPV-induced carcinogenesis (Rösl and Schwarz, 1997) (see **1.2.3**).

1.2.1. Composition of the transcription factor AP-1

AP-1 stands for a group of dimeric transcription factors that differ in their composition of Jun- (c-Jun, JunB and JunD), Fos- (c-Fos, FosB, Fra-1 and Fra-2) and ATF-family members (ATF-2, ATF-3 and B-ATF). Jun family members are able to form homodimers or heterodimers with members of the Fos- or ATF-family through a bZIP-motif (*basic region leucine zipper*) (Angel and Karin, 1991; Shaulian and Karin, 2002).

The expression of single AP-1 proteins is dependent on species, cell type, developmental state and cell cycle phase (Lallemand *et al.*, 1997). Additionally, the repressing or activating potential of AP-1 is determined by multiple factors: different *trans*-activating capabilities of single AP-1 members, post-translational modifications, interactions with other regulatory factors and extra cellular stimuli modulating the abundance of AP-1 subunits, e.g. through differential transcriptional rates or mRNA stabilities (Eferl and Wagner, 2003; Hess *et al.*, 2004). Thus, AP-1 is able to exert varying functions in the same genomic context. By different homo- or heterodimerization patterns, the composition of AP-1 can be very variable. In principle, dimerization of Jun- and Fos- family members leads to 18 different combinations (Karin *et al.*, 1997; Chinenov and Kerppola, 2001).

AP-1 dimers composed of Jun- and Fos-family members, preferentially bind to an asymmetric, heptanucleotide recognition motif, 5'-TGA(G/C)TCA-3', that is present in promoters of many cellular and viral genes. This AP-1 consensus sequence is termed TRE (*TPA (12-O-tetradecanoylphorbol-13-acetate) responsive element*) (Tseng and Verma, 1995). In a complex with ATF-family members, Jun:ATF heterodimers or ATF:ATF homodimers, AP-1 binds with higher affinity to the symmetric, octanucleotide CRE-motif (*cAMP-responsive element*) that varies slightly from TRE, 5'-TGACGTCA-3' (Angel and Karin, 1991; Shaulian and Karin, 2002; Eferl and Wagner, 2003).

	c-Jun	JunB	JunD	c-Fos	FosB	Fra-1	Fra-2
c-Jun	+	+	+	+	+	+	+
JunB		+	+	+	+	+	+
JunD			+	+	+	+	+
c-Fos							
FosB							
Fra-1							
Fra-2							

Table 1-1: Dimer combinations of Jun- and Fos-family proteins

Only Jun family members are capable of forming dimers among themselves. Fos family members only form heterodimers with Jun proteins.

1.2.2. AP-1 family members: characteristics, function and regulation

The two mayor subgroups of AP-1, the Jun- and Fos- families, are characterized by a high degree of homology. Binding affinities to TRE- and CRE-motifs, however, are different among Jun family members (Ryseck and Bravo, 1991), whereas Fos proteins show different trans-activating capabilities. Fos family proteins do not bind to DNA themselves – regulatory activity is mediated through a Jun family member. A third family of dimerization partners is the ATF family (ATF-2, ATF-3 and B-ATF) that preferentially interacts with CRE rather than TRE binding sites (Karin *et al.*, 1997; Chinenov and Kerppola, 2001).

The Jun family is composed of c-Jun, JunB and JunD. Regulation of c-Jun is achieved at transcriptional, translational and post-translational levels. c-Jun protein content is set by transcriptional and translational control mechanisms, whereas post-translational regulation is mainly responsible for rapid responses to stimuli that activate c-Jun. Activation of human c-Jun is achieved through phosphorylation and dephosphorylation events which control DNA binding and transcriptional regulatory activity (Boyle *et al.*, 1991; Pulverer *et al.*, 1991; Franklin *et al.*, 1992).

First, *c-jun* promoter is highly conserved and contains potential binding sites including Sp-1, nuclear factor-jun, CCAAT transcription factor and AP-1. Induction of human and murine *c-jun* expression is mediated through a TRE-like site located in the proximal region of the promoter, which is preferentially recognized by c-Jun:ATF-2 heterodimers (Steinmüller *et al.*, 2001). Despite this inducible expression, many human (Mechta-Grigoriou *et al.*, 2001) and murine (Lamph *et al.*, 1988; Ryder and Nathans, 1988) cell types contain basal levels of c-Jun protein prior to stimulation by growth factors, UV irradiation or cytokines. Additionally, human phosphorylated c-Jun induces its own transcription through a positive feed-forward loop (Berry *et al.*, 2001; Mechta-Grigoriou *et al.*, 2001).

Second, chicken c-Jun mRNA contains long 5' and 3' UTRs (*untranslated region*) implying additional levels of control (Sehgal *et al.*, 2000). The 5'UTR comprises ~1000nt and is characterized by GC-rich sequences, which was shown to generally block efficient translation (Kozak, 1989, 1991). Translation, however, is modulated by the presence of an IRES (*internal ribosomal entry site*) allowing translation even under stress conditions when overall protein synthesis is reduced (Sehgal *et al.*, 2000). The 3'UTR contains several AUUUA motifs, termed AU-rich elements that confer rapid degradation of mRNA (Vogt and Bos, 1990; Aharon and Schneider, 1993; Curatola *et al.*, 1995).

Third, at protein level, c-Jun is unstable with a 90min half-life time that is partially due to a PEST motif, which is involved in proteasomal degradation of short-living proteins upon ubiquitination. When phosphorylated by JNK (*c-Jun N-terminal Kinase*) at Ser^{63}, Ser^{73} and Thr^{91} or Thr^{93} polyubiquitination was suppressed and consequently the half-life time of murine c-Jun was extended (Musti *et al.*, 1997). Contrarily, phosphorylation by GSK-3 (*glycogen synthase kinase 3*) at Thr^{239} and Ser^{243} generates an attachment site for the E3 ligase Fbw7 (*F-box and WD repeat domain containing 7*), which targets human c-Jun for polyubiquitination and subsequent proteasomal degradation (Wei *et al.*, 2005).

The *JunB* promoter contains several putative regulatory elements including a STAT3 binding site and CRE and SRE (*serum response element*) recognition sequences. Its biological properties differ from c-Jun, since it negatively regulates cell growth. This functional difference is due to its decreased dimerization potential and the absence of JNK phosphorylation sites, what results in a lower *trans*-activation capacity (Mechta-Grigoriou *et al.*, 2001).

In contrast to *c-jun* and *junB*, *junD* is unresponsive to serum stimulation and shows high basal expression in many cell types. The promoter contains several identified regulatory elements: CRE, Sp-1 binding site, octamer motif, CAAT-box and AP-1 consensus site. JunD expression is primarily regulated by the octamer motif that is specifically recognized by Oct-1 (Mechta-Grigoriou *et al.*, 2001). Alternative initiation of translation leads to two predominant JunD proteins, a full-length (JunD-FL) and a shorter isoform (ΔJunD) (Short and Pfarr, 2002).

The Fos family comprises c-Fos, FosB, Fra-1 and Fra-2 that are all immediate early genes being rapidly expressed after stimulation. c-Fos protein and mRNA are undetectable in most quiescent cells and expression depends on stimulation of hormones, serum mitogens or other ligands (Distel and Spiegelman, 1990). Stimulation induces rapid and transient transcription of *c-fos* mediated by several elements, e.g. CRE, SIE (*sis-inducible enhancer*) and SRE (Karin *et al.*, 1997). Additionally, c-Fos is regulated at the level of mRNA stability by AREs (*adenylate uridylate-rich elements*) and mCRD (*major protein-coding region determinant of instability*). ARE and mCDR elements determine the mRNA turn-over by deadenylation of the poly(A) tail and subsequent nuclease digestion of the mRNA body by the exosom (Chen *et al.*, 1995; Grosset *et al.*, 2000; Chen *et al.*, 2002). Furthermore, c-Fos protein is degraded by the ubiquitin-proteasome pathway (Tulchinsky, 2000).

FosB transcription is rapidly and transiently induced upon stimulation with serum, growth factors or phorbol esters like *c-fos*. However, expression drops below detection levels within 3h (Tulchinsky, 2000).

Transcription of the *fosB* gene leads to two functionally distinct proteins via alternate splicing, FosB and FosB2, of which FosB is larger due to an additional C-terminal domain. Functionally, FosB is a more potent transcriptional activator than FosB2 (Skinner *et al.*, 1997; Herdegen and Waetzig, 2001; Jochum *et al.*, 2001).

Fra-1 and *fra-2* harbor functional TRE sequences (intronic enhancer of *fra-1*, promoter of *fra-2*) possibly controlling transcription via a positive auto-regulatory loop. Fra-1 and Fra-2 lack the C-terminal *trans*-activation domain, which points towards an inhibitory function that is consistent with their delayed *de-novo* synthesis after stimulation (Tulchinsky, 2000).

1.2.3. Role of AP-1 in HPV

AP-1 binds to two recognition sequences in the URR of HPV, located in the enhancer and in the promoter region, thereby positively regulating viral transcription (Hoppe-Seyler and Butz, 1994). Upon deletion of one of the two AP-1 recognition sequences, viral transcription is greatly diminished (Butz and Hoppe-Seyler, 1993).

Besides its role as a positive regulator, AP-1 can also inhibit transcription. Antioxidant-induced changes of the stoichiometry of AP-1 in HPV-16 immortalized keratinocytes were paralleled by a selective suppression of E6/E7 transcription (Rösl *et al.*, 1997). Furthermore, a shift from predominant c-Jun:c-Jun homodimers to c-Jun:Fra-1 heterodimers upon TNF-α treatment lead to a selective reduction of HPV-transcription (Soto *et al.*, 1999).

The composition of AP-1 is characteristic for tumorigenic and non-tumorigenic HPV-positive cell lines and the expression profile of AP-1 members reflects the *in vitro* and *in vivo* phenotype of the cells. For example, in HPV-immortalized, non-tumorigenic cell lines AP-1 is composed of Jun family member homodimers or heterodimers with Fra-1 whereas c-Fos is not expressed. Contrarily, tumorigenic HPV16/18 cervix carcinoma cell lines HeLa, SiHa or SW756 contain predominantly c-Fos and not Fra-1 leading to Jun:c-Fos heterodimers (O'Hara *et al.*, 1987; Soto *et al.*, 1999; Soto *et al.*, 2000; de Wilde *et al.*, 2008).

In contrast to other AP-1 members, the stoichiometry of Fra-1 and c-Fos in non-tumorigenic and tumorigenic HPV16/18-positive cell lines shows an inverse correlation. This correlation is not only characteristic but determinant for the *in vitro* and *in vivo* phenotype of HPV-positive cell lines as shown by ectopic overexpression experiments. Overexpression of *c-fos* in a non-tumorigenic HPV18-positive cell line shifted the balance from Jun:Fra-1 dimers to Jun:c-Fos dimers. As a result, cells underwent morphological changes *in vitro* and gained the capability of tumor formation in immuno-suppressed mice *in vivo* (Soto *et al.*, 1999). Contrarily, ectopic overexpression of *fra-1* in tumorigenic HPV18-positive cells did not affect the stoichiometry of AP-1 dimers and did not reverse the tumorigenic phenotype probably because of different phosphorylation marks (De-Castro Arce, 2003).

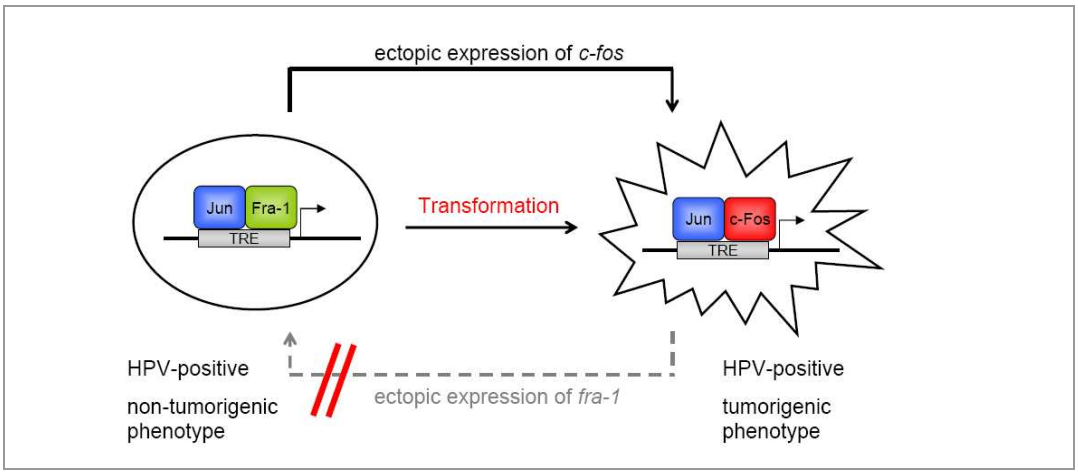

Figure 1-2: Phenotype-dependent composition of AP-1 in HPV-positive cell lines

Constitutive expression of *c-fos* induces tumorigenic transformation of HPV-immortalized cells. Fra-1 expression is a marker for a non-tumorigenic phenotype, but can not revert tumorigenicity.

1.3. microRNAs

MicroRNAs or miRNAs were first discovered in 1993. It could be shown that a 22nt RNA, termed *lin-4*, is required for the appropriate timing of post-embryonic development in *Caenorhabditis elegans* (Lee *et al.*, 1993; Wightman *et al.*, 1993). Since then, miRNAs have been identified in diverse animals and also plants. miRNAs form a family of noncoding small RNAs of 20-24nt in length, regulating the expression of protein-coding genes post-transcriptionally. This is achieved by regulating mRNA translation or stability in the cytoplasm (Bartel, 2004). Thereby, miRNAs are involved in crucial processes, including development, differentiation, apoptosis and proliferation. Current estimates suggest that about 30% of human mRNAs are conserved miRNA targets (Lewis *et al.*, 2005) that are regulated by predicted ~1000 different miRNAs, many of which are also conserved in other vertebrates (Bentwich *et al.*, 2005; Berezikov *et al.*, 2005). This makes miRNAs the most abundant class of regulatory genes. Each vertebrate miRNA targets about 200 transcripts and multiple miRNAs can synergistically regulate one single target (Krek *et al.*, 2005; Tay *et al.*, 2008).

Target sites are mainly localized in the 3'UTR (*untranslated region*) of mRNAs. There are, however, studies reporting target sites in the coding region (Duursma *et al.*, 2008; Tay *et al.*, 2008) and in the 5'UTR of mRNAs (Orom *et al.*, 2008). The exact mechanism how target mRNAs are repressed is not fully deciphered, yet. Indeed, there are several models (see **1.3.3**).

1.3.1. Biogenesis of microRNAs

Genes encoding miRNAs are mostly transcribed by RNA polymerase II (Pol II) (Cai *et al.*, 2004; Lee *et al.*, 2004) and less by Pol III (Borchert *et al.*, 2006). miRNA genes can be categorized according to their genomic location.

First, miRNAs can be encoded in introns, e.g. miR-135b in intron 1 of the TU ENSESTG0000000249 (*transcription unit*) (Rodriguez *et al.*, 2004), and also in exons of non-protein-coding transcripts, e.g. miR-155 in exon 3 of BIC (*B-cell integration cluster*) (Tam, 2001). Second, miRNAs can be part of protein-coding genes, e.g. miR-21 in intron 10 of TMEM49 (*transmembrane protein 49*) (Fujita *et al.*, 2008) or, as the only representative so far, miR-650 in the leader exon of the IGVL gene (*immunoglobulin lambda variable region gene*) (Das, 2009). In addition, miRNAs are encoded by individual genes or by clusters of genes expressing a polycistronic transcript, e.g. miR-17-92 cluster (Lee *et al.*, 2002).

Transcription by Pol II leads to capped, polyadenylated primary transcripts (pri-miRNAs) that are normally several kilo bases long and that embody local stem-loop hairpin structures of 60-110nt (see Fig. 1-2). These stem-loops are cleaved in the nucleus during the first step of miRNA maturation. The liberated product, the small hairpin, is named precursor miRNA (pre-miRNA) (Lee *et al.*, 2002). This cleavage is processed by the nuclear RNase III-type protein Drosha and its cofactor DGCR8 (*DiGeorge syndrome critical region gene 8 protein*) forming together the microprocessor complex (Gregory *et al.*, 2004; Han *et al.*, 2004). Alternatively, Ruby et al. found intronic miRNA precursors, termed mirtrons that bypass Drosha processing in *Drosophila melanogaster* and *Caenorhabditis elegans* (Ruby *et al.*, 2007). Instead of stem-loop formation, which is needed for pri-miRNA cleavage by Drosha (Han *et al.*, 2006), introns have conserved canonical splice sites and are dependent on a functional splicing and debranching pathway and not on Drosha processing. After splicing, mirtrons fold into the characteristic hairpin pre-miRNA structure and enter the common biogenesis pathway. Compared to flies and nematodes, mammals have few pre-miRNA-sized mirtrons (Lim and Burge, 2001; Yandell *et al.*, 2006),which might explain why mirtrons have not yet been found among the annotated mammalian miRNAs (Griffiths-Jones, 2004).

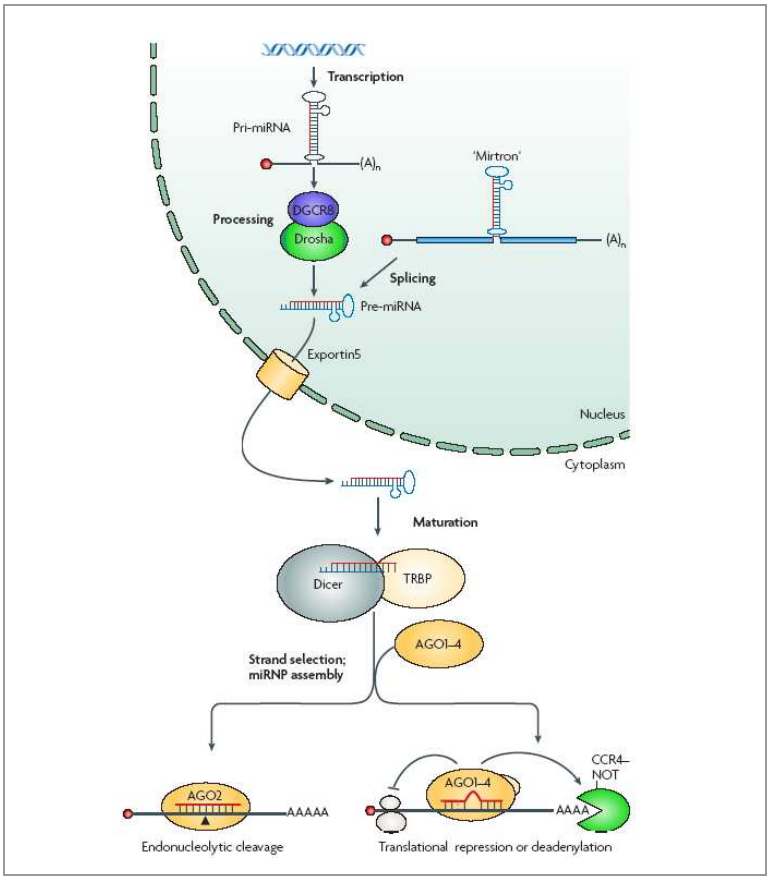

Figure 1-3: Biogenesis of miRNAs (Filipowicz *et al.*, 2008)

For details see chapter 1.3.1

After nuclear cleavage, pre-miRNAs are exported to the cytoplasm (Yi *et al.*, 2003) by exportin 5, which belongs to the nuclear transport receptor family (Bohnsack *et al.*, 2004; Lund *et al.*, 2004; Yi *et al.*, 2005). Following export from the nucleus, pre-miRNAs are cleaved near the terminal loop by the cytoplasmic RNase III-type protein Dicer, releasing ~22nt miRNA duplexes (Bernstein *et al.*, 2001; Hutvágner *et al.*, 2001).

After Dicer cleavage, one strand of the resulting ~22nt dsRNA is loaded into the effector complex. Two sorts of effector complexes can be distinguished depending on composition and mode of action: miRISC (*miRNA induced silencing complex*) and miRNP (*miRNA ribonucleoprotein complex*), see **1.3.2**. Since only one strand represents the mature and active miRNA (also termed "guide strand"), the complementary strand (also termed "passenger strand") is degraded. The thermodynamic stability of the two ends of the duplex determines strand selection (Khvorova *et al.*, 2003; Schwarz *et al.*, 2003). This process, however, is not yet fully understood since some hairpins produce miRNAs from both strands in equal amounts. The core component of the effector complexes is an Ago protein (*Argonaute*) that exercises miRNA-mediated repression. The Ago protein family consists of four members, Ago1-4, that, however, do not differ by the set of miRNAs they bind to (Meister *et al.*, 2004; Azuma-Mukai *et al.*, 2008).

1.3.2. Repression mechanisms of miRNAs

Mechanisms by which miRNAs repress their respective target mRNAs can be divided into two groups, depending on the degree of complementarity with their targets (see Fig. 1-3). miRNAs exhibiting a nearly perfect degree of complementarity with their target mRNA sequences trigger endonucleolytic cleavage by Ago2 in an RNAi-like mechanism (Meister *et al.*, 2004). Ago2 is the core component of the effector complex miRISC (*miRNA induced silencing complex*).

In most cases, however, miRNAs pair imperfectly with the mRNA due to central mismatches. In this case, target recognition is achieved through perfect base pairing between a "seed" sequence located at positions 2-7 in the miRNA sequence and target sequences in the mRNA (Brennecke *et al.*, 2005). Although less important, 3'end pairing might contribute to target recognition, especially when seed-pairing is weaker. Besides, functional miRNA sites not following the "seed-rule" are also reported (Stern-Ginossar *et al.*, 2007; Orom *et al.*, 2008). Imperfect pairing of miRNA:mRNA duplexes leads to post-transcriptional repression, which can be mediated by all four Ago proteins, Ago1-4. Repression is mediated by the effector complex miRNP (*miRNA-ribonucleoprotein complex*) that does not primarily involve endonucleolytic cleavage. Contrarily, target mRNAs are transported to P-bodies, where translation is repressed by different mechanisms:

(1) block of initiation. The central domain of Ago proteins contains limited sequence homology to the cap-binding region of eIF4E (Kiriakidou *et al.*, 2007), which is a subunit of the eukaryotic translation initiation complex. It was shown that Ago proteins can compete with eIF4E for m^7G binding and thus repress translation at the initiation step. Additionally, decap-

ping by the Dcp1-Dcp-2 complex leaves the mRNA susceptible for 5'→3' decay (Lykke-Andersen, 2002; van Dijk *et al.*, 2002).

(2) post-initiation repression. Ago proteins interact with the P-body protein GW182 (Jakymiw *et al.*, 2005; Liu *et al.*, 2005), which is thought to recruit the CCR4-NOT deadenylating complex (Behm-Ansmant *et al.*, 2006). Partial deadenylation of mRNAs is a necessary step of P-body formation (Zheng *et al.*, 2008) and of subsequent mRNA decay (Chen and Shyu, 1995; Chen *et al.*, 1995; Chen and Shyu, 2003; Parker and Song, 2004; Wu *et al.*, 2006). Target mRNAs with shortend poly(A) tails are then further deadenylated and finally degraded by the exosome, 3'→5' direction (Yamashita *et al.*, 2005).

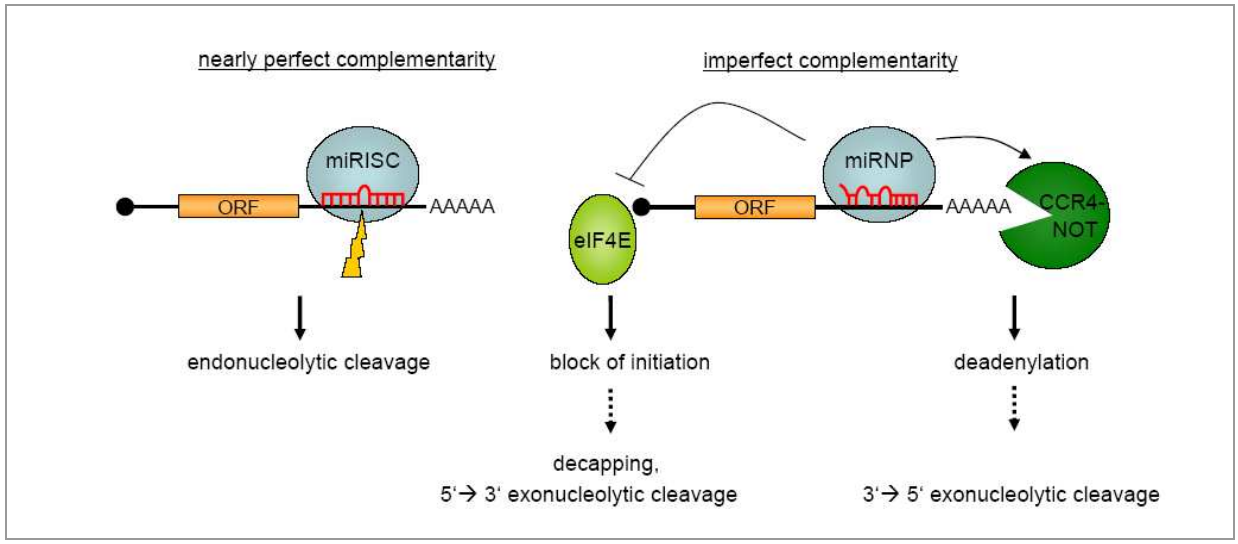

Figure 1-4: Repression mechanism of miRNAs

Modified according to (Filipowicz *et al.*, 2008), for details see chapter **1.3.2**

1.3.3. microRNAs and cancer

It is well known that carcinogenesis is marked by a broad deregulation of normally fine-tuned genes, what can even be used to classify different types of cancers (Ramaswamy *et al.*, 2001; Su *et al.*, 2001). Of those genes, protein-coding oncogenes and tumor suppressor genes are of particular interest. Due to their role in post-transcriptional gene regulation, miRNAs have been viewed as potential oncogenes or tumor suppressor genes and were thus studied in the context of tumorigenicity.

Many high-throughput expression profiling studies were conducted for different types of cancers (Michael *et al.*, 2003; Calin *et al.*, 2004a; Iorio *et al.*, 2005) that state the same ob-

servation: global deregulation and global down regulation of miRNAs in tumor versus normal tissues.

Deregulation is not surprising since miRNA expression patterns are highly specific for cell-type and cellular differentiation status (Aravin *et al.*, 2003; Bernstein *et al.*, 2003; Abbott *et al.*, 2005). Cancer cells, undergoing malignant transformation, differ in phenotype and differentiation status from healthy surrounding tissue by e.g. acquiring the capability to evade apoptosis, to loose contact-inhibition, to be resistant to anti-growth signals or to sustain neoangiogenesis (Hanahan and Weinberg, 2000). A deregulated miRNA expression profile can then be cause and / or consequence of this event.

Furthermore, the second finding that miRNAs are largely down regulated supports the idea on an altered differentiation status. Undifferentiated embryonic cells also express low levels of miRNAs; the increase of miRNA expression parallels the start of the differentiation process (Wienholds *et al.*, 2005). A possible disturbance of the miRNA processing machinery (Dicer, Drosha, Ago2 and DGCR8) as an obvious reason for reduced miRNA levels was not found in cancer cells (Lu *et al.*, 2005).

Since the expression profile of miRNAs is so specific, it is likely that much of the altered miRNA expression is a secondary effect of the loss of cellular identity that accompanies malignant transformation. Thus, up- or down regulation of a miRNA in a certain tumor-type is not necessarily indicative of a causative role in tumorigenesis. Nevertheless, data obtained from profiling studies can be used to classify human cancers according to the developmental lineage, differentiation state and the distinct mechanism of transformation of the tumor (Pavlidis and Fizazi, 2005).Classification based on expression data of miRNAs was even found to be superior to those of mRNAs (Lu *et al.*, 2005).

To address the question, if certain miRNAs play a causative role in carcinogenesis, the same criteria of protein-coding oncogenes or tumor suppressor genes, must be applied. Four types of evidence should be at least partially fulfilled by a miRNA before it can surely be viewed as a tumor suppressor or oncogene (Kent and Mendell, 2006): (1) data showing widespread deregulation in different cancers, (2) gain or loss of miRNA function, (3) direct documentation of tumor-suppressing or tumor-promoting activity using animal models, and (4) the identification of cancer-relevant target genes that depict mechanisms through which a miRNA contributes to oncogenesis.

A few miRNAs that partially or completely fulfill these criteria were already described. Known tumor suppressor miRNAs are the let-7 family, repressing, amongst others, RAS oncogene (Johnson *et al.*, 2005).Reduced expression of let-7 was linked to poor survival of lung cancer patients (Takamizawa *et al.*, 2004; Yanaihara *et al.*, 2006). Further tumor suppressors are miR15a and miR-16-1 that target BCL2 (B-cell CLL/lymphoma 2) (Cimmino *et al.*, 2005)

and that are frequently deleted in CLL (chronic lymphocytic leukemia), mantle cell lymphoma and multiple myeloma (Calin *et al.*, 2002; Calin *et al.*, 2005) and in prostate cancer (Dong et al., 2001). Down-regulation of miR-143/-145 was observed in several cancer types: colorectal cancer (Michael et al., 2003), breast cancer (Iorio et al., 2005) and myelodysplastic syndrome (Calin *et al.*, 2004b). In smooth muscle cells, it was shown that miR-143/-145 synergistically target a network of transcription factors including Klf4 (*Kruppel-like factor 4*), myocardin and Elk-1, which represses proliferation (Cordes *et al.*, 2009).

Besides, oncogenic miRNAs, also termed “oncomirs”, have been found to be up-regulated in various tumors. Levels of miR-155 are increased in B-cell lymphoma and Burkitt lymphomas (Eis *et al.*, 2005), papillary thyroid carcinoma (He *et al.*, 2005a) and in breast, lung and colon cancer (Volinia *et al.*, 2006). miR-155 negatively regulates AT1R (*angiotensin II receptor, type 1*) (Martin *et al.*, 2006), which plays a mayor role in fluid homeostasis, and it can, similarly to c-myc, induce oncogenesis in chicken embryonic fibroblasts (Tam *et al.*, 2002). The miR17-92 cluster, which comprises the six miRNAs, miR-17, -18a, -19a, -19b-1, -20a and -92-1, targets, amongst others, E2F1 (*E2F transcription factor 1*) (O'Donnell *et al.*, 2005) and the tumor suppressor PTEN (*phosphatase and tensin homolog*) (Lewis *et al.*, 2003). The cluster is up-regulated in B-cell lymphoma (Ota *et al.*, 2004; He *et al.*, 2005b), lung cancer (Hayashita *et al.*, 2005; Volinia *et al.*, 2006) and in breast, colon, pancreas and prostate cancer (Volinia *et al.*, 2006). Lastly, the oncogenic miRNA miR-21 possesses anti-apoptotic properties in glioblastomas (Chan *et al.*, 2005) and is also up-regulated in breast, colon, lung, pancreas, stomach and prostate cancer (Volinia *et al.*, 2006).

1.3.4. microRNAs and cervical cancer

Several studies have been published on the relation of microRNAs and HPV-infection or cervical cancer. Mostly, they report the (deregulated) expression of miRNAs and early functional studies with the overexpression or inhibition of single miRNAs. But, except for one study, respective target genes have not been identified, yet.

In contrast to other pathogenic DNA viruses that are known to express miRNAs (polyomavirus SV40, adenovirus hAV, herpesviruses) (Andersson *et al.*, 2005; Grey *et al.*, 2005; Pfeffer *et al.*, 2005; Sullivan *et al.*, 2005; Aparicio *et al.*, 2006), human papillomaviruses do not express miRNAs (Pfeffer *et al.*, 2005; Cai *et al.*, 2006; Lui *et al.*, 2007).

miRNA array expression studies were conducted reporting deregulation of miRNAs in cervical carcinoma cell lines (Lui *et al.*, 2007; Martinez *et al.*, 2008), in cervical cancer cell lines and tissues (Wang *et al.*, 2008b) and in early stage ISCCs (*invasive squamous cell car-*

cinomas) (Lee *et al.*, 2008). Down regulation of miR-143, which is reported in other types of cancer, was also observed in cervical cancer (Lui *et al.*, 2007; Wang *et al.*, 2008b). Furthermore, some miRNAs were analyzed for their physiological effects in cervical cancer cell lines, e.g. knockdown of miR-199a suppressed cell growth *in vitro*, which was potentiated by the anticancer drug cisplatin (Lee *et al.*, 2008). Overexpression of miR-143 and miR-145 had a growth suppressive effect, whereas overexpression of miR-146a increased cell proliferation (Wang *et al.*, 2008b). Targets for miR-143, -145, -146a and -199a were not found. Contrarily, miR-218 and its host-gene, SLIT2 tumor suppressor gene, were characterized in more detail. High-risk, but not low-risk, E6 protein reduced the expression of miR-218 and SLIT2, which lead to the up-regulation of LAMB3 (*laminin-5 β3 protein*), a target of miR-218. The binding site of miR-218, however, was not verified (Martinez *et al.*, 2008). Since LAMB3 is known to increase cell migration and tumorigenicity (Dajee *et al.*, 2003; Calaluce *et al.*, 2004), down regulation of miR-218 by high-risk HPV E6 and consequential up regulation of LAMB3 contributes to tumorigenesis.

Furthermore, HPV-infected cell lines expressed a different set of miRNAs, when they were grown in organotypic raft culture instead of monolayer cell culture. The miRNA expression profile was changed during the differentiation process; however, it was not altered by the status of the HPV genome, integrated or episomal (Wang *et al.*, 2008b).

Interestingly, Drosha, located at 5p13.3, was the most significantly up-regulated transcript in a study showing the gain of chromosome 5 in cervical SCCs (*squamous cell carcinomas*) and SILs (*squamous intraepithelial lesions*) (Muralidhar *et al.*, 2007). Drosha overexpression resulted in a differential regulation of a subset of miRNAs, some of which are also reported to be deregulated in other cancer types.

1.3.5. microRNAs and AP-1

AP-1 can potentially regulate the expression of miRNAs by acting as a transcriptional activator or repressor. On the other hand, AP-1 family members can theoretically also be subjected to miRNA-mediated regulation.

So far, c-Fos is the only subunit of AP-1 that is reported to be regulated by miRNAs. It was shown that miR-7b, which is over expressed in the hypothalamus of mice after hyperosmolar stimulation, inhibits c-Fos translation with no effect on c-Fos mRNA levels (Lee *et al.*, 2006). The search engine miRanda predicted two putative target sites of miR-7b in the 3'UTR of c-Fos that are both conserved among mammalian species. If both or only one of the putative sites is a true binding site for miR-7b, remains to be determined. Secondly, it was pub-

lished that miR-101 represses the expression of c-Fos oncogene (Li *et al.*, 2009). miRNA expression profiling of human hepatocellular carcinomas compared to surrounding normal tissues revealed down-regulation of miR-101. In the 3'UTR of c-Fos, the search engine TargetScan predicted one putative binding site, which is conserved among many species. By mutation experiments, the putative target site was confirmed to be a true binding site for miR-101.

Besides being a target of miRNAs, AP-1 can also regulate the expression of miRNAs. RAS oncogene activity can be found in a variety of tumor types, e.g. in adenocarcinomas of the pancreas (90%), the colon (50%), and the lung (30%) (Bos, 1989). The induction of AP-1 activity by RAS and RAS-dependent AP-1-compositional changes are described in various cell systems (Mechta *et al.*, 1997; Casalino *et al.*, 2003). In a rat thyroid cell line, the overexpression of RAS induced differential expression of AP-1 subunits such as Fra-1 (Talotta *et al.*, 2009). Newly-expressed Fra-1 containing dimers activated the expression of miR-21 through three AP-1 responsive elements in its promoter. Among the target genes of miR-21 is the tumor suppressor PDCD4 that, in turn, inhibits AP-1 activity (Yang *et al.*, 2003; Wang *et al.*, 2008a). This constitutes an auto-regulatory loop in which miR-21 is a direct target and an indirect regulator of AP-1. The finding of this circuit was further confirmed by a study of vascular smooth muscle cells (Lin *et al.*, 2009).

Furthermore, AP-1 dimers are also reported to bind to the promoter of BIC (*B-cell integration cluster*), which constitutes the pri-miRNA of miR-155 (Yin *et al.*, 2008). During B-cell maturation, transcription of the oncogenic miRNA-155 is activated via ERK and JNK signaling pathways. JunB:FosB dimers were shown to be recruited to a conserved AP-1 site in the promoter.

1.4. Aim of this study

The transcription factor AP-1 plays a decisive role in HPV-induced carcinogenesis, since it positively or negatively regulates transcription of the viral oncogenes E6 and E7. Besides, the composition of AP-1 is an important marker of the *in vitro* and *in vivo* phenotype of HPV-positive cells. miRNAs are potent post-transcriptional regulators of protein-coding genes and are known to enhance and cause transformation. Deregulated miRNA expression might contribute to an altered dimerization pattern of AP-1 during carcinogenesis.

This study wants to decipher and characterize miRNAs that regulate AP-1 proteins and that are potentially differentially regulated in non-tumorigenic and tumorigenic cells.

2. Material

2.1. Chemicals and reagents

[γ-^{32}P] dATP 10mCi/ml	Amersham-Pharmacia, Braunschweig
Acrylamide/bis-Acrylamide (29:1), 30% (v/v)	Sigma, Deisenhofen
Agarose	Invitrogen, Karlsruhe
Boric acid	Sigma, Deisenhofen
BSA (Albumin bovine Fraction V)	BIOMOL, Hamburg
Bradford-Reagent	Bio-Rad Laboratories, Munich
Bromophenol blue	Serva Feinbiochemica, Heidelberg
Chloroform	Merck, Darmstadt
DEPC	Sigma, Deisenhofen
DTT	Sigma, Deisenhofen
DMSO	Merck, Darmstadt
E-64	Roche Diagnostics, Mannheim
ECL-Reagent	NEN Lifescience Products, Cologne
EDTA	Roche Diagnostics, Mannheim
EGTA	Sigma, Deisenhofen
Ethanol absolute	Merck, Darmstadt
Ehtidium bromide solution, 1%	Fluka BioChemika, Gillingham (UK)
ExpressHyb™ Hybridization Solution	Clontech, Mountain View, CA (USA)
Formaldehyde	Merck, Darmstadt
Formamide	Fluka BioChemika, Deisenhofen
Glycerin, 86%	Merck, Darmstadt
Glycine	Sigma, Deisenhofen
Glycogen, 20µg/µl	Roche Diagnostics, Mannheim
HEPES	Gerbu, Gaiberg
Hydrochloric acid	Merck, Darmstadt

Isoamyl alcohol	Merck, Darmstadt
Magnesium chloride	Merck, Darmstadt
2-Mercaptoethanol	Sigma, Deisenhofen
Methanol	Merck, Darmstadt
Milk powder	Carl Roth, Karlsruhe
MOPS	Gerbu, Karlsruhe
Nonidet® P-40 (NP-40), 10% (w/v)	Roche Diagnostics, Mannheim
dNTPs	Invitrogen, Karlsruhe
PBS	Gibco, Eggenstein
Pefabloc SC	Roche Diagnostics, Mannheim
PMSF	Sigma, Deisenhofen
Poly(dI-dC).poly(dI-dC)	Amersham-Pharmacia, Freiburg
Potassium chloride	Merck, Darmstadt
2-Propanol	Merck, Darmstadt
Random primers $p(dN)_6$	Boehringer, Mannheim
RNasin Plus RNase Inhibitor, 40 U/µl	Promega, Mannheim
Roti-Phenol, pH 4.0	Carl Roth, Karlsruhe
Sigmacote, SL2	Sigma-Aldrich, St. Louis, MO (USA)
Sodium acetate	Merck, Darmstadt
Sodium citrate	Sigma, Deisenhofen
Sodium chloride	Merck, Darmstadt
Sodium dodecyl sulfate	Sigma, Deisenhofen
Sodium fluoride	Merck, Darmstadt
Sodium hydroxide	Carl Roth, Karlsruhe
Sodium ortho-vanadate	Sigma, Deisenhofen
TEMED	Gibco Life Technologies, Carlsbad, CA (USA)
TRIS	Sigma, Deisenhofen
Trypan blue	Sigma, Deisenhofen

Tween® 20	Sigma, Deisenhofen
Urea	Merck, Darmstadt
Xylene cyanol	Serva Feinbiochemica, Heidelberg

2.2. Reagents and media for bacteria culture

Ampicillin	Roche Diagnostics, Mannheim
Bacto™ Agar	Becton Dickinson, Heidelberg
Kanamycin	BIOTREND Chemikalien, Cologne
LB-Medium (Lennox)	Carl Roth, Karlsruhe
S.O.C. Medium	Invitrogen, Karlsruhe

2.3. Reagents and media for cell culture

DMEM + GlutaMAX™-I cat #21885, lot #514126	Invitrogen, Karlsruhe
OPTI-MEM® –I cat #11058, lot# 492516	Invitrogen, Karlsruhe
Tet System approved FBS cat #631106, lot #6B0314	Clontech, Mountain View, CA (USA)
Pen Strep cat #15140, lot #577998 +10,000U/ml Penicillin +10,000µg/ml Streptomycin	Invitrogen, Karlsruhe
0.25% Trypsin-EDTA cat #25300, lot #578150	Invitrogen, Karlsruhe

2.4. Oligonucleotides

2.4.1. siRNAs and miRIDIAN® miRNA mimics for knock-down experiments

siRNA	Sequence	Manufacturer	Reference
siDrosha	5'-TGTCATATAAGTCACGAAGCCTA-3' processed from shRNA sequence	Dharmacon, Chicago	(Aagaard *et al.*, 2007)
siDicer	5'-AAGGCTTACCTTCTCCAGGCT-3'	Dharmacon, Chicago	(Tang *et al.*, 2007)
siLuciferase	5'-CGTACGCGGAATACTTCGATT-3'	Dharmacon, Chicago	(Elbashir *et al.*, 2001)
siScramble	5'-AACAGTCGCGTTTGCGACTGG-3'	Dharmacon, Chicago	(Schneider *et al.*, 2006)
miR-495	miRIDIAN Mimic cat # C-300762-05-0005	Dharmacon, Chicago	
let-7a	miRIDIAN Mimic cat # C-300475-05-0005	Dharmacon, Chicago	
miRIDIAN Mimic Negative control #1	5'-UCACAACCUCCUAGAAAGAGUAGA-3' cat # CN-001000-01-05	Dharmacon, Chicago	

All siRNAs were synthesized with processing option A4 and ordered with a dTdT overhang at the 3' end.

2.4.2. double-stranded oligonucleotides for gene analysis by EMSA

Oligo	Sequence	Origin	Reference
AP-1 consensus	5'-cgcttgatgactcagccggaa-3'	Collagenase gene	(Lee *et al.*, 1987)
Oct-1 consensus	5'-tgtcgaatgcaaatcactagaa-3'		(Scheidereit *et al.*, 1988)

2.4.3. Single-stranded oligonucleotides as Northern probes for miRNA analysis

Probe	Sequence
has-let-7a	5'-aactatacaacctactacctca-3'
5S	5'-ttagcttccgagatcagacga-3'

2.4.4. Oligonucleotides for protein-coding gene analysis by RT-PCR

Gene	Sequence	T_A	Size	Reference
atf-2	F 5'-ctccagctcacacaactcca-3' R 5'-tgtttcagctgtgccacttc-3'	55℃	247 bp	
dicer1	F 5'-ggtccaccaatgagctgtgt-3' R 5'-ctttcccaactggcatcaaa-3'	53℃	112 bp	
drosha	F 5'-catgcaccagattctcctgta-3' R 5'-gtctcctgcataactcaactg-3'	57℃	267 bp	
c-fos	F 5'-aacttcattcccacggtcac-3' R 5'-ccttctccttcagcaggttg-3'	55℃	397 bp	(De-Castro Arce *et al.*, 2004)
fosB	F 5'-gggaacgaaataaactagca-3' R 5'-aaactccagacgttccttct-3'	51℃	154 bp	
fra-1	F 5'-gcgcctaggccttgtatctccctttcccc-3' R 5'-ccgctcgaggcgaggagggttggagagcc-3'	61℃	212 bp	(De-Castro Arce *et al.*, 2004)
fra-2	F 5'-gctgtagtggtgaaacagga-3' R 5'-aggataggtgaagacgaggt-3'	55℃	203 bp	
gapdh	F 5'-tggatattgttgccatcaatgacc-3' R 5'-gatggcatggactgtggtcatg-3'	65℃	461 bp	(Griffiths *et al.*, 1997)
jdp2	F 5'-agcccgtgaaaagtgagcta-3' R 5'-cagtgggttgccttctgact-3'	55℃	284 bp	
c-jun	F 5'-tcgacatggagtcccagga-3' R 5'-cgagttctgagctttcaagg-3'	57℃	143 bp	
junB	F 5'-cgactcatacacagctacgg-3' R 5'-gagccctgaccagaaaagta-3'	57℃	186 bp	

junD	F 5'-ggtgcccgacgtgccgagctt-3' R 5'-gtacgccgggacctggtgc-3'	61℃	307 bp	(De-Castro Arce *et al.*, 2004)
net	F 5'-acccaaaggcttggaaatct-3' R 5'-agtgtggggaactggaacag-3'	53℃	258 bp	(Hitschler, 2007)
oct-1	F 5'-agccaaactaccatctctcg-3' R 5'-cacacggatgttggtctcta-3'	55℃	213 bp	

Newly designed primers were chosen with Primer3 (http://frodo.wi.mit.edu/).

2.4.5. Oligonucleotides for miRNA analysis by RT-PCR

Gene	Sequence	T_A	Size	Cycles
hsa-miR-32	F 5'-ggagatattgcacattactaagt-3' R 5'-gaaaatatcacacacactaaattg-3'	57℃	70 bp	35
hsa-miR-92-1	F 5'-ctttctacacaggttgggatc-3' R 5'-ccaaactcaacaggccggg-3'	57℃	78 bp	35
hsa-miR-340	F 5'-ttgtacctggtgtgattataaag-3' R 5'-taagataccaggtatggctataa-3'	57℃	95 bp	35
hsa-miR-495	F 5'-tggtacctgaaaagaagttgc-3' R 5'-tgataccgaaaaagaagtgcac-3'	57℃	82 bp	35
hsa-let-7a-3	F 5'-gggtgaggtagtaggttgta-3' R 5'-aggaaagacagtagattgtatag-3'	57℃	74 bp	35

2.4.6. Oligonucleotides for 3'UTR cloning by RT-PCR

Gene	Primer sequence	T_A	Size
Without linkers, full-length 3'UTR:			
Jun 3'UTR	F 5'-ggtgccaactcatgctaacg-3' R 5'-ttggtatttgaatacatttattgtga-3'	59℃	1299 bp
Oct-1 3'UTR	F 5'-gcacagtgagctgggcaga-3' R 5'-aatttttggttagaaagttctcca-3'	57℃	286 bp

With linkers, full-length 3'UTR:			
Dicer 3'UTR	F 5'-agggcgatcgcctcgagtagctgaaaccgctttttaaaat-3' R 5'-cgtgcggccgcgtttaaacgaacagacgataactttattgg-3'	55℃	4312 bp
Fra-1 3'UTR	F 5'-agggcgatcgcctcgagtcgctttgtgaggcgcctga-3' R 5'-cgtgcggccgcgtttaaaccacagcttcaagccttttattc-3'	57℃	712 bp
c-Jun 3'UTR	F 5'-agggcgatcgcctcgagacattttgaagagagaccgtcg-3' R 5'-cgtgcggccgcgtttaaacttggtatttgaatacatttattgtga-3'	57℃	1329 bp
Net 3'UTR	F 5'-agggcgatcgcctcgagaaatcctgatgacgtctggcc-3' R 5'-cgtgcggccgcgtttaaactcgatgtttattgtctaaatatgg-3'	57℃	696 bp
Oct-1 3'UTR	F 5'-agggcgatcgcctcgaggcacagtgagctgggcaga-3' R 5'-cgtgcggccgcgtttaaacaatttttggttagaaagttctcca-3'	57℃	322 bp
With linkers, single segments:			
Fra-1 3'UTR Seg 1	F 5'-agggcgatcgcctcgagtcgctttgtgaggcgcctga-3' R 5'-cgtgcggccgcgtttaaactagggctccagaggacctct-3'	59℃	326 bp
Fra-1 3'UTR Seg 2	F 5'-agggcgatcgcctcgagagactttgtagatccttagagg-3' R 5'-cgtgcggccgcgtttaaacagctgtgcggttcaggagg-3'	59℃	216 bp
Fra-1 3'UTR Seg 3	F 5'-agggcgatcgcctcgagaggtgattggaccaggccatt-3' R 5'-cgtgcggccgcgtttaaaccacagcttcaagcctttattc-3'	59℃	219 bp
c-Jun 3'UTR Seg 1	F 5'-agggcgatcgcctcgagacattttgaagagagaccgtcg-3' R 5'-cgtgcggccgcgtttaaacccctttaatactgaatgagatcgaa-3'	55℃	351 bp
c-Jun 3'UTR Seg 2	F 5'-agggcgatcgcctcgaggaactgcatggacctaacattc-3' R 5'-cgtgcggccgcgtttaaacactcagagtgctccaaatctct-3'	55℃	360 bp
c-Jun 3'UTR Seg 3	F 5'-agggcgatcgcctcgagccagtgttgtttgtaaataagag-3' R 5'-cgtgcggccgcgtttaaacgtccctctccactgcaacc-3'	55℃	414 bp
c-Jun 3'UTR Seg 4	F 5'-agggcgatcgcctcgaggtttcaggaggctggaggaa-3' R 5'-cgtgcggccgcgtttaaacttggtatttgaatacatttattgtga-3'	55℃	295 bp

2.4.7. Oligonucleotides for sequencing

Primer	Primer sequence	3'UTRs
Check2 Seq	F 5'-gaaggtgaagggcctccactt-3'	c-Jun, Fra-1, Net, Oct-1, Dicer
dicer1 Seq 1	F 5'-atgatctttggctaaacaccc-3'	Dicer
dicer1 Seq 2	F 5'-taattccgatttggaaccttag-3'	Dicer
dicer1 Seq 3	F 5'-aagcattgcacttggtaccat-3'	Dicer

2.5. Plasmids

2.5.1. Original plasmids

Plasmid	Insert	Reference
pAP-1-Luc, (pTRE-Luc)	(TRE)-Firefly luciferase	Stratagene
pRL-TK	(HSV-TK)-Renilla luciferase	Promega
psiCHECK™-2	(SV40)-Renilla luciferase (HSV-TK)-Firefly luciferase	Promega
pCR2.1-TOPO-GAPDH	(promoter less)-GAPDH	Dr. Bachmann Laboratory Prof. Dr. Rösl

The promoter of each expression plasmid is mentioned in brackets.

2.5.2. Modified plasmids

Plasmid	Insert
psiCHECK-2-c-Jun 3'UTR	Fusion mRNA: *Renilla* luciferase - 3'UTR of c-Jun
psiCHECK-2-Fra-1 3'UTR	Fusion mRNA: *Renilla* luciferase - 3'UTR of Fra-1
psiCHECK-2-Net 3'UTR	Fusion mRNA: *Renilla* luciferase - 3'UTR of Net
psiCHECK-2-Dicer 3'UTR	Fusion mRNA: *Renilla* luciferase - 3'UTR of Dicer
psiCHECK-2-Oct-1 3'UTR	Fusion mRNA: *Renilla* luciferase - 3'UTR of Oct-1
psiCHECK-2-c-Jun seg 1	Fusion mRNA: *Renilla* luciferase - 1st segment of c-Jun 3'UTR

psiCHECK-2-c-Jun seg 2	Fusion mRNA: *Renilla* luciferase - 2nd segment of c-Jun 3'UTR
psiCHECK-2-c-Jun seg 3	Fusion mRNA: *Renilla* luciferase - 3rd segment of c-Jun 3'UTR
psiCHECK-2-c-Jun seg 4	Fusion mRNA: *Renilla* luciferase - 4th segment of c-Jun 3'UTR
psiCHECK-2-ra-1 seg 1	Fusion mRNA: *Renilla* luciferase - 1st segment of Fra-1 3'UTR
psiCHECK-2-Fra-1 seg 2	Fusion mRNA: *Renilla* luciferase - 2nd segment of Fra-1 3'UTR
psiCHECK-2-Fra-1 seg 3	Fusion mRNA: *Renilla* luciferase - 3rd segment of Fra-1 3'UTR

The plasmid maps are displayed in chapter **3.4.11.2**.

2.6. Enzymes

AccuPrime Pfx DNA Polymerase, 2.5 U/µl	Invitrogen, Karlsruhe
CIAP, 1 U/µl	MBI Fermentas, Vilnius, Lithuania
NotI, 10 U/µl	New England Biolabs, Schwalbach
Pfu DNA Polymerase recombinant, 2.5 U/µl	MBI Fermentas, Vilnius, Lithuania
Platinum Taq DNA Polymerase, 5 U/µl	Invitrogen, Karlsruhe
PmeI, 5 U/µl	MBI Fermentas, Vilnius, Lithuania
PRECISOR High-Fidelity DNA Polymerase, 2 U/µl	BioCat, Heidelberg
RNaseH, 5 U/µl	New England Biolabs, Schwalbach
SuperScript™ II Reverse Transcriptase, 200 U/µl	Invitrogen, Karlsruhe
SuperScript™ III Reverse Transcriptase, 200 U/µl	Invitrogen, Karlsruhe
T4 Polynucleotide Kinase, 10,000 U/ml	New England Biolabs, Schwalbach
T4 DNA Ligase, 400 U/µl	New England Biolabs, Schwalbach
XhoI, 20 U/µl	New England Biolabs, Schwalbach

2.7. Size Markers

BenchMark™ Prestained Protein Ladder	Invitrogen, Karlsruhe
GeneRuler™ DNA Ladder Mix	MBI Fermentas, Vilnius, Lithuania
PageRuler™ Plus Prestained Protein Ladder	MBI Fermentas, Vilnius, Lithuania

2.8. Kits

Dual-Luciferase® Reporter Assay System	Promega, Mannheim
Effectene® Transfection Reagent	Qiagen, Hilden
HiPerFect Transfection Reagent	Qiagen, Hilden
LightCycler® FastStart DNA Master^{PLUS} SYBR Green I	Roche, Mannheim
Lipofectamine™ 2000	Invitrogen, Karlsruhe
MinElute Gel Extraction Kit	Qiagen, Hilden
miRNeasy Kit	Qiagen, Hilden
One Shot® TOP10 competent cells	Invitrogen, Karlsruhe
QIAquick Gel Extraction Kit	Qiagen, Hilden
Qiagen® Plasmid Purification Maxi Kit	Qiagen, Hilden
QIAprep® Miniprep Kit	Qiagen, Hilden
RNeasy® Kit	Qiagen, Hilden
Zero Blunt® Topo® PCR Cloning Kit	Invitrogen, Karlsruhe

2.9. Antibodies

Antibody	**Manufacturer**	**Epitope**	**Application**
Actin (Clone 4) mouse monoclonal IgG cat # 691001 lot # 5029J	MP Biomedical, Eschwege	Chicken gizzard actin	Western, 1:100,000

ATF2 (N-96) rabbit polyclonal IgG cat # sc-6233x lot # A2607	Santa Cruz Biotechnology, Santa Cruz	Amino acids 1-96 of human ATF-2	Western, 1:10,000
Dicer [13D6] mouse monoclonal IgG cat # ab14601 lot # 348991	Abcam, Cambridge (UK)	N-terminus of human Dicer	Western, 1:1,000
Drosha rabbit polyclonal IgG cat # ab12286 lot # 291586	Abcam, Cambridge (UK)	Synthetic peptide derived from within residues 1-100 of human Drosha	Western, 1:400
c-Fos rabbit polyclonal IgG cat # 06-341 lot # 23255	Upstate Cell Signaling, Hamburg	Amino acids 3-16 of human c-Fos	Western, 1:10,000
c-Fos rabbit polyclonal IgG cat # sc-52x lot # I0403 lot # J1008	Santa Cruz Biotechnology, Santa Cruz	N-terminus of human c-Fos	EMSA, 2µg
Fra-1 rabbit polyclonal IgG cat # sc-605x lot # I0106	Santa Cruz Biotechnology, Santa Cruz	N-terminus of Fra-1 of rat origin	Western, 1:10,000 EMSA, 2µg
c-Jun rabbit polyclonal IgG cat # sc-1694 lot # I3004	Santa Cruz Biotechnology, Santa Cruz	Amino acids 1-79 mapping at the N-terminus of human c-Jun p39	Western, 1:500
p-c-Jun mouse monoclonal IgG_1 cat # sc-822x lot # E0704	Santa Cruz Biotechnology, Santa Cruz	Amino acids 56-69 of human c-Jun	EMSA, 2µg

Anti-rabbit IgG HRP cat # W401B lot # 21357802	Promega, Mannheim	Secondary antibody, HRP conjugated	Western, 1:10,000
Anti-mouse IgG HRP cat # W402B lot # 2157906	Promega, Mannheim	Secondary antibody, HRP conjugated	Western, 1:10,000

All antibodies being used for Western blot analysis were diluted with blocking buffer.

2.10. Consumables

Cell culture flaks	(Corning) Sigma-Aldrich, Munich
Cell culture plates	Greiner Bio-One, Frickenhausen
Cell scraper	Carl Roth GmbH & Co, Karlsruhe
Cryotubes	Greiner Bio-One, Frickenhausen
Cristal pipette tips	Greiner Bio-One, Frickenhausen
Eppendorf tubes	Eppendorf, Hamburg
Films Hyperfilm ECL	Amersham Bioscience, Freiburg
Graduated pipettes	Hirschmann, Eberstadt
Hybond-N+ Nylon membrane	Amersham Bioscience, Freiburg
MicroSpin™ G-25 Columns	GE Healthcare, Buckinghamshire
Pipette tips	Eppendorf, Hamburg
Photometer plastic cuvettes	Greiner Bio-One, Frickenhausen
Polypropylene conical tubes	(Falcon) BD, Heidelberg
Protrans membrane	Schleicher & Schüll, Dassel
PVDF membrane (Immobilon P)	Millipore, Eschborn
15% Polyacrylamide / TBE-Urea gel	Bio-Rad, Hercules, CA (USA)
Saran wrap	Toppits, Minden
Scalpels, disposable	Feather Safety Razor Company, Osaka (JP)
Sterile needles, Microlancer™ 3	Becton Dickinson, Heidelberg

Sterile filters MILLEX®-GS 0.22µm	Millipore, Molsheim (F)
TipOne Pipette Filter Tips	Starlab, Ahrensburg
Whatman 3MM filter paper	Schleicher & Schüll, Dassel
X-ray films, Super RX	Fuji, Tokyo (JP)

2.11. Apparatuses & laboratory equipment

Agilent 2100 Bioanalyzer	Agilent Technologies, Waldbronn
Analytical Scale AE 160	Mettler, Gießen
Analytical Scale basic	Sartorius, Göttingen
Autoradiography cassettes	Kodak, Stuttgart
Bacteria shaker G25	Infors, Bottmingen (CH)
Bioruptor	Diagenode, Liège (B)
BioPhotometer	Eppendorf, Hamburg
Camera, UV light	Renner, Dannstadt
Centrifuge Biofuge, Varifuge RF	Heraeus, Hanau
Centrifuge 5415 R	Eppendorf, Hamburg
Centrifuge MIKRO 120	Hettich, Tuttlingen
Developer machine Curix 60	AGFA, Cologne
DNA Engine DYAD and Tetrad 2 Cycler	Bio-Rad Laboratories, Munich
Geiger counter LB 1210B	Berthold, Wildbad
Gel drier 483	Bio-Rad Laboratories, Munich
Hybridization oven /shaker	Bibby Scientific Ltd, Stone (UK)
Lab Dancer Mini Vortexer	VWR, Lutterworth (UK)
LightCycler 1.5	Roche, Mannheim
Microscope CKX41SF	Olympus Corporation, Tokyo (JP)
Minifuge	Heraeus, Hanau
Mini-PROTEAN II™	Bio-Rad Laboratories, Munich
NanoDrop® ND-1000	NanoDrop Technologies, Wilmington (USA)

Neubauer counting chamber	Bender & Hobein, Bruchsal
PCR ThermoCycler MultiCycler PTC2000	Bio-Rad Laboratories, Munich
pH-meter Calimatic 765	Knick, Egelsbach
Photometer Ultraspec 3000	Amersham Bioscience, Freiburg
BioPhotometer	Eppendorf, Hamburg
Plate reader Mithras LB 940	Berthold Technologies, Bad Wildbad
Pipetboy acu	Hirschmann, Eberstadt
Pipettes 2.5µl, 10µl, 20µl, 200µl, 1000µl	Eppendorf, Hamburg
Power Supply PHERO-stab 500	Biotech-Fischer, Reiskirchen
Shaker Polymax 2040	Heidolph Instruments, Schwabach
Scale 1216 MP	Sartorius, Göttingen
Software MikroWin 2000	Mikrotek Laborsysteme, Overath
Sonifier 250	Branson/Heinemann, Schwäbisch Gmünd
SterilGARD Hood	Baker Company, Sanford, Maine (USA)
STERI-CULT 200 Incubator	Forma Scientifc, Marietta, Ohio (USA)
Thermomixer compact	Eppendorf, Hamburg
UV Stratalinker® 1800	Stratagene, La Jolla, CA (USA)
Water bath	Julabo, Seelbach
Blotting chamber, semi-dry	Hoefer Pharmacia Biotech, San Francisco, CA (USA)

2.12. Cell lines

Cell line	Characteristics	Reference
HeLa	*Species:* human, female, adult *Tissue:* Cervix, adenocarcinom *Viral status:* HPV18-positive *In vivo phenotype:* tumorigenic after s.c. injection into $nu^{-/-}$ mice	(Boshart *et al.*, 1984) (Schwarz *et al.*, 1985)

	caryotype: aneuploid	
444	HeLa x fibroblast hybrids *Viral status:* HPV18-positive *In vivo phenotype*: non-tumorigenic after s.c. injection into $nu^{-/-}$ mice *caryotype*: tetraploid	(Stanbridge, 1984)
CGL3	HeLa x fibroblast hybrids (segregant of 444) *Viral status:* HPV18-positive *In vivo phenotype:* tumorigenic after s.c. injection into $nu^{-/-}$ mice *caryotype:* tetraploid	(Stanbridge, 1984)

2.13. Solutions and buffers

All buffers were prepared with bidistilled water, if not mentioned otherwise.

Ampicillin	50mg/ml Aliquoted, storage at -20℃
APS	10% (w/v) Aliquoted, storage at -20℃
Blocking buffer (Western blot)	1xTBS, pH 7.6 0.1% (v/v) Tween 20 5% (w/v) Milk powder Storage at 4℃
BSA (protein quantification)	1µg/µl Aliquoted, storage at -20℃
BSA (EMSA binding buffer 5x)	60mg/ml Storage at -20℃

Buffer A	10mM HEPES, pH 7.9 10mM KCl 0.1mM EDTA, pH 8.0 0.1mM EGTA, pH 7.9 Storage at -20℃ Addition of protease and phosphatase inhibitors prior to use (see **3.2.1)**
Buffer C	20mM HEPES, pH 7.9 400mM NaCl 1mM EDTA, pH 8.0 1mM EGTA, pH 7.9 25% Glycerin Storage at -20℃ Addition of protease and phosphatase inhibitors prior to use (see **3.2.1**)
CIA	49 parts Chloroform 1 part Isoamyl alcohol Storage light protected at 4℃
DEPC water	0.1% (v/v) DEPC Incubation overnight, then autoclavation
DMEM, complete	500ml DMEM 50ml FBS 100U/ml Penicillin 100µg/ml Streptomycin Storage at 4℃
DMEM, freezing medium	60% (v/v) DMEM complete 30% FBS 10% DMSO sterile filtered through 0.22µm filter
DNA lysis buffer (3x)	1.5% (w/v) SDS 150mM Tris, pH 7.8 150mM EDTA, pH 8.0
DTT	0.1M Aliquoted, storage at -20℃

EDTA	0.5M, pH 8.0 Adjust pH with NaOH conc.
EGTA	0.25M, pH 7.9
EMSA binding buffer (5x)	50% (v/v) Glycerin 60mM HEPES, pH 7.9 20mM TRIS, pH 8.0 300mM KCl 5mM EDTA, pH 8.0 3µg/µl BSA Addition of protease and phosphatase inhibitors prior to use (see **3.2.5**)
E-64	2.5mg/ml in 50% ethanol Aliquoted, storage at -20℃
Freezing medium	10% (v/v) DMSO 30% (v/v) FBS 60% (v/v) DMEM Storage at -20℃
Kanamycin	30mg/ml Aliquoted, storage at -20℃
Laemmli buffer (10x)	0.25M TRIS 1.9M Glycine 1% (w/v) SDS
LB-Medium	10g NaCl 10g Bacto Krypton 5g yeast extract ad 1000ml Adjust to pH 7.2
LB-ampicillin agar plates	2% Bacto-Agar in LB-medium 50µg/ml Ampicillin
LB-kanamycin agar plates	2% Bacto-Agar in LB-medium 30µg/ml Kanamycin

MOPS buffer (20x)	400mM MOPS 100mM NaAc 20mM EDTA DEPC water Adjust to pH 7.0 Storage light protected
Pefabloc SC	23.8mg/ml Aliquoted, storage at -20℃
PMSF	0.01mg/ml in isopropanol Storage at -20℃
Poly(dI/dC).poly(dI/dC)	1mg/ml (10U=500µg) in TNE Annealing: 10min at 45℃, cooling to 20℃ Aliquoted, storage at -20℃
Ripa (1x)	10mM TRIS, pH 8.0 150mM NaCl 1mM EDTA, pH 8.0 1% NP-40 0.1% SDS
RNA loading buffer (2x)	50% Formamide 2.2M Formaldhyde 1% (w/v) Ficoll 400 0.02% (w/v) Bromophenol blue 1x MOPS buffer DEPC water Storage at -20℃
RNA loading buffer (3x) (miRNA Northern blot)	8M Urea 1x TBE 30mM EDTA 20% (v/v) Glycerin 0.03% (w/v) Bromophenol blue 0.03% (w/v) Xylencyanol DEPC water Storage at -20℃

RNase A	10mg/ml RNase A 10mM Tris, pH 7.5 15mM NaCl 80℃, 20min Storage at -20℃
SDS	10% (w/v)
SDS loading buffer (5x)	10% (w/v) SDS 0.03% (w/v) Bromophenol blue 12.5% (v/v) 2-Mercaptoethanol 5mM EDTA, pH 8.0 50% (v/v) Glycerin 300mM TRIS, pH 6.8 Aliquoted, storage at -20℃
SOC medium	2% (w/v) Bacto-Trypton 0.5% (w/v) yeast extract 10mM NaCl 2.5mM KCl 10mM $MgCl_2$ 10mM $MgSO_4$ 20mM glucose
Sodium fluoride	500mM NaF Aliquoted, storage at -20℃
Sodium ortho-vanadate	10mM Na_3VO_4 Adjust to pH 10.0 Aliquoted, storage at -20℃
SSC (20x)	3M NaCl 0.3M Na_3Citrate pH 7.0
Stripping solution (miRNA Northern blot)	0.5% SDS (w/v) DEPC water
TAE (50x)	2M TRIS 0.25M NaAc 0.05M EDTA, pH 8.0 Adjust to pH 7.8 with acetic acid

TBE (10x)	0.9M TRIS 0.9M Boric acid 0.02M EDTA, pH 8.0
TBS (10x)	100mM TRIS 1.37M NaCl Adjust to pH 7.6
TBST (1x)	1xTBS pH 7.6 0.1% (v/v) Tween 20
TE (1x)	10mM TRIS 1mM EDTA, pH 8.0
TNE (1x)	1x TE, pH 8.0 100mM NaCl Adjust to pH 7.4 with NaOH conc.
Towbin (10x)	250mM TRIS 1.92M Glycine Add 10% (v/v) Methanol prior to use
Transfer buffer (miRNA Northern blot)	1xTBE DEPC water
Trypan blue	0.25% (w/v) in 1xPBS
Wash solution 1 (miRNA Northern blot)	2xSSC 0.05% SDS EPC water
Wash solution 2 (miRNA Northern blot)	0.1xSSC 0.1% SDS DEPC water

2.14. Search engines

Search engine	Internet address	Reference
TargetScan Release: 5.1 (04/2009)	http://www.targetscan.org/	(Lewis *et al.*, 2005) (Grimson *et al.*, 2007) (Friedman *et al.*, 2009)

PicTar Release: 03/26/2007	http://pictar.mdc-berlin.de/	(Krek *et al.*, 2005) (Lall *et al.*, 2006)
miRBase Release: 5 (11/2007)	http://microrna.sanger.ac.uk/targets/v5/	(Enright *et al.*, 2003) (Griffiths-Jones *et al.*, 2006) (Griffiths-Jones *et al.*, 2008)
DIANA-microT Release: 3.0 (04/2009)	http://diana.cslab.ece.ntua.gr/microT/	(Maragkakis *et al.*, 2009)

3. Methods

3.1. Cultivation of eukaryotic cells

3.1.1. Cell culture

Cells were cultured in complete DMEM. When reaching 80-90% confluence, they were split by washing once with 1xPBS and trypsinizing at 37℃ for 5min. Then, Trypsin was inactivated with fresh media and cells were plated again at various dilutions ranging from 1:5 to 1:30, depending on scheduled experiments. All media were prewarmed at 20℃.

3.1.2. Cryoconservation and reactivation of eukaryotic cells

Cells were trypsinized as described in **3.1.1** and resuspended in complete DMEM. Then, cells were centrifuged at 800rpm for 5min. DMEM complete was replaced by freezing medium, precooled to 4℃. Afterwards, cell suspensi ons were aliquoted into cryotubes, which were rolled into a thick pile of paper towels and subsequently stored at -80℃. After two weeks, cryotubes were transferred into the cell tank for long-term conservation at -196℃.

When fresh cells were needed, a cryotube was slowly thawed on ice and the cell suspension was transferred into a falcon tube with 5ml complete DMEM, prewarmed at 25℃. After washing, cells were resuspended with complete DMEM and plated into a cell culture dish. After 2-3 passages cell were used for experiments.

3.1.3. Cell counting

100µl of a cell suspension in complete DMEM were mixed with 100µl Trypan blue solution and loaded onto the Neubauer chamber. All four quadrants (each comprising 16 fields) were counted and numbers were added up. The final cell concentration [cells/ml] was calculated as described by the formula:

$$\frac{\text{cell number}}{2} \cdot 10^4 = \left[\frac{\text{cells}}{\text{ml}}\right]$$

3.2. Preparation and analysis of proteins

3.2.1. Nuclear protein preparation (Schreiber *et al.*, 1989)

Nuclear protein extracts were prepared applying the method from Schreiber *et al.*, 1989. Furthermore, phosphatase and protease inhibitors were added to buffers A and C at concentrations according to the manufacturers' suggestions.

60cm^2 cell culture plates with 90-100% confluent cells were washed twice with isotonic 1xPBS. Then, 1.2ml buffer A were added, cells were scraped from the plates, transferred into Eppendorf tubes and incubated for 15min to allow hypotonic swelling of the cells. Subsequently, 75µl non-ionic detergent Nonidet® P40 (10% aqueous solution) were added (final concentration 0.59%) and cell suspensions were vortexed 10sec to lyse the plasma membranes. After centrifugation at 13,000rpm, 1min, intact nuclei were separated from the supernatants containing cytoplasmic proteins and RNA.

Supernatants were subsequently used for RNA preparation (see **3.3.1**).

Pellets were resuspended in 100µl high-salt buffer C and incubated for 30min while tubes were shaken every 5min. Finally, extracts were centrifuged at 13,000rpm, 5min, and the clarified supernatants containing nuclear proteins were transferred into fresh Eppendorf tubes and stored at -80℃. All steps, buffers and centrif ugations were done and applied at 4℃.

Protein concentrations were determined with the Bradford assay (see **3.2.3**).

Inhibitor	Function	Stock solution	Final concentration
DTT	Reducing agent	0.1 M	1 mM
E-64	Cysteinprotease inhibitor	2.5 µg/ml	5 µg/ml
NaF	Phosphatase inhibitor	0.5 M	1 mM
Na_3VO_4	Phosphatase inhibitor	10 mM	0.2 mM
Pefabloc SC	Serinprotease inhibitor	23.8 mg/ml	0.5 mg/ml

Table 3-1: Additives for buffers A and C

3.2.2. Whole cell protein preparation (RIPA) (Klotz *et al.*, 1999)

Whole cell protein extracts were prepared with chilled Ripa buffer supplemented with PMSF. 20cm^2 cell culture plates with 90-100% confluent cells were washed twice with isotonic 1xPBS. Then, 400µl Ripa buffer were added, cells were scraped from the plates and trans-

ferred into Eppendorf tubes. To lyse cell membranes, cell suspensions were sonified twice, 10sec, with Sonifier 250 set to: timer “hold”, duty cycle “50%” and output control “5”. Subsequently, suspensions were incubated at 4°C, 30min to allow complete protein extraction. After vortexing 2sec and centrifugation at 13,000rpm, 5min, supernatants, containing whole cell proteins, were transferred into fresh tubes and stored at -80°C. All work was done on ice at 4°C.

Protein concentration was determined with the Bradford assay (see **3.2.3**).

Inhibitor	Function	Stock solution	Final concentration
PMSF	Serinprotease inhibitor	10 mg/l (isopropanol)	0.1 µg/ml

Table 3-2: Additive for RIPA buffer

3.2.3. Protein quantification according to Bradford (Bradford, 1976)

All protein extracts were quantified with the colorimetric Bradford assay basing on the dye Coomassie Brilliant Blue G-250. The read-out depends upon the change of absorbance at a wave-length of 595nm when G-250 binds to proteins containing arginine and aromatic amino acids. The assay was carried out as follows: 800µl of bidistilled water were mixed with 200µl Bradford reagent and 1-10µg BSA to generate a straight calibration line or 2µl of protein extracts. Solutions were vortexed 2sec and measured with a spectrophotometer, calibrated with water and Bradford reagent. Protein concentrations were calculated with their repective extinction values using the straight calibration line.

3.2.4. Western blot analysis

3.2.4.1. SDS-polyacrylamide gel electrophoresis

(Laemmli, 1970; Hames and Rickwood, 1990)

With SDS-polyacrylamide-gel electrophoresis (SDS-PAGE), proteins were separated according to their size. This system is based on a discontinuous SDS-polyacrylamide-gel with a low-percentage stacking gel and a high-percentage running gel. The stacking gel concentrates the samples whereas they are separated in the running gel. Negatively charged SDS in loading buffer and gels attaches to hydrophobic regions of proteins in a constant weight ratio, thereby over-neutralizing positive charges, denaturing and solubilizing proteins. The scaffold

of the gels, the polyacrylamide, serves as a molecular filter separating proteins only according to their size, while they are migrating towards the anode. Resolution depends on the concentration of polyacrylamide. For an optimal separation, 10% running gels for proteins of 40-70kDa and 6% running gels for bigger proteins were used.

	Stacking gel	**Running gel, 6%**	**Running gel, 10%**
Tris, pH 6.8	0.126M	-----	-----
Tris, pH 8.8	-----	0.376M	0.376M
SDS	0.1% (w/v)	0.1% (w/v)	0.1% (w/v)
Acrylamide/bis-Acrylamide (29:1)	3% (w/v)	6% (w/v)	10% (w/v)
APS	0.05% (w/v)	0.05% (w/v)	0.05% (w/v)
TEMED	0.12% (v/v)	0.06% (v/v)	0.06% (v/v)

Table 3-3: Composition of stacking and running gels

For analysis, 12-15µg of nuclear or whole cell protein extracts were mixed with SDS loading buffer (1x final concentration) and incubated at 99℃, 3min. Immediately afterwards, samples were cooled on ice for 5min, centrifuged and loaded onto the wells. In order to determine the size of the proteins of interest, a prestained protein ladder was used as a size marker. Gels were first run at 15mA/gel and then at 30mA/gel when proteins reached the running gel. Electrophoresis was stopped when bromophenol blue exited the gel.

3.2.4.2. Western-blot transfer (Gallagher *et al.*, 1997)

Proteins separated by SDS-PAGE (see **3.2.4.1**) were subsequently transferred with the “semi-dry” method onto a Polyvinylidendifluorid-membrane (PVDF) (Towbin *et al.*, 1979; Gallagher *et al.*, 1997). After gel-electrophoresis, the gel was placed on top of the membrane that had been hydrated with methanol for 1min, washed with bidistilled water for 5min and then placed in Towbin buffer for 15min. The top and the bottom of the pile was composed of Whatmann 3MM filter paper that had been placed in Towbin buffer to serve as a reservoir for ions. Membrane and filter papers matched the size of the polyacrylamide gel. The assembly looked as follows from top to bottom: cathode – 8 sheets of filter paper – gel – membrane – 8

sheets of filter paper – anode. The transfer was conducted at 4°C, with 1.2mA/cm^2/gel for 70min.

3.2.4.3. Immuno-detection and "enhanced chemiluminescence" (ECL)

In the last step, proteins were detected indirectly with a specific, first antibody against the protein of interest and a secondary antibody raised against the species of origin of the first antibody (Schneppenheim *et al.*, 1991). The secondary antibody was conjugated with horseradish peroxidase (HRP) that oxidized in the presence of hydrogen peroxide luminol to a dioxetan compound. The product was unstable and decomposed while emitting light. Finally, this light was detected as "enhanced chemiluminescence" via autoradiography.

In order to inhibit unspecific binding, the membrane was blocked in blocking solution for at least 1h at 20°C. Then, the membrane was incubated with the first antibody in the respective dilution on a shaker at 4°C overnight. Next day (all steps were carried out at 20°C), the membrane was washed with TBST, 30min, incubated with the secondary antibody for 1h and subsequently washed again with TBST, 30min. Finally, the membrane was incubated for 1min with the ECL reagent and proteins were detected via autoradiography by exposing to X-ray films for seconds to minutes depending on the intensity of the signal.

3.2.4.4. Stripping of PVDF membranes

In order to detect different proteins on the same membrane, the previous protein-specific, first antibody was removed as follows (each step lasting 5min): washing with TBST and bidistilled water, stripping with 0.2 M NaOH to remove the old antibody while keeping the epitopes of the proteins for new antibody binding, and subsequently washing with bidistilled water and TBST. Finally, the membrane was blocked again with blocking buffer for 1h. Then, the membrane was ready to be reincubated with another antibody as described in **3.2.4.3**.

3.2.5. Electrophoresis mobility shift assay (EMSA)

The electrophoresis mobility shift assay (EMSA) determines the interaction between DNA and DNA-binding proteins, such as the interaction of transcription factors with their corresponding regulatory regions. The electrophoresis mobility shift assay, also known as gel re-

tention assay, bases on different migration abilities through a non-denaturizing polyacrylamide gel of protein-DNA complexes and DNA alone. Protein-DNA complexes migrate more slowly due to their increased size than unbound, double-stranded oligonucleotides. By adding specific antibodies to the reaction prior to the gel run, complexes are further increased in size and thus further retarded, allowing identification of the bound proteins. The employed oligonucleotides were made with an Applied Biosystems synthesizer using phosphoramitide chemistry and subsequent HPLC purification.

Oligonucleotide strands (sense and antisense) were annealed in TNE in a PCR machine applying the following program: 85°C for 10min followed by a temperature decrease of 0.5°C every 30sec. 200ng of annealed oligonucleotides were end-labeled with 3,000Ci/mmol [γ-^{32}P] dATP and T4 polynucleotide kinase at 37°C for 30 min. Non-incorporated oligonucleotides were removed by gel-purification: 15% polyacrylamide/1xTBE-gel electrophoresis at 200V for 90min. Subsequently, the radioactively labeled oligonucleotide was excised from the gel and extracted in TNE by shaking overnight at 4°C.

The binding assay was performed in a 20µl reaction volume containing 1xEMSA binding buffer, 2µg poly(dI/dC).poly(dI/dC), 2µg nuclear protein extract and additives (Pefabloc SC2,5mg/ml, E-64 25µg/ml, NaF 5mM, DTT 5mM, Na_3VO_4 1mM). The mixture was incubated at 20°C, 5min. Then, 10,000cpm of 5' end labeled, double-stranded oligonucleotide probe were added and incubated for 30min at 20°C. Afterwards, for supershift analysis, 2µg of the specific antibody were added and the mixture was additionally incubated at 4°C, 1h. Finally, protein-DNA complexes were resolved in a 5.5% non-denaturizing polyacrylamide/1xTBE-gel which was subsequently dried on a Whatmann 3MM filter paper and exposed to X-ray films at -80°C for hours to days depending on the intensity of the signal.

3.3. Preparation and analysis of nucleic acids

3.3.1. Genomic DNA preparation

Cells were washed twice with 1xPBS, incubated with 3ml DNA lysis buffer for 10min at 20°C, scrapped and transferred into 15ml falcon tubes. Proteinase K was added (200ng/µl final concentration) and the mixture was incubated at 56°C for 1 hr. Nucleic acids were purified using phenol/chloroform extraction. After centrifugation, the upper, DNA-containing, aqueous phase was transferred into a new tube where DNA was precipitated after addition of ammonium acetate (2M final concentration) and 0.8 volumes of isopropanol. The mixture was centrifuged and the pellet was washed twice with 70% ethanol, air-dried and resuspended in TE

buffer. Finally, gDNA was treated with RNAse A (Ribonuclease A, 10µg/ml) 10 minutes at 37℃. gDNA was stored at 4℃.

3.3.2. Cytoplasmic RNA preparation

Cytoplasmic RNA was isolated from buffer A extracts after separation from the nuclei (see **3.2.1**) with the RNeasy Kit according to the manufacturer's instructions. 1 volume supernatant was mixed with 2 volumes RLT buffer containing 1% β-mercaptoethanol and 1.5 volumes EtOH, loaded stepwise onto a column and centrifuged at 10,000rpm, 15sec. For washing, the column was centrifuged once with 700µl RW1 buffer and twice with 500µl RPE buffer. Afterwards, the column was dried by centrifuging at 10,000rpm, 15sec. Finally, RNA was eluted with 30µl RNase-free water and stored at -80℃.

3.3.3. Total RNA preparation

Total RNA including miRNAs was isolated with the miRNeasy Kit according to the manufacturer's instructions. $3x10^6$ "444" and $5x10^6$ "CGL3" and HeLa cells were seeded in 60cm^2 cell culture plates and grown until 90-100% confluence was reached: "444" cells after 1d, "CGL3" and HeLa cells after 2d. First, cells were washed twice with ice-cold 1xPBS and scrapped off the plates in 1ml 1xPBS. Cell suspension was transferred into an Eppendorf tube which was centrifuged at 2,000rpm, 2min, to replace the 1xPBS with 700µl QIAzol. The suspension was vortexed until all cells were dissolved and then the solution was incubated at 20℃, 5min. Afterwards, 140µl Chloroform were added , the mixture was vigorously shaken for 15sec and incubated for 3min. The dispersion was transferred into a fresh tube and centrifuged at 13,000rpm for 15min at 4℃. The upper, aqu eous phase was transferred into a new tube (~350µl) and 1.5 volumes EtOH (~525µl) were added. After vortexing, the solution was loaded stepwise onto a column and centrifuged at 10,000rpm, 15sec. For washing, the column was centrifuged once with 700µl RWT buffer and twice with 500µl RPE buffer. Afterwards, the column was dried by centrifuging twice at 10,000rpm, 2min. Finally, total RNA was eluted with 30µl RNase-free water and stored at -80℃.

3.3.4. Nucleic acid quantification

RNA, prepared according to 3.3.2 or **3.3.3,** plasmid DNA (see **3.4.11**) and genomic DNA (see 3.3.1) were quantified using the Nanodrop® ND-1000 Spectrophotometer according to the manufacturer's instructions. Absorbances at 230nm, 260nm and 280nm were measured. Sample concentrations were automatically calculated according to the Beer-Lambert equation:

$c = (A * e)/b$

c = concentration [ng/µl]

A = absorbance at 260nm [AU]

e = wavelength-dependent extinction coefficient [ng*cm/µl]

dsDNA: 50

ssDNA: 33

RNA: 40

b = path length [cm]

To determine nucleic acid purity the quotient 260nm/230nm, which should be 1.8-2.2, and the quotient 260nm/280nm, which should be ~2.0, were calculated.

3.3.5. RNA agarose gel electrophoresis

RNA that had been prepared according to **3.3.2** or **3.3.3** was separated in 1% agarose / 1xMOPS / ethidium bromide gels under non-denaturing conditions. 1µg RNA were incubated with RNA-loading buffer at 65℃ for 10min and cooled down to 4℃ for 3min prior to loading. Gels were run at 100V and bands were visualized with UV-light. Equal intensities of ribosomal RNAs indicated correct quantifications (see **3.3.4**) and RNA quality was assessed by the absence of degradation products of the ribosomal RNAs 28S and 18S.

3.3.6. Reverse transcription

3.3.6.1. Reverse transcription with SuperScript™ II

1-2µg cytoplasmic RNA (see **3.3.2**) were used with 200ng random primers for all cDNAs analyzed in quantitative RT-PCRs (see **3.3.8**). 2µg total RNA were used with 0.05nmol oligo $d(T)_{23}$ primer for cloning purposes (see **3.4**). 2µg total RNA (see **3.3.3**) were used for semi-quantitative RT-PCR analysis of pri-/pre-miRNAs (see **3.3.7.2**).

According to the manufacturer's instructions, RNA was incubated with random primers or oligo $d(T)_{23}$ at 70°C for 10min and cooled down on ice. Then, the mixture was supplemented with 1x First-Strand Buffer (50mM Tris-HCl, 75mM KCl, 3mM $MgCl_2$), 10mM DTT and 0.5mM dNTPs and incubated at 25°C for 10min. After annealing of the primers, 100U SuperScript™ II was added and the reaction was incubated at 42°C for 50min, then heated up to 70°C for 15min and finally cooled down to 4°C. cDNA was stored at -20°C.

3.3.6.2. Reverse transcription with SuperScript™ III

According to the manufacturer's instructions SuperScript™ III was used to clone the 3'UTR of Dicer. 3µg cytoplasmic RNA (see **3.3.1**) were incubated with 0.05nmol oligo $d(T)_{23}$ primers and 0.5mM dNTPs at 70°C for 10min and subsequently cooled down to 4°C. Then, 1x First-Strand Buffer, 10mM DTT and 400U SuperScript™ III were added and the mixture was incubated at 55°C for 60min, at 70°C for 15min and finally cooled down to 4°C. cDNA was stored at -20°C.

3.3.7. Semi-quantitative polymerase chain reaction

3.3.7.1. Primer test for qRT-PCR

Semi-quantitative RT-PCR was used to test the specificity of primers that were used in quantitative RT-PCRs. cDNA was obtained with random primers and SuperScript™ II (see **3.3.6.1**). PCRs were performed in 25µl total volume with 2.5U Platinum Taq DNA Polymerase, 1.5mM $MgCl_2$, 0.8mM dNTPs, 1x PCR buffer (20mM Tris-HCl, 50mM KCl), 0.8µM primers and 1µl cDNA. All PCR reactions were run with 35 cycles with a denaturation step at 94°C for 30sec, an annealing step at primer-specific temperature for 45sec, an extension step at 72°C for 45sec and a final elongation step at 72°C for 10min. The PCR fragment was visualized in a 2% agarose / ethidium bromide gel.

3.3.7.2. Analysis of pri-/pre-miRNA expression

Semi-quantitative RT-PCR was also used to analyze the expression of pri-/pre-miRNAs. cDNA was obtained with random primers and SuperScript™ II from total RNA (see **3.3.6.1**) that was, following reverse transcription, RNase H digested (see **3.4.2**). PCRs were performed in 25µl total volume with 2.5U Platinum Taq DNA Polymerase, 1.5mM $MgCl_2$, 0.8mM dNTPs, 1x PCR buffer, 0.8µM primers and 0.5µl cDNA. All PCR reactions were run with 35 cycles with a denaturation step at 94°C for 30sec, an annealing step at primer-specific temperature for 45sec, an extension step at 72°C for 45sec and a final elongation step at 72°C for 10min. The PCR fragment was visualized in a 4% agarose / ethidium bromide gel.

3.3.8. Quantitative polymerase chain reaction

The relative amount of cDNA of all analyzed genes was determined by quantitative RT-PCR using SYBR Green I according to the manufacturer's instructions. SYBR Green I binds to dsDNA which results in a fluorescence dye absorbing blue light of 494nm and emitting green light of 521nm. An increase in DNA product during PCR leads to a linear increase in fluorescence intensity, which is measured at the end of each cycle, therefore allowing DNA concentrations to be quantified. With reference to a standard dilution of 5 different amounts of pGAPDH (7.5ng, 750pg, 75pg, 7.5pg, 0.75pg), the cDNA concentrations of the genes of interest could be determined. For correction of possible differences in RNA quantity and quality or inefficiency of the reverse transcription reaction, values of target genes were normalized against the internal reference gene GAPDH. The Ct-values (*cycle threshold*), which determines the cycle when the fluorescence intensity significantly rises for the first time above the background fluorescence, were then used for the calculations.

Primers were tested according to **3.3.7** and cDNA was prepared with random primers and SuperScript™ II (see **3.3.6.1**). For relative quantifications, a straight calibration line consisting at least out of 3 of the 5 GAPDH values was generated. The values were chosen considering two criteria: inclusion of the cycle thresholds of the samples and a minimal error, usually 0.003 – 0.04. cDNA of target genes was relatively quantified by first subtracting the background (sample was water) and then by normalizing against GAPDH. Finally, values were displayed in Excel tables as percentages compared to control siRNA set to 100%.

PCRs were performed in 10µl total volume with 1x SYBR Green (FastStart Taq DNA Polymerase, reaction buffer, $MgCl_2$, SYBR Green I dye, dNTP mix), 2µM Primer and 1µl cDNA. PCRs were run following this program:

	Temp	Hold Time	Slope	Acquisition Mode
Denaturation	95℃	10min	20℃/sec	None
Amplification	95℃	10sec	20℃/sec	None
50 cycles	Gene specific	5sec	20℃/sec	None
	72℃	20sec	20℃/sec	Single
Melting Curve	95℃	0sec	20℃/sec	None
	Gene specific - 10℃	15sec	20℃/sec	None
	95	0	0.1℃/sec	Continuous
Cooling	40℃	30sec	20℃/sec	None

Table 3-4: qRT-PCR protocol

3.3.9. Northern blot analysis

Northern blotting was applied to control the down-regulation of miRNAs upon knock-down of Drosha or Dicer. In principle, the technique is identical to Western blotting (see **3.2.4**) where the focus is on proteins. Due to similarities, the techniques have been named according to the points of the compass after starting off with Southern blotting of DNA developed by Edwin Southern (Southern, 1975). First, RNA molecules are separated according to their size. Then, they are transferred onto a Nylon membrane, permanently fixed and autoradiographically detected.

3.3.9.1. RNA PAGE electrophoresis

Total RNA was obtained as described in **3.3.3**, quantified (see **3.3.4**) and quality-checked (see **3.3.5**). First, 10µg total RNA were filled up with Nuclease-free ddH_2O to 10µl, mixed with 8µl RNA loading buffer (for miRNAs) and heated to 80℃ for 10min and subsequently cooled down to 4℃. Then, samples were loaded onto a 15% Polyacrylamide / TBE-Urea Ready gel (Bio-Rad) that had been prerun at 125V for 45min. The gel was run at 90V with 0.5xTBE until the bromophenol blue (~10nt) reached the end of the gel. Afterwards, to compare for equal loading, the ribosomal RNA bands were visualized with ethidium bromide.

3.3.9.2. Northern-blot transfer and crosslink

RNAs, separated by PAGE electrophoresis (see **3.3.9.1**), were subsequently transferred onto a membrane and cross-linked. After gel-electrophoresis, the gel was placed on top of the membrane that had been dampened with transfer buffer. Top and bottom of the pile were composed of Whatmann 3MM filter papers that had also been dampened with transfer buffer to serve as a reservoir for ions. Membrane and filter papers matched the size of the polyacrylamide gel. The assembly looked as follows from top to bottom: cathode – 9 sheets of filter paper – gel – membrane – 9 sheets of filter paper – anode. The transfer was conducted at 20℃, with 20V for 40min/gel. Afterwards, RNA was twice UV-cross-linked with the UV Stratalinker® set to "Autocrosslink" (120,000µJ). The filter was then stored at -80℃.

3.3.9.3. Probe labeling

Complementary ssDNA-oligonucleotides (Invitrogen) were used as probes against mature miRNAs. The kinase reaction was incubated for 60min at 37℃. Then, 30µl Nuclease-free ddH_2O were added and the solution was transferred onto a MicroSpin™ G-25 Column. The column was centrifuged at 3,000rpm for 2min and the eluate, containing the radioactive-labeled probe, was used immediately or stored at -20℃.

	Final concentration	**Volume**
T4 Polynucleotide kinase [10U/µl]	0.5U/µl	1µl
PNK buffer (10x)	1x	2µl
ssDNA oligo [10µM]	1pmol/µl	2µl
[γ-^{32}P] dATP [10µCi/µl]	1µCi/µl	2µl
Nuclease-free ddH_2O	ad 20µl	13µl
Final volume		20µl

Table 3-5: Kinase reaction

3.3.9.4. Hybridization, washing, detection

Membranes were prehybridized in 5ml ExpressHyb™Hybridization Solution for 30min while rolling in the oven at 37℃. Then, membranes were hybridized for 60min and subsequently washed in the following order: 5min washing with wash solution 1, rolling in the oven, and 1min washing with wash solution 2, shaking on a rocking table. All wash solutions were at 20℃. Finally, membranes were wrapped in saran wrap and signals were detected by autoradiography. Filters were exposed to an X-ray film at -80℃ for hours to days which were subsequently processed in a developer machine.

3.3.9.5. Stripping

In order to hybridize membranes multiple times, the previous probe was removed by shaking the filters at 20℃ with 100℃ hot strippin g solution for 30min. This step was repeated until any radioactive signal was removed.

3.4. Cloning techniques: preparation of reporter plasmids

Full-length 3'UTRs of c-Jun, Fra-1, Net, Dicer and Oct-1 and segments of the 3'UTRs of c-Jun and Fra-1 were cloned behind the ORF of *Renilla* luciferase gene into the multiple cloning site of psiCHECK™-2.

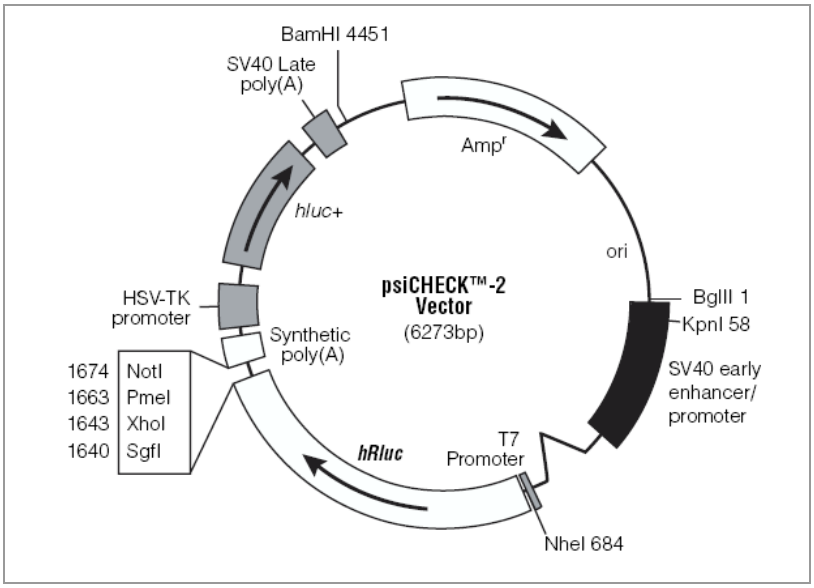

Figure 3-1: Vector map of psiCHECK™-2, © Promega

3.4.1. Cloning strategies

The following cloning strategy (**A**) was applied to clone the 3'UTRs of c-Jun, Fra-1, Dicer, Oct-1 and the segments of c-Jun and Fra1. For Net 3'UTR the strategy was slightly modified (**B**).

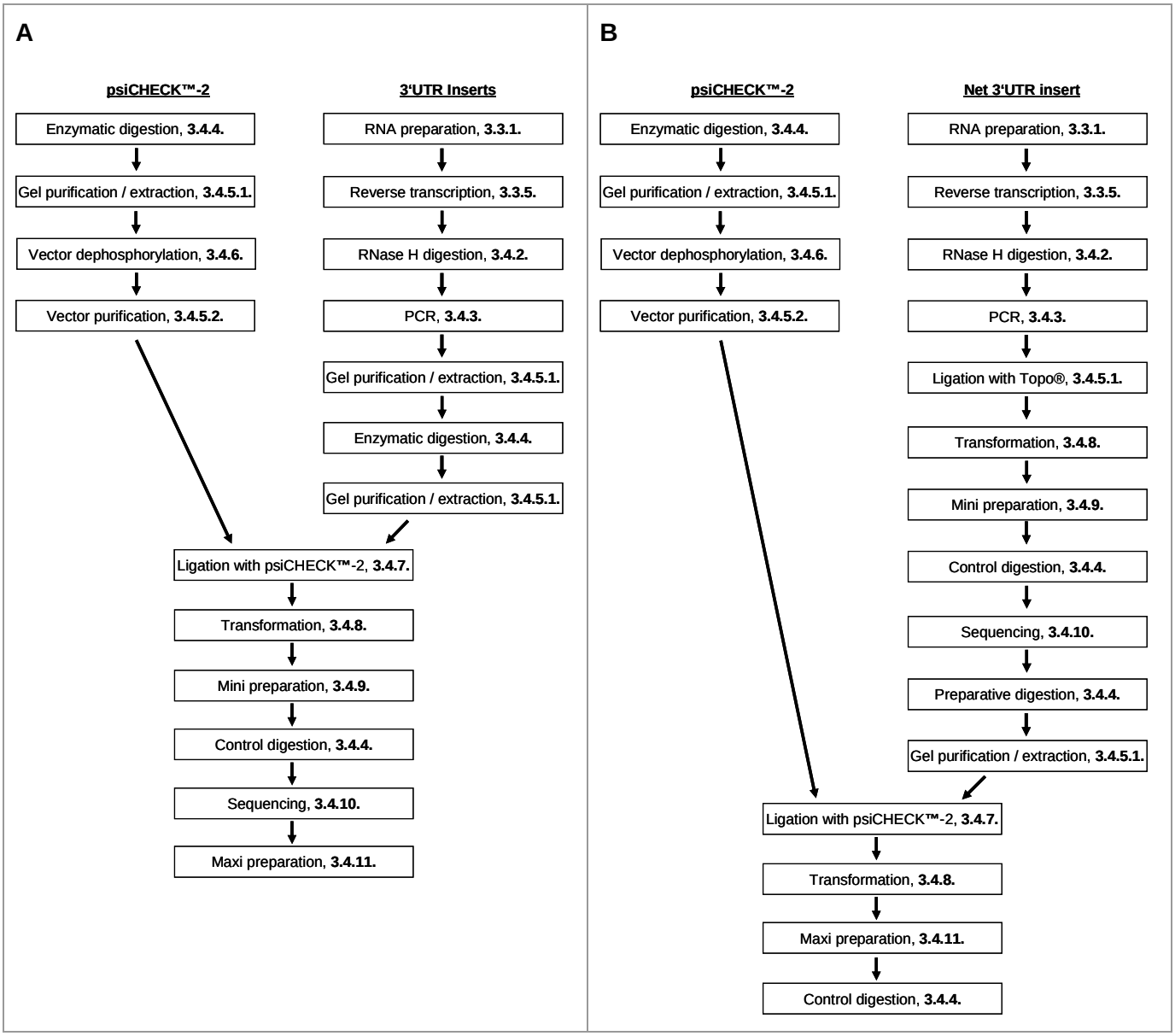

Figure 3-2: Cloning strategies for different 3'UTRs

3.4.2. RNase H digestion

cDNA that was used for cloning, was digested with RNase H to hydrolyze RNA which was hybridized to cDNA. cDNA was mixed with 10U RNase H and 1x RNase H buffer (50mM Tris-HCl, 75mM KCl, 3mM $MgCl_2$, 10mM Dithiothreitol) and the mixture was incubated at 37℃, 2h. Then, RNase H was heat-inactivated at 65° C, 20min. cDNA was stored at -20℃.

3.4.3. Semi-quantitative PCR to amplify 3'UTRs for cloning

Primers were chosen to harbor recognition sequences for SgfI, XhoI, PmeI and NotI – the restriction enzymes cutting in the multiple cloning site of psiCHECK™-2. All PCRs were run 5-8 folds in parallel to obtain enough amounts of fragments.

Forward primer

	overhang	SgfI	XhoI	binding to cDNA
5'-	agg	gcgatcgc	ctcgag	xxxxxxxxxxxxxxx -3'

Reverse primer

binding to cDNA	PmeI	NotI	overhang	
3'- xxxxxxxxxxxxxxx	caaatttg	cgccggcg	tgc	-5'

Table 3-6: Design of forward and reverse cloning primers

3'UTRs of Fra-1 and Net were amplified using Pfu DNA Polymerase according to the manufacturer's instructions. PCRs were performed in 25µl total volume with 1U Pfu DNA Polymerase, 3mM $MgSO_4$, 0.8mM dNTPs, 1x PCR reaction buffer (20mM Tris-HCl, 10mM $(NH_4)_2SO_4$, 10mM KCl, 0.1% (v/v) TritonX-100, 0.1mg/ml BSA), 0.8µM primers and 1.5µl cDNA. All PCR reactions were run with 35 cycles with a denaturation step at 94℃ for 30sec, an annealing step at 57℃ for 45sec, an extension step at 72℃ for 60sec and a final elongation step at 72℃ for 10min. The PCR fragment was visualized in a 1% agarose / ethidium bromide gel.

The 3'UTR of c-Jun was amplified using AccuPrime Pfx DNA Polymerase according to the manufacturer's instructions. The PCR was first run with primers without linkers. After extraction of the band from the agarose gel (see **3.4.5.1**), a nested PCR with primes harboring the linkers was prepared. PCRs were performed in 25µl total volume with 1.25U AccuPrime

Pfx DNA Polymerase, 1x PCR reaction buffer, 0.8µM primers and 1µl cDNA. All PCR reactions were run with 35 cycles with a denaturation step at 94°C for 30sec, an annealing step at 59°C for 45sec (or 57°C for nested PCR), an extensi on step at 68°C for 60sec and a final elongation step at 68°C for 10min. The PCR fragment was visualized in a 1% agarose / ethidium bromide gel.

The 3'UTR of Oct-1 was amplified using Platinum Taq DNA Polymerase according to the manufacturer's instructions. The PCR was first run with primers without linkers. After extraction of the band from the agarose gel (see **3.4.5.1**), a nested PCR with primers harboring the linkers was prepared. PCRs were performed in 25µl total volume with 2.5U Platinum Taq DNA Polymerase, 1.5mM $MgCl_2$, 0.8mM dNTPs, 1x PCR reaction buffer, 0.8µM primers and 1µl cDNA. All PCR reactions were run with 35 cycles with a denaturation step at 94°C for 30sec, an annealing step at 57°C for 45sec, an exte nsion step at 72°C for 45sec and a final elongation step at 72°C for 10min. The PCR fragment was visualized in a 1% agarose / ethidium bromide gel.

3'UTR of Dicer was amplified using Precisor High-Fidelity DNA Polymerase according to the manufacturer's instructions. PCR was performed in 25µl total volume with 0.4U Precisor High-Fidelity DNA Polymerase, 1x GC PCR reaction buffer, 0.8µM primers, 0.8mM dNTPs and 0.75µl cDNA. PCR reaction was run with 35 cycles with a denaturation step at 97°C for 30sec, an annealing step at 55°C for 45sec, an exte nsion step at 72°C for 5min and a final elongation step at 72°C for 10min. The PCR fragment was visualized in a 1% agarose / ethidium bromide gel.

3'UTR segments of c-Jun and Fra-1 were amplified using AccuPrime Pfx DNA Polymerase according to the manufacturer's instructions. PCRs were performed in 25µl total volume with 1.25U AccuPrime Pfx DNA Polymerase, 1x PCR reaction buffer, 0.8µM primers, 2% DMSO and 10pg psiCHECK-2-c-Jun or psiCHECK-2-Fra-1, respectively. All PCR reactions were run with 35 cycles with a denaturation step at 94°C for 30sec, an annealing step at 55°C (c-Jun) or 59°C (Fra-1) for 45sec, an extension ste p at 68°C for 60sec and a final elongation step at 68°C for 10min. PCR fragments were visualiz ed in a 1% agarose / ethidium bromide gel.

3.4.4. Analytical and preparative restriction enzyme digestion

For analytical purposes, plasmids from mini preparations (see **3.4.9**) were digested with restriction enzymes to identify positive clones with the respective insert. 500ng plasmid were digested in a mixture of 1x appropriate restriction buffer, 1x BSA and 10U of each re-

striction enzyme at 37℃, 1h. The fragment pattern was visualized in a 1% agarose / ethidium bromide gel. Positive plasmids were sent to sequencing (see **3.4.10**).

For preparative purposes, psiCHECK™-2 and PCR products were digested with restriction enzymes to obtain compatible, sticky ends. PCRs were prepared (see **3.4.3**) and PCR products were isolated from 1% agarose gels (see **3.4.5.1**). Then, fragments or empty vector were digested in a mixture of 1x appropriate restriction buffer, 1x BSA and 10U of each restriction enzyme at 37℃, 1h. Afterwards, fragments or vector were purified again with a 1% agarose / ethidium bromide gel (see **3.4.5.1**).

3.4.5. Purification of DNA

3.4.5.1. Gel purification / extraction

Fragments or vector were run in a 1-2% agarose / ethidium bromide gel to isolate them. Then, they were excised from the gel, extracted and purified by using the QIAquick Gel Extraction Kit according to the manufacturer's instructions. The gel slice was first dissolved in QG buffer at 50℃. Then, isopropanol was added and the mixture was passed through the column by centrifuging at 10,000rpm for 1min. For washing, the column was centrifuged with 500µl QG buffer and 750µl PE buffer and afterwards dried at 13,000rpm for 1min. Finally, DNA was eluted with 20-30µl EB buffer. DNA was stored at -20℃.

3.4.5.2. MinElute Cleanup

After dephosphorylation of the vector (see **3.4.6**), pDNA was purified from the reaction mixture by using the MinElute Gel Extraction Kit according to the manufacturer's instructions. 300µl ERC buffer were added to the plasmid mixture, transferred onto a column and centrifuged at 10,000rpm for 1min. Then, DNA was washed with 750µl PE buffer and the column was dried at 13,000rpm for 1min. Finally, DNA was eluted with 20µl EB buffer and stored at -20℃.

3.4.6. Dephosphorylation of vector

The vector was dephosphorylated prior to the ligation reaction to prevent the backbone from spontaneous re-ligation. The dephosphorylation reaction was carried out at 37℃ for 30min and subsequently purified as described in **3.4.5.2**.

	Final concentration	**Volume**
pDNA		x µl
CIAP [1U/µl]	0.04U/µl	2µl
CIAP buffer [10x]	1x	5µl
ddH_2O	ad 50µl	x µl
Final volume		50µl

Table 3-7: Dephosphorylation reaction

3.4.7. Ligation

The required volumes of backbone and insert to achieve a suitable ratio in the ligation reaction were estimated visually by running a 1% agarose / ethidium bromide gel. The ligation reaction was carried out overnight at 16℃. 3'UTRs of Fra-1, Net and Dicer were ligated via XhoI and NotI cutting sites, 3'UTRs of c-Jun and Oct-1 via XhoI and PmeI.

Ligation reaction	**Final concentration**	**Volume**
T4 DNA Ligase [400U/µl]	20.0U/µl	1 µl
Ligase buffer [10x]	1x	2 µl
psiCHECK™-2	ratio (vector: insert):	x µl
insert	1:5 – 1:8	x µl
ddH_2O	ad 20µl	x µl
Final volume		20µl

Table 3-8: Ligation reaction

For Net 3'UTR, a different strategy was applied. Since the amount of Net 3'UTR was too low from the PCR for direct digestion and subsequent cloning into psiCHECK™-2, the fragment was first cloned into TOPO vector (ZeroBlunt® Topo® PCR Cloning Kit). Ligation was carried out at 20℃, 30min, according to the manufacturer's instructions. Positive colonies were selected, mini DNA preparations were made (see **3.4.9**) and sequenced. Then, Net 3'UTR was prepared in sufficient amount by restriction enzyme digestion and cloned into psiCHECK™-2.

3.4.8. Transformation of chemically competent *E. coli*

Ligation reaction was heated up to 65℃ for 10min to inactivate the ligase. Then, 2µl of the ligation mixture were transfected into 25µl of TOP10 chemically competent cells according to the manufacturer's instructions. Bacteria were incubated with the plasmid solution on ice for 30min, then heat-shocked at 42℃ for 30sec and incubated while shaking for 1h with pre-warmed S.O.C. medium at 37℃. Subsequently, bacteria were spread onto LB-agar plates containing the selective antibiotic and incubated at 37℃ overnight to allow colony growth.

3.4.9. Mini preparation of plasmid DNA

Plasmid DNA was purified with the QIAprep® Miniprep Kit following manufacturer's instructions. 7ml LB medium were inoculated with one colony from the agar plate (see **3.4.8**) and were incubated at 37℃ overnight. Then, bacteria were pelleted and resuspended in 250µl P1 buffer. For lysis, 250µl P2 buffer were added and the lysis reaction was stopped after 5min. Subsequently, 350µl N3 buffer were added and the mixture was centrifuged at 13,000rpm for 10min. The clarified supernatant was centrifuged through a QIAprep spin column which was then washed with 500µl PB buffer and 750µl PE buffer. The column was dried at 13,000rpm, 1min. Finally, plasmid DNA was eluted with 30µl EB buffer. pDNA was stored at -20℃.

3.4.10. Sequencing of reporter plasmids

Plasmids were sequenced by GATC Biotech AG, Konstanz, to ensure absence of point mutations.

3.4.11. Maxi preparation of plasmid DNA

Large amounts of pDNA were prepared with the Qiagen® Plasmid Purification Maxi Kit following the manufacturer's instructions. 7ml LB medium were inoculated with either one colony from the LB agar plate (see **3.4.8**) or with bacteria culture, left over from the mini preparation (see **3.4.9**). The culture was incubated at 37℃ for 8h at 225rpm on a shaker. Then, the culture was transferred into 300ml LB medium and incubated further at 37℃ for 12-14h at 225rpm on a shaker. Then, the suspension was transferred into centrifuge tubes and bacteria were centrifuged at 6,000rpm for 15min at 4℃. The clarified supernatant was removed and the bacteria pellet was resuspended in 10ml P1 buffer, then lysed by adding 10ml P2 buffer at 20℃ for 5min. Subsequently, lysis was stopped with 10ml P3 buffer and the mixture was neutralized at 4℃ for 20min. Then, the supernatant containing the plasmid DNA was clarified by centrifuging at 4℃ for 30min at 13,000rpm before it was transferred onto the column. Afterwards, the column was washed twice with 30ml GC buffer and pDNA was eluted with 15ml QF buffer into a Falcon tube containing 10.5ml isopropanol for precipitation. Subsequently, the pDNA dispersion was centrifuged at 4℃, 4,000rpm, 1h. Finally, the pelleted pDNA was washed with ice-cold 70% ethanol twice and dissolved in 200µl TE buffer. pDNA was stored at -20℃.

3.4.11.1. Cryoconservation and reactivation of bacteria

In order to have permanent stocks of bacterial strains, bacteria were cryoconserved. 800µl of an exponentially growing bacterial suspension were mixed with the same volume of 86% glycerin and shock-frozen in liquid nitrogen. The strains were then stored at -80℃. For reactivation, a pipette tip was dipped into the glycerin culture and used to inoculate a LB-agar plate, which was subsequently incubated at 37℃ overnight.

3.4.11.2. Plasmid maps

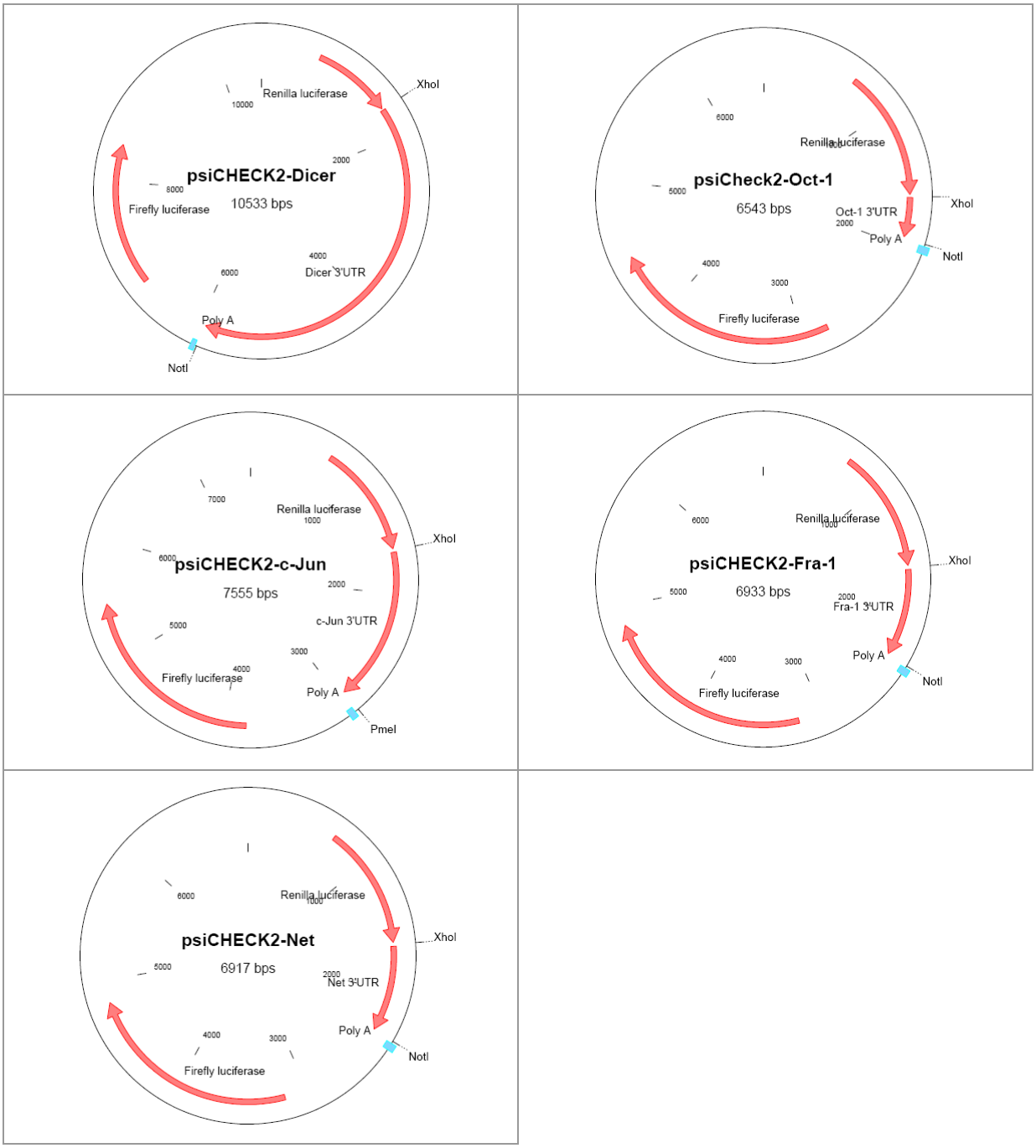

3.5. Reporter gene analysis

In reporter gene assays the Dual-Luciferase® Reporter Assay System was applied to analyze functional implications of miRNAs. The assay makes use of two luciferases: *Firefly*-luciferase derived from firefly *Photinus pyralis* and Renilla-luciferase derived from sea pansy *Renilla reniformis*. The system benefits from the absence of human equivalents, the short half-life time of mRNAs and proteins and the high sensitivity (de Wet *et al.*, 1987).

The two luciferase enzymes catalyze the oxidation of their respective substrates, which is accompanied by light emission. The light intensities are directly proportional to the amount of luciferases. Therefore, the number of impulses indirectly allows quantification of the proteins and conclusions about the biological activity of miRNAs. Since the substrates and the peak emission wavelengths are different, the activities of *Firefly*- and *Renilla*-luciferase can be determined in parallel.

3.5.1. Transfection of reporter genes

3.5.1.1. Transfection of plasmid DNA

For reporter gene analysis, reporter constructs were transfected using Effectene™. Effectene® is a non-liposomal lipid reagent that forms micelle structures that incorporate condensed DNA which is then able to pass through the cell membrane. Transfections were done according to the manufacturer's instructions including 4-6 biological replicates per experimental setup. Cells were seeded 24h prior to transfection in 6-well plates: "444" cells $1.3x10^5$, "CGL3" and HeLa cells $3.5x10^5$. Next day, medium was removed and replaced with 2.0ml fresh complete DMEM.

For pAP-1-luciferase assays, for one single transfection, 95ng of pAP-1-Luc and 5ng of pRL-TK were mixed with EC buffer and 0.8µl enhancer and incubated at 20℃, 5min. Then, 2.5µl Effectene were added, vortexed 10sec and incubated at 20℃, 10min, to allow formation of micelles. Then, the mixture was slightly agitated together with complete DMEM and finally the complete 300µl transfection mixture was added drop wise to the well.

For psiCHECK™-2 luciferase assays, the protocol was slightly different due to the low amount of Effectene reagent. For one single transfection, 5ng of the respective psiCHECK-2 construct were mixed with EC buffer and 0.08µl enhancer and incubated at 20℃, 5min. Then, 0.25µl Effectene that had been diluted with EC buffer were added, vortexed 10sec and incubated at 20℃, 10min. Then, the mixture was slightly agitated together with complete DMEM and finally the complete 300µl transfection mixture was added drop wise to each well.

To reduce errors in biological replicates, master mixes were prepared for all transfections. Next day, 24h later, cells were harvested (see **3.5.2**).

3.5.1.2. Co-transfection of plasmid DNA and miRNA mimics

For reporter gene analysis, reporter constructs and miRNA mimics were transfected using Lipofectamine™ 2000. Lipofectamine™ 2000 forms cationic liposomes that encapsulated pDNA and miRNA mimics which were then able to pass through the cell membrane. Transfections were done according to the manufacturer's instructions including 4 biological replicates per experimental setup. $1x10^4$ "444" cells were seeded 24h prior to transfection in 96-well plates. Next day, medium was removed and replaced with 50µl fresh DMEM only supplemented with serum.

For one single 96-well transfection, 0.2ng of psiCHECK2-3'UTR construct and 15pmol miRNA mimic (final concentration 150nM) were diluted in 25µl OPTI-MEM without additives. 0.583µl Lipofectamine™ 2000 were diluted separately in the same volume of OPTI-MEM without additives and incubated for 5min. Then, both mixtures were combined, slightly agitated and incubated for 20min. Finally, the complete 50µl transfection mixture was added drop wise to the well.

3.5.2. Cell extracts for reporter gene analysis

Cell extracts for reporter gene analysis were harvested 24h after transfection (see **3.5.1**). 6-well plates (see **3.5.1.1**) were washed twice with 1xPBS. Then, 80µl of 1x Passive Lysis buffer (Dual-Luciferase® Reporter Assay kit) were added to each well and cells were scrapped and transferred into Eppendorf tubes. Cell suspensions were incubated for 30min to allow for complete cell lysis, then vortexed for 3sec and centrifuged at 13,000rpm for 2min. The clarified supernatants were transferred into fresh tubes and signal intensity was quantified immediately (see **3.5.3**) or stored at -80°C. Alternatively, cells in 96-well plates (see **3.5.1.2**) were lysed with 35µl of 1x Passive Lysis buffer after washing with 1xPBS. Lysis occurred while shaking on a Thermomixer at 4°C, for 1h. Subsequently, 15µl of the suspension were used for the measurement. All steps were carried out at 4°.

3.5.3. *Firefly-* / *Renilla*-luciferase measurements

Luciferase measurements were done with the Mithras plate reader and the MicroWin 2000 software. 10µl of each extract were loaded onto a 96-well plate. LARII and Stop&Glow buffer were prepared according to the manufacturer's instructions. The program was as fol-

lows: injection of 50µl LARII, 2sec incubation, 10sec reading, injection of 50µl Stop&Glow, 2sec incubation and 10sec reading. Readings were exported to a MS Excel file and analyzed.

Results for pAP-1-luciferase assays are given as RLU [%] by dividing *Firefly*-luciferase readings with *Renilla*-luciferase readings. Graphics show the increase in percentage [%] compared to a control treatment set to 100%.

Results for psiCHECK™-2 luciferase assays are given as RLU [%] by first dividing *Renilla*-luciferase readings with *Firefly*-luciferase readings and second by dividing this figure with the one obtained from the control plasmid without an insert (psiCHECK™-2_empty). Graphics show the increase in percentage [%] compared to a control treatment set to 100%.

3.6. RNA-interference (RNAi)

RNA-interference is a mechanism by which genes are post-transcriptionally silenced either by endogenous or exogenous, artificial, double-stranded siRNA (*small interfering RNA*). siRNAs recognize their respective target genes via Watson-Crick base-pairing to mRNA resulting in selective degradation of the mRNA and therefore inhibiting *de-novo* protein synthesis (Elbashir *et al.*, 2001; Meister and Tuschl, 2004).

siRNAs were transfected with HiPerFect Transfection Reagent according to the manufacturer's suggestions. 20µl of siRNA (40µM) were mixed with 1.0ml DMEM without additives and 40µl HiPerFect, vortexed 3sec and incubated at 20℃, 10min. Then, $2x10^6$ cells of "444" or "CGL3" were seeded in a $60cm^2$ cell culture plate with a final volume of 7.0ml complete DMEM. Transfection solution was added drop wise to the cell suspension resulting in 8.0ml total volume and 100nM final siRNA concentration. Cell culture plates were agitated slightly and placed in the incubator. On day 2, 24h later, cells were trypsinized (see **3.1.1**), counted (see **3.1.3**) and plated in 6-well plates for reporter gene assays (see **3.5**) or split in $20cm^2$ and $60cm^2$ cell culture plates to obtain nuclear extracts (see **3.2.1**) and whole cell extracts (see **3.2.2**) on day 4.

3.6.1. Diagram of the workflow of a standard experiment

All experiments requiring Drosha and Dicer knock-down and subsequent pDNA transfection were carried out following this overview:

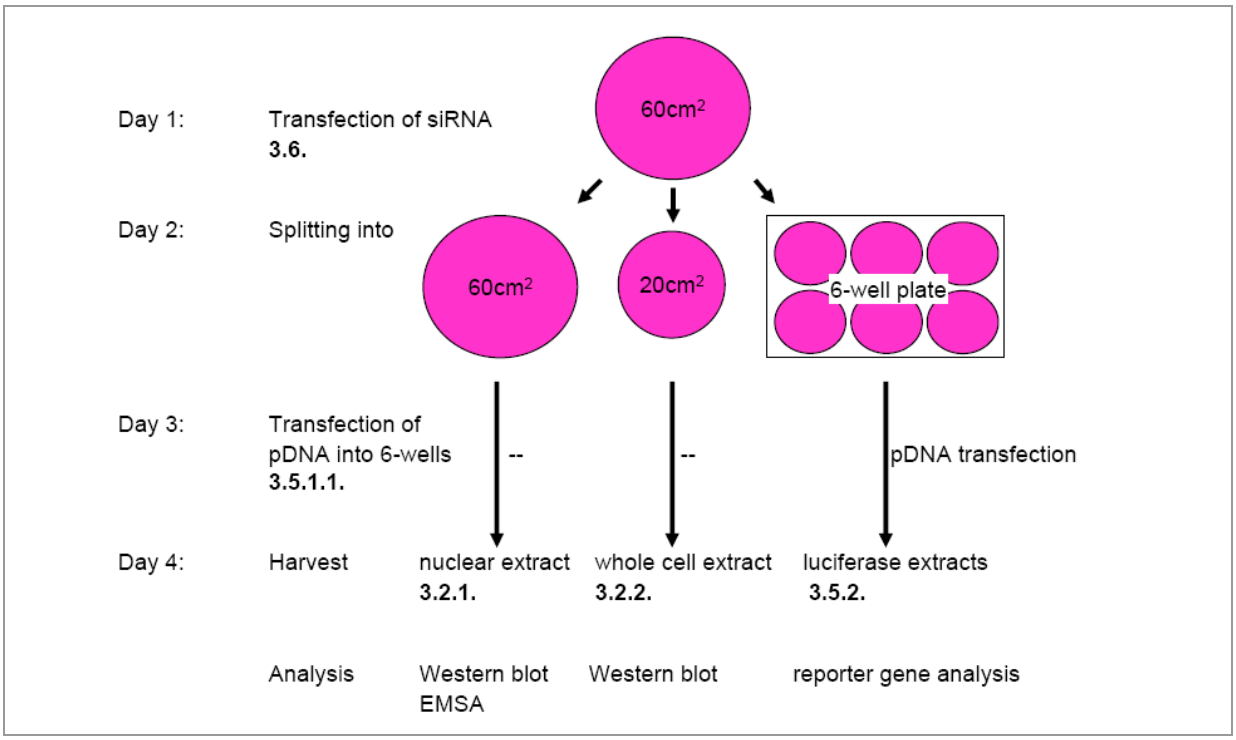

Figure 3-3: Workflow of standard experiment requiring depletion of Drosha and Dicer

3.7. miRNA prediction software analysis

To obtain a comprehensive list of miRNAs that are predicted to regulate c-Jun and Fra-1, prediction software tools were used: TargetScan, PicTar, miRBase and DIANA-microT.

TargetScan classifies its predictions in:
conserved sites for miRNA families broadly conserved among vertebrates
conserved sites for miRNA families conserved only among mammals
poorly conserved sites and sites for poorly conserved miRNA families
Predictions from all three categories were included in the common list.

PicTar was searched by setting the parameters:
“species” to “vertebrate”
“dataset” to “target predictions for all human microRNAs based on conservation in mammals (human, chimp, mouse, rat, dog)”.
All given predictions were included in the common list.

miRBase was searched setting the parameter “genome” to “homo sapiens”.
All given predictions were included in the common list.

DIANA-microT was used setting the “score threshold” to “7.3” which is considered to be a loose criterion and searching in “homo sapiens genome”.
All predictions were included in the common list.

Once the comprehensive list was assembled, the predicted miRNAs were ranked according to the frequency of their respective nomination by the software programs and by the number of the predicted binding sites. The classification was as follows:

4/4	predicted by all 4 search engines
3/4 +double	predicted by 3 search engines with 2 binding sites
3/4	predicted by 3 search engines
2/4 + double	predicted by 2 search engines with 2 binding sites
2/4	predicted by 2 search engines
1/4 + double	predicted by 1 search engine with 2 binding sites

Locations of predicted miRNA binding sites in the 3’UTR are displayed in a table, see **7.2**.

3.8. Illumina miRNA array

The Illumina miRNA array was performed by Dr. Bernhard Korn, Genomics and Proteomis Core Facility, German Cancer Research Center.

3.8.1. RNA analysis

Total RNA was prepared according to **3.3.3** and subsequently checked by gel analysis using the Total RNA Nanochip assay on an Agilent 2100 Bioanalyzer. Only samples with RNA index values greater than 7 were selected for microRNA profiling. RNA concentrations were determined using the NanoDrop spectrophotometer.

3.8.2. Probe labeling and Illumina BeadArray Hybridization

The method is a modification of an assay that was developed for high-throughput gene expression profiling, the DASL® Assay (cDNA-mediated annealing, selection, extension and ligation, (Fan *et al.*, 2004)). The miRNA method similarly targets specific sequences with sets of oligonucleotides that are extended, and then labeled during PCR amplification. If not stated otherwise, 200 ng of total RNA were first polyadenylated using Poly-A Polymerase, incubated

at 37℃ for 60 min, then heat inactivated at 70℃ f or 10 min. The introduced poly A tail was then used as a priming site for cDNA synthesis, incubated at 42℃ for 60 min, then heat inactivated at 70℃ for 10 min. The primer used for cDN A synthesis was biotinylated and contained a universal PCR primer sequence that was used later in the assay. After cDNA synthesis, miRNAs were individually interrogated using specific oligonucleotides. A single miRNA-specific oligo (MSO) is designed against each mature miRNA sequence, which consists of three parts: at the 5′-end is another universal PCR priming site; in the middle is an address sequence used for capturing the product on the array; and at the 3′-end is a miRNA-specific sequence. The second universal PCR priming site is shared among all MSO's, and each address sequence is associated uniquely with each of the 470 miRNA targets (miRBase database v9.1). As controls, central mismatch probes for miRNAs hsa-let-7a, let-7c, let-7f, miR-152 and miR-182, and 3′-end mismatch probes for small nuclear RNAs RNU24 and RNU66 were used. The subsequent assay process and array hybridization were performed as described previously (Fan *et al.*, 2004). Briefly, 15 µl of the cDNA synthesis reaction was added to 5 µl of the multiplexed MSO pool and 30 µl of a reagent containing streptavidin paramagnetic particles, heated to 70℃, and allowed to ann eal to 40℃. All 470 human miRNAs were assayed simultaneously. After binding and washing, the annealed MSOs were extended through the cDNA primer, forming an amplifiable product. The extended oligos were eluted from the streptavidin beads and added to a PCR reaction, in which one of the universal primers was Cy3 labeled and the other universal primer was biotinylated. The PCR products were captured on streptavidin paramagnetic beads, washed and denatured to yield single-stranded fluorescent molecules to hybridize to the arrays. The universal arrays used for fluorescent reporting consist of capture oligos immobilized on beads and randomly assembled onto the ends of fiber optic bundles, which are arranged in a matrix to match a 96-well plate (Sentrix® Array Matrix, Illumina, (Fan *et al.*, 2006)). The identity of each bead is determined before hybridization to the miRNA assay product. Arrays were scanned on the BeadArray Reader, and automatic image registration and intensity extraction software was used to derive intensity data per bead type corresponding to each miRNA (Galinsky, 2003).

3.8.3. Microarray data analysis

The array intensity data were imported into Beadstudio version 3 (Illumina), a software package that permits visualization and normalization of the data. The quantile normalization method for all the analyses reported here was used (Chudin *et al.*, 2006). miRNA expression statuses were assessed by signal intensity and p-values. The threshold was defined as signal intensity ≥ 400 and p-value ≤ 0.01.

4. Results

4.1. Model system: HPV18-positive non-malignant and malignant cell lines

To analyze the impact of miRNAs on the stoichiometry of AP-1 members in HPV-positive cell lines with different phenotypes, an *in vitro* model system was applied. The cell system bases on the fusion of the HPV18-positive cervical carcinoma cell line HeLa with the male fibroblast cell strain GM77, thereby generating HeLa-fibroblast-hybrids, termed “444”. Inoculation into immuno-compromised mice showed that 444 cells are non-malignant (Stanbridge, 1984). However, 444 cells are genetically unstable that leads to segregants upon long-term *in vitro* cultivation. These segregants were referred as “CGL3” and display a tumorigenic phenotype in nude mice (Stanbridge, 1984) (**Fig. 4-1A**). In non-malignant HeLa-fibroblast-hybrids, AP-1 is mainly composed of c-Jun:Fra-1 heterodimers, whereas the malignant counterpart CGL3 is characterized by reduced levels of c-Jun and c-Jun:c-Fos heterodimers (Soto *et al.*, 1999) (**Fig. 4-1B**).

A

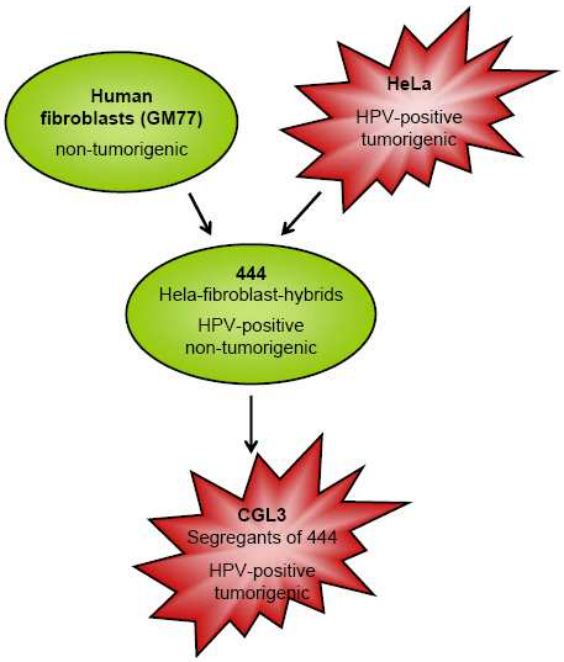

B

	c-Jun	Fra-1	c-Fos
HeLa	++	+	+
444	+++	++	-
CGL3	+	-	++

Figure 4-1: Model system of non-tumorigenic and tumorigenic HPV18-positive cell lines

(**A**) Fusion of the cervical carcinoma cell line HeLa with the male fibroblast cell strain GM77 generated non-tumorigenic HeLa-Fibrobast-Hybrids (“444”). Confluent and enduring cultivation leads to their clonal segregants (“CGL3”), which possess a tumorigenic phenotype (Stanbridge, 1984; Soto *et al.*, 1999). (**B**) AP-1 composition of both cell hybrids and the parental HeLa cells are displayed (Soto *et al.*, 1999)

4.2. Differential expression of AP-1 members upon disruption of the miRNA biogenesis machinery

miRNAs can post-transcriptionally inhibit gene expression by targeting mRNAs. Thus, a widely used strategy to detect such repressed genes is to deplete cells from the miRNA containing effector complexes, miRISC and miRNP. This is achieved by knocking down key components of the miRNA biogenesis machinery or of the effector complexes (Schmitter *et al.*, 2006; Kuehbacher *et al.*, 2007; Lee and Dutta, 2007; Tang *et al.*, 2007). Here, Drosha and Dicer, two miRNA processing enzymes, were knocked down using specific siRNAs against target sequences located in the ORFs (*open reading frame*). Following depletion of Drosha and Dicer, the expression of AP-1 family members was analyzed on mRNA and protein levels in order to decipher possible miRNA-regulated proteins (**Fig. 4-2, 4-3**).

Drosha mRNA (**Fig. 4-2, lane 1**) and protein (**Fig. 4-3**) were steadily down-regulated with nearly 100% efficiency in all three cell lines after 72h post-transfection. Dicer protein was reduced to a lesser extent (**Fig. 4-3**), while Dicer mRNA was re-expressed at normal levels in 444 and CGL3 cells (**Fig. 4-2, lane 2**), compared to control transfections. As exemplified by let-7a Northern blotting in 444 samples (**Fig. 4-4**), the knock-downs of Drosha and Dicer led to a substantial decrease in mature miRNAs. Let-7a was analyzed because it belongs to the let-7 family, let-7a-g and let-7i that is known to regulate Dicer (Tokumaru *et al.*, 2008).

In order to demonstrate functional consequences on endogenous miRNA target genes, the positive control Dicer, which is regulated by the let-7 family (Tokumaru *et al.*, 2008), was analyzed. Upon depletion of Drosha, Dicer was increased on mRNA levels in 444 and CGL3 cells (**Fig. 4-2, lane 2**) and also on protein levels in 444, CGL3 and HeLa cells (**Fig. 4-3**).

Besides the positive control, the transcription factor Oct-1 was unresponsive in all cell lines. Oct-1, also known as POU2F1, is a member of the POU transcription factor family (Phillips and Luisi, 2000). Oct-1 mRNA levels did not change upon Drosha or Dicer down-regulation neither 444 nor CGL3 cells (**Fig. 4-2, lane 3**). Additionally, Oct-1 protein also remained unaltered, as shown in EMSA assays for 444, CGL3 and HeLa cells (see **4.3, Fig. 4-5A**). Therefore, Oct-1 served as a negative control, thereby predefining the threshold levels, where mRNA changes were not considered to be significant. Additionally, Oct-1 proved specificity for the observed effects.

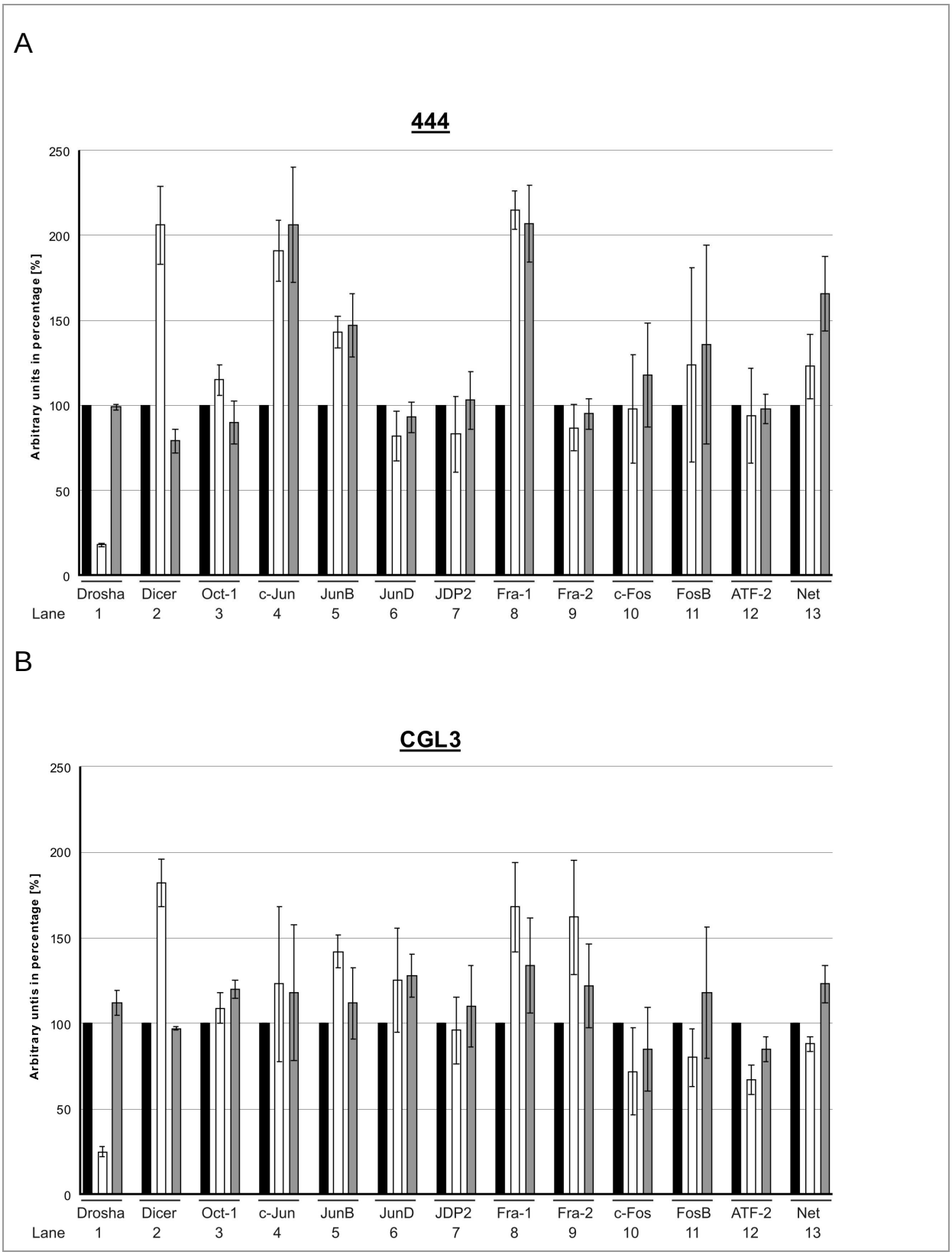

Figure 4-2: Changes in mRNA levels upon disruption of the miRNA pathway

(**A**) 444 and (**B**) CGL3 cells were treated for 72h with siLuciferase (black bars), siDrosha (white bars) and siDicer (grey bars) RNA. qRT-PCRs of the indicated genes were preformed and normalized against GAPDH. Relative increases in signal intensities compared to siLuciferase for each gene were plotted in percentage. Error bars represent s.d. from three independent experiments.

The mRNA analysis of AP-1 family members (**Fig. 4-2**) revealed that c-Jun (**lane 4**) and JunB (**lane 5**) levels were up-regulated in 444, while in CGL3 cells only JunB was up-regulated upon siDrosha treatment. JunD (**lane 6**) and JDP2 (**lane 7**) levels did not change in either cell line. Fra-1 mRNA (**lane 8**) was up-regulated in 444 and to a lesser extent also in CGL3 cells, whereas Fra-2 (**lane 9**) was only increased in CGL3 cells under siDrosha treatment. c-Fos (**lane 10**) and ATF-2 (**lane 12**) were unaltered in 444 cells, and FosB (**lane 11**) was slightly increased. Contrarily, CGL3 cells displayed a slight reduction for c-Fos (**lane 10**) and ATF-2 (**lane 12**) mRNA levels, while FosB was slightly reduced upon depletion of siDrosha and unchanged upon depletion of Dicer. The transcription factor Net (**lane 13**), which is a transcriptional repressor of *c-fos* (van Riggelen *et al.*, 2005), was only up-regulated in the non-tumorigenic cell line 444 upon depletion of Dicer.

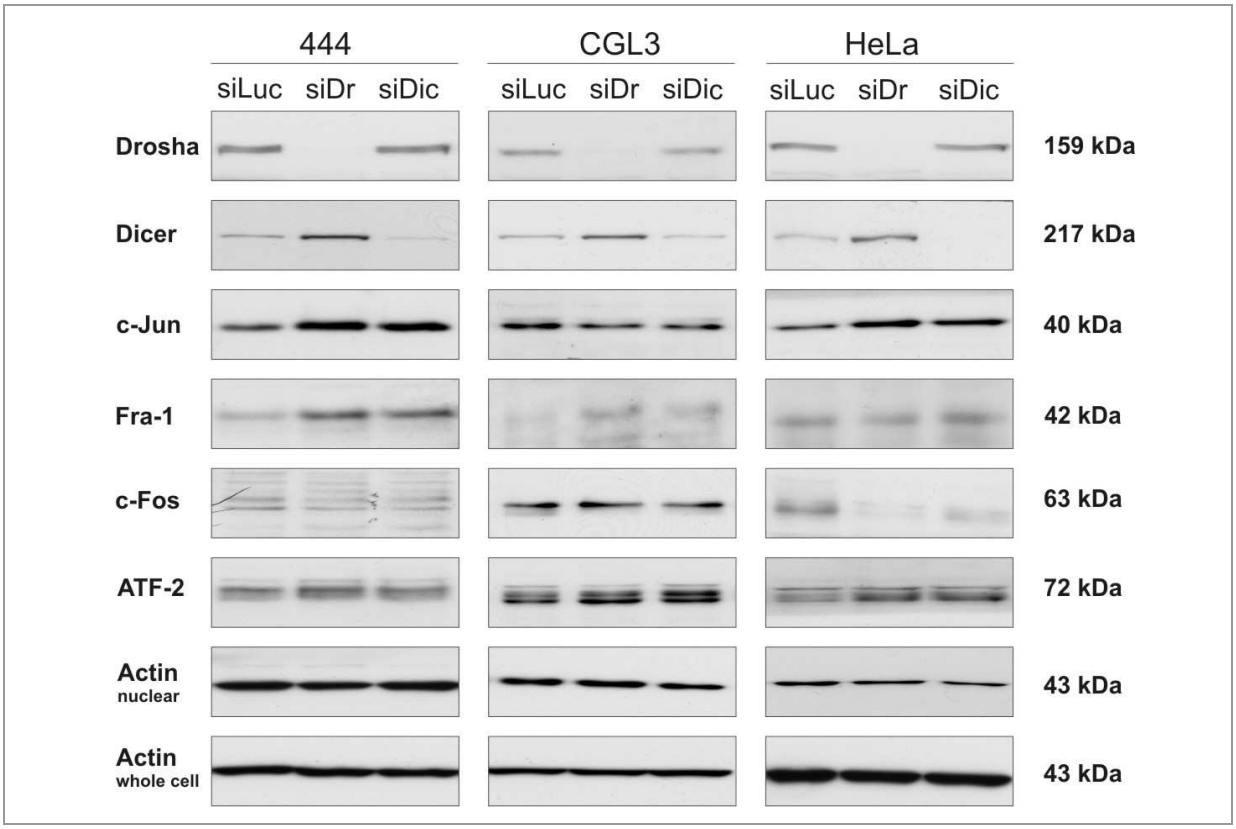

Figure 4-3: Changes in protein levels upon disruption of the miRNA pathway

12-15µg nuclear protein extract of 444, CGL3 and HeLa cells were used for all Western Blots, except 15µg whole cell lysate was used for Dicer. Actin served as a loading control. Sizes in kDa are indicated. Proteins were resolved in 6-10% Polyacrylamid gels, followed by incubation with the indicated primary antibodies. Protein amounts were assessed by chemiluminescence.

Furthermore, protein extracts from the same experiments were also used to analyze AP-1 family members by Western blotting to monitor, whether the observed changes in mRNA also resulted in different protein levels. Additionally, parental tumorigenic HeLa cells were also included in the analysis (**Fig. 4-3**).

c-Jun was up-regulated in 444 and HeLa cells, whereas CGL3 did not show any difference. Fra-1 was up-regulated in 444 and CGL3, whereas it was unchanged in HeLa cells. ATF-2 was unchanged in 444 and CGL3 and slightly increased in HeLa cells. c-Fos did not change in the two hybrid cell lines, while it was reduced in HeLa cells.

Taken together, the mRNA and protein data revealed that a subset of AP-1 members was differentially regulated upon knock-down of the miRNA biogenesis pathway (**Tbl. 4-1**). Concerning the AP-1 proteins c-Jun, Fra-1 and c-Fos, which are important for HPV-transcription in the cell system, the comparative analysis displayed some differences: Fra-1 was up-regulated in 444 and CGL3 cells. c-Jun was increased only in the parental HeLa cells and in the non-tumorigenic hybrids. Contrarily, on mRNA level, CGL3 cells showed a slight reduction of c-Fos, which was, however, largely reduced in HeLa cells on protein levels.

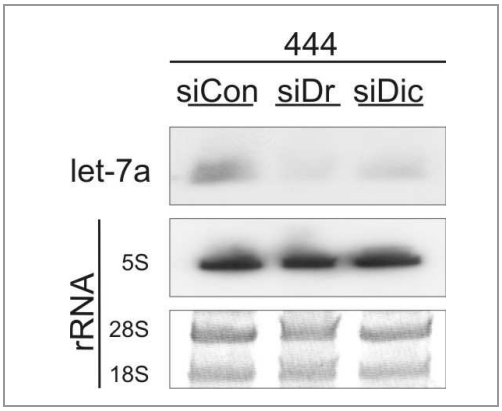

Figure 4-4: Reduction of let-7a upon knockdown of Drosha or Dicer

444 cells were transfected for 72h with si-Control, siDrosha and siDicer RNA. Abundance of mature let-7a was analyzed by Northern blotting of 20µg total RNA. RNA quality was monitored by polyacrylamide gel electrophoresis; 5S, 18S, 28S ribosomal RNA were used as loading controls.

	HeLa	444	CGL3
c-Jun	+	+	0
Fra-1	0	+	+
c-Fos	-	0	0
ATF-2	+	0	0

Table 4-1: AP-1 members are differentially modulated upon knockdown of Drosha or Dicer

The table gives a summary on modulated levels of AP-1 family members, which are confirmed by Western blotting, upon knock-down of Drosha and Dicer. +, increased; 0, unchanged; -, decreased levels.

4.3. Modulation of AP-1 composition upon disruption of the miRNA pathway

Having shown that Drosha / Dicer knock-down affected c-Jun, Fra-1 and c-Fos levels, the possible consequences for amount, composition and activity of AP-1 dimers were studied. To address the question if the abundance of functional AP-1 dimers was altered, electro-mobility-shift-assays (EMSA) were employed (**Fig. 4-5A**). In 444 cells, an enhanced binding of AP-1 to its consensus sequence after Drosha and Dicer knock-down was observed, whereas CGL3 and HeLa cells did not show this effect. The negative control Oct-1 remained unaltered in all three cell lines. The slight up-regulation of sample 444 siDr was not considered to be significant.

Additionally, the composition of AP-1 dimers was monitored by EMSA with super shifting antibodies (**Fig. 4-5B,C,D**). In 444 cells, the supershift showed that the enhanced AP-1 binding is mediated by increased dimerization between c-Jun:c-Jun homodimers c-Jun:Fra-1 heterodimers (**Fig. 4-5B**). c-Fos incorporation did not change, as expected. In CGL3 cells, however, the increase of Fra-1 protein (**Fig. 4-3**) did not result in an enhanced incorporation into the AP-1 complex (**Fig.4-5C**). Additionally, c-Jun and c-Fos proteins in the AP-1 complex were not altered, as expected from unchanged protein levels. In HeLa cells, the incorporation of Fra-1 was not altered (**Fig. 4-5D**), while c-Jun was up-regulated. c-Fos, however, was reduced, reflecting down-regulation of c-Fos protein as shown by Western blotting (**Fig. 4-3**).

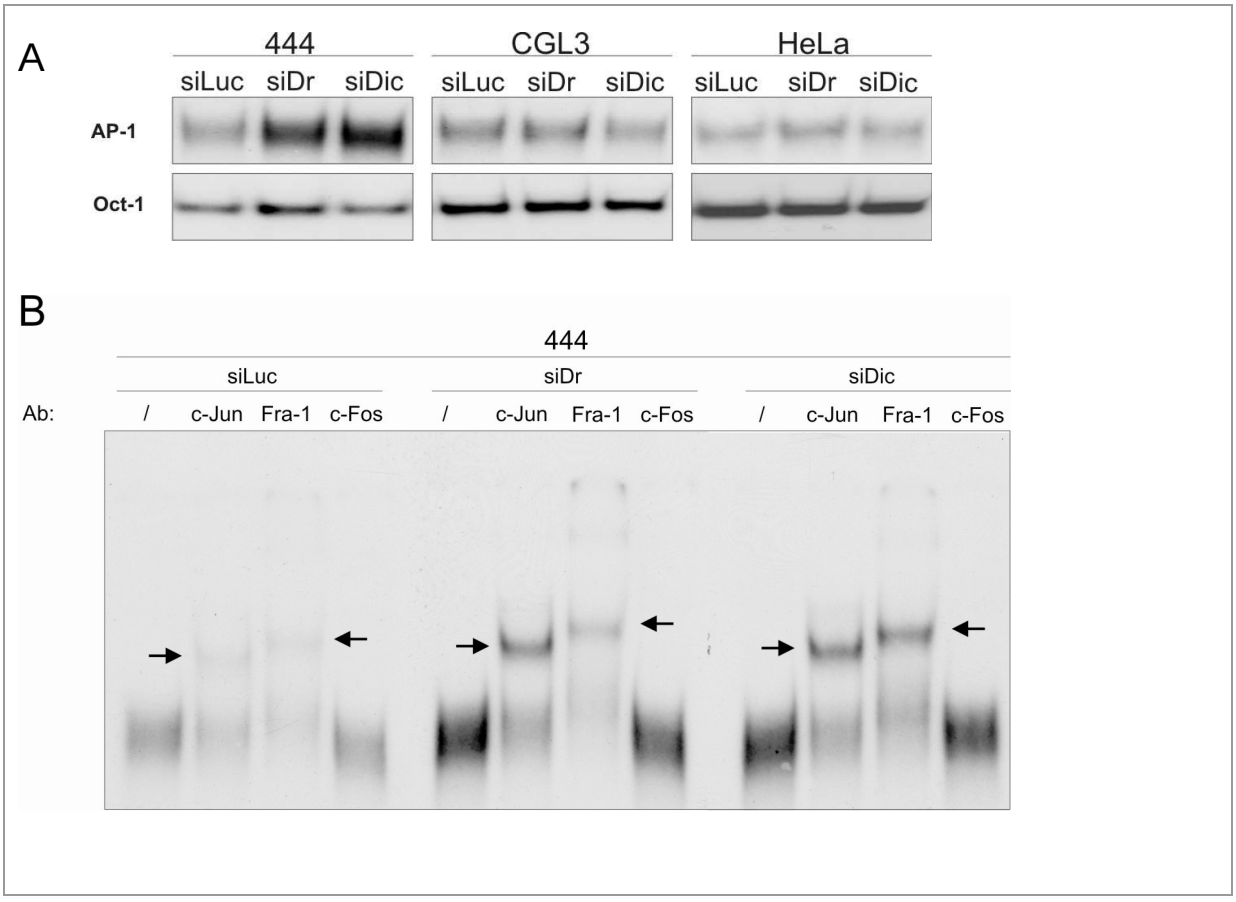

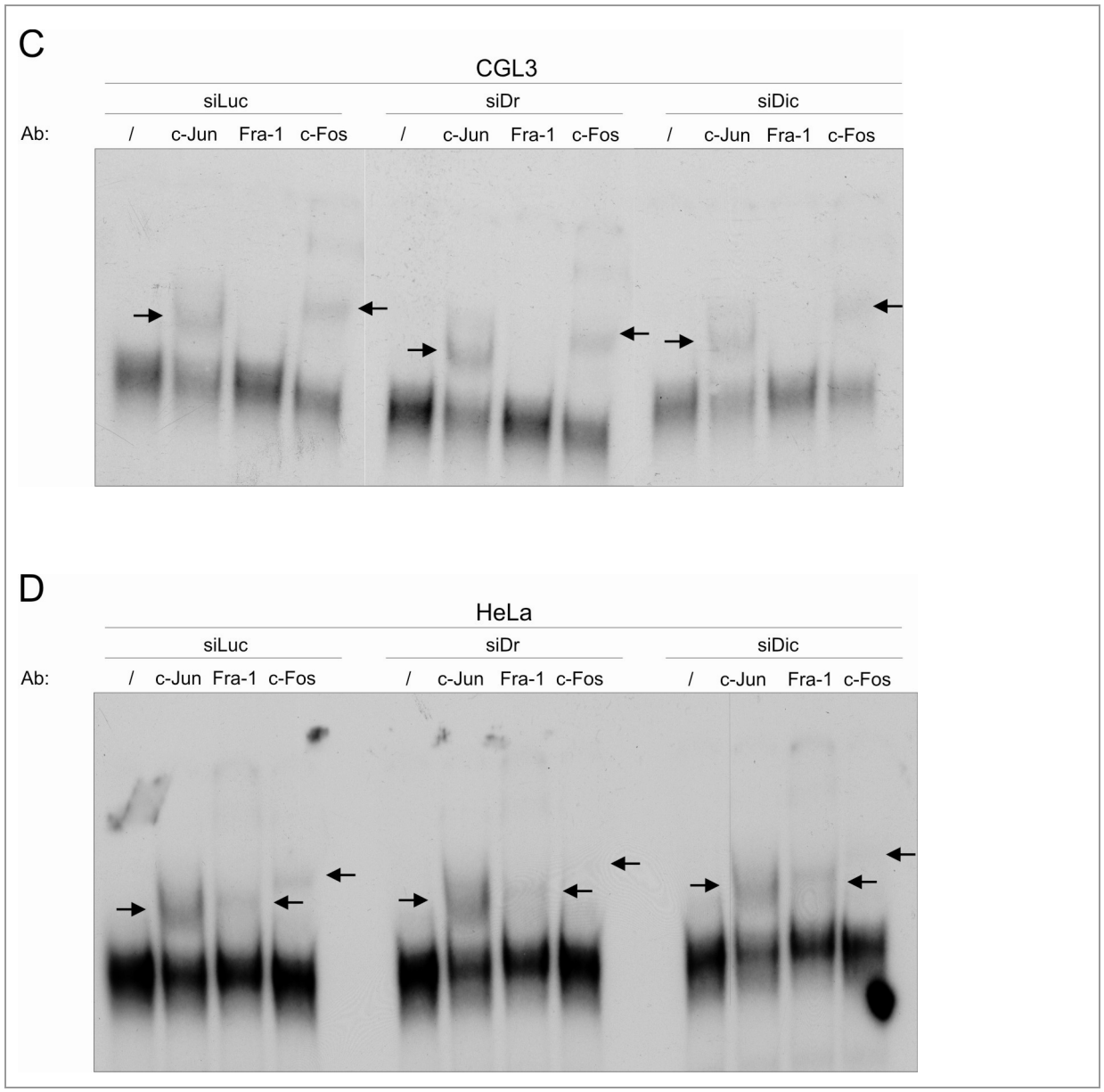

Figure 4-5: Changes in AP-1 levels and composition upon disruption of the miRNA pathway

AP-1 binding and composition were analyzed by EMSA (**A**) "shift-" and (**B,C,D**) "super-shift-" analysis. 2µg nuclear extracts from figure 4-3 were incubated with 10,000 cpm ^{32}P-radiolabeled AP-1 / Oct-1 consensus sequence. For super-shift reactions, 2µg antibody against p-c-Jun, Fra-1 or c-Fos were added. The analysis was performed in 5.5% native polyacrylamid gels, followed by autoradiography.

4.4. Changes in AP-1 activity upon disruption of the miRNA biogenesis machinery

To answer the question, if differential AP-1 binding in EMSAs upon depletion of Drosha and Dicer (**Fig. 4-5A**) affects the transcriptional activity of AP-1, the reporter plasmid pAP-1 was used. In this vector, the expression of *Firefly* luciferase is controlled by five AP-1 consensus sequences, also termed "TRE"-sites (*TPA (12-O-tetradecanoylphorbol-13-acetate) responsive element*) (Tseng and Verma, 1995), that are fused to a core promoter only containing a TATA box.

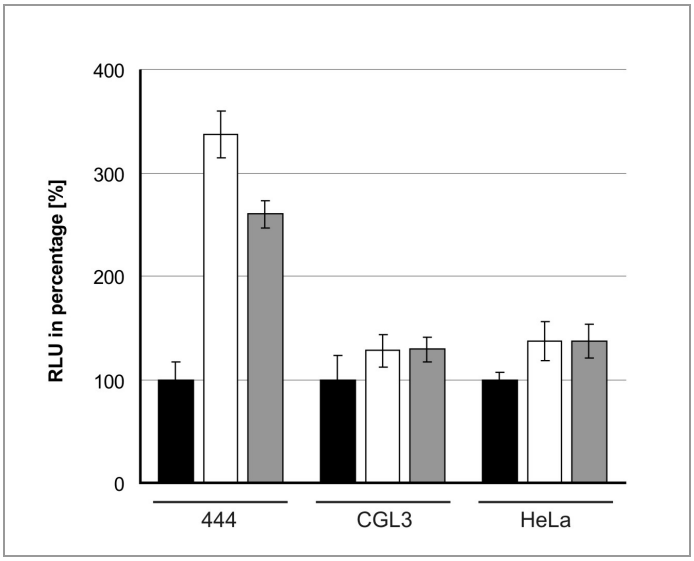

Figure 4-6: Higher AP-1 activity in 444 upon disruption of the miRNA pathway

444, CGL3 and HeLa cells were transfected for 72h with siControl (black bars), siDrosha (white bars) and siDicer (grey bars) RNA. 24h prior to harvest, an AP-1 responsive reporter plasmid, pAP-1 *Firefly*-luciferase, and a control plasmid, pRL-*Renilla*-luciferase, were transfected. Relative increases in signal intensities compared to siControl were plotted in percentage. Error bars represent s.d. from 4 replicates.

444 cells showed an about 3-fold increased expression of *Firefly* luciferase after knock-down of Drosha and Dicer. CGL3 and HeLa cells, however, did not show enhanced AP-1 transcriptional activity under either treatment (**Fig. 4-6**).

These results indicate that the transcriptional activity of AP-1 is selectively modulated by miRNAs in 444 cells, but not in CGL3 and HeLa cells, through a direct or an indirect effect.

4.5. c-Jun, Fra-1 and Net are direct targets of miRNAs

Previous experiments have shown that AP-1 members are differentially and selectively modulated by miRNAs in the non-malignant cell lines 444 and in the malignant cell lines CGL3 and HeLa. However, the question, whether the modulation was achieved through a direct or an indirect effect, has not been addressed. A commonly used approach is the cloning of the full-length 3'UTR (*untranslated region*) of the respective gene behind a luciferase reporter gene in order to generate a Luciferase-target gene 3'UTR fusion transcript (Garzon *et al.*, 2006; Lee *et al.*, 2006; Schultz *et al.*, 2008; Tay *et al.*, 2008). Direct interactions of miRNAs

and putative target genes are assessed by luciferase assays based on selective degradation or translational repression of Luciferase-target gene 3'UTR fusion transcripts.

The most comprehensive data encompassing results on mRNA, protein and biological functionality were obtained for c-Jun and Fra-1. In addition, besides c-Fos, both proteins constitute the important AP-1 family members regulating HPV-transcription. Therefore, further analysis focused on c-Jun and Fra-1. Additionally, Net, the transcriptional repressor of c-Fos (van Riggelen *et al.*, 2005), was also further examined, since Net showed differential regulation in the non-malignant and malignant hybrids (**Fig. 4-2**).

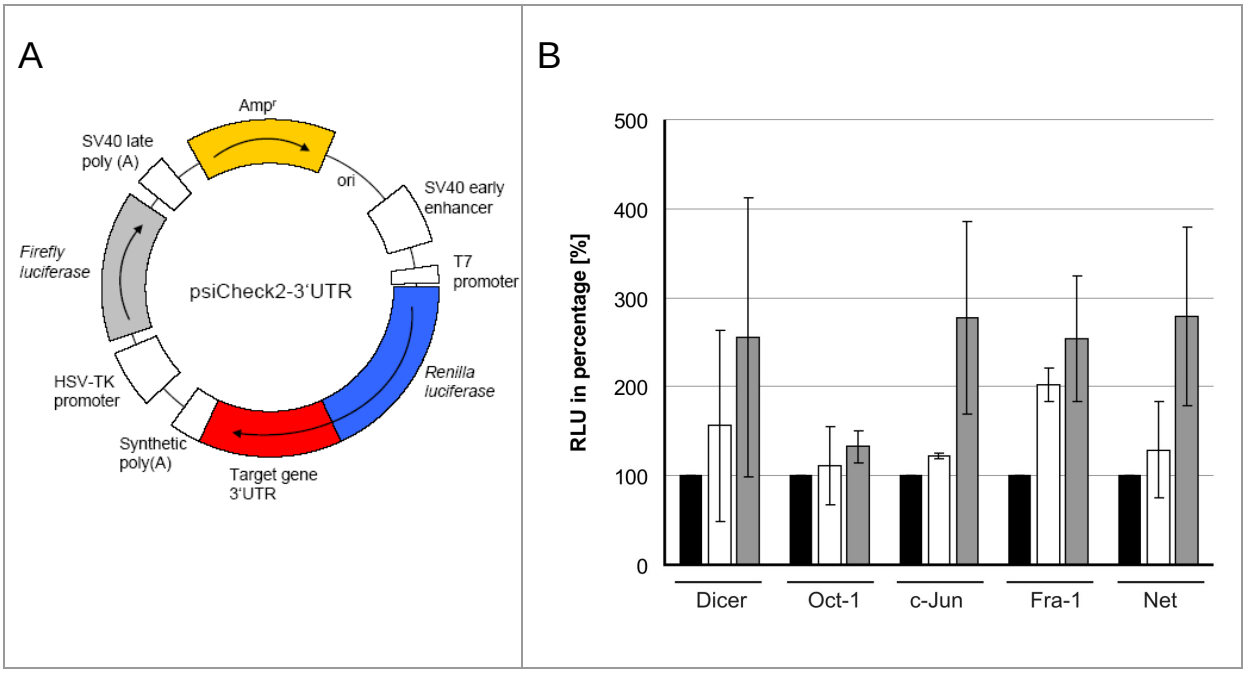

Figure 4-7: c-Jun-, Fra-1- and Net-3'UTR reporter genes are responsive to miRNA regulation

(**A**) Full-length 3'UTRs of Dicer, Oct-1, c-Jun, Fra-1 and Net were cloned into psiCHECK2 to give rise to a fusion transcript of *Renilla*-target gene 3'UTR; the internal *Firefly*-luciferase gene served as a normalization control. (**B**) 444 cells were transfected for 72h with siControl (black bars), siDrosha (white bars) and siDicer (grey bars) RNA. 24h prior to harvest, the respective psiCHECK2-3'UTR plasmid was transfected. Values were normalized against the empty plasmid. Relative increases in signal intensities compared to siControl for each gene were plotted in percentage. Error bars represent s.d. from 3 independent experiments.

The full-length 3'UTRs of c-Jun, Fra-1, Net, Dicer (positive control) and Oct-1 (negative control) were cloned downstream of *Renilla* luciferase. The assay was done in 444 cells that had already shown the up-regulation of c-Jun, Fra-1 and Net at mRNA and / or protein levels (**Fig. 4-2, 4-3**) after knock-down of Drosha and Dicer. Depletion of Drosha led to a ~1.5 fold and depletion of Dicer to a ~2.5 fold increased activity of the reporter gene *Renilla*-Dicer 3'UTR, as expected for the positive control. The negative control *Renilla*-Oct-1 3'UTR showed only marginal effects (**Fig. 4-7**). The activities of *Renilla*-c-Jun 3'UTR and *Renilla*-Net 3'UTR

were only significantly increased upon knock-down of Dicer, whereas the activity of *Renilla*-Fra-1 3'UTR was augmented under both treatments.

Taken together, these results demonstrated that c-Jun, Fra-1 and Net are directly regulated by miRNAs in non-malignant 444 cells.

4.6. Identification of putative miRNAs regulating c-Jun and Fra-1

In order to identify the miRNAs that regulate c-Jun and Fra-1, a bioinformatics approach was conducted by using the prediction software tools miRBase (Enright *et al.*, 2003), TargetScan (Lewis *et al.*, 2005; Grimson *et al.*, 2007; Friedman *et al.*, 2009), DIANA microT (Maragkakis *et al.*, 2009) and PicTar (Krek *et al.*, 2005; Lall *et al.*, 2006). Thereby, TargetScan bases its predictions on the presence of conserved 8mer and 7mer sites within 3'UTRs that match the seed region, nucleotides 2-7 from the 5' end, of each miRNA (Lewis *et al.*, 2005). PicTar calculates "binding scores" according to sequence conservation of the 3'UTRs and to optimal free energies that result from binding with the seed region and from additional hybridizations in the middle or at the 3' end of the miRNA (Krek *et al.*, 2005). DIANA microT takes into account sequence conservation for up to 27 species of the MRE (*miRNA recognition element*), which is the seed sequence that is allowed to be of 6 to 9 nucleotides of length. Additional binding via the 3' end of the miRNA is also considered (Maragkakis *et al.*, 2009). miRBase predictions rely on the presence of a conserved seed sequence, for which up to 37 genomes are analyzed, and on the estimated accessibility via RNA folding and thermodynamic stability (Enright *et al.*, 2003; Griffiths-Jones *et al.*, 2006; Griffiths-Jones *et al.*, 2008).

Putative miRNAs were classified according to the frequency of predictions and according to the number of predicted binding sites within the respective 3'UTR. For c-Jun, miR-139-5p, -340, -495, -200b, -32 and -522 are the most likely candidates (**Tbl. 4-2A**). For Fra-1, miR-34a, -449a, - 19a, -22, -34c-5p, -138, -149 and -593 are the most likely candidates (**Tbl. 4-2B**). Due to the high number of predicted miRNAs, the 3'UTRs of c-Jun and Fra-1 were dissected. Single segments were used in the luciferase reporter system to identify the responsible segments that harbor the miRNA binding sites and to decrease the number of predicted miRNAs (**Tbl. 4-3**). Luciferase assays were conducted in 444 cells that showed the repressive effect of miRNAs for both proteins. Although abrogation of Drosha and Dicer led to increased levels of c-Jun mRNA (**Fig. 4-2**) and protein (**Fig. 4-3**), only depletion of Dicer gave clear results in the luciferase assay for unknown reasons (**Fig. 4-7**). For Fra-1, both treatments led to equal effects in the luciferase assay (**Fig. 4-7**); therefore 444 cells were depleted from Drosha to analyze Fra-1 segments and from Dicer to analyze c-Jun segments.

For all segments of c-Jun and Fra-1, the relative increases compared to control transfections exceeded the relative increases of the full-length 3'UTR reporter constructs, which served as positive controls (**Fig. 4-8**). Fra-1 segment 3 was the only exception that showed a similar increase compared to the Fra-1 full-length 3'UTR construct. Thus, the assays revealed that every segment of the 3'UTRs of c-Jun and Fra-1 harbors at least one miRNA binding site. Therefore, the number of putative miRNAs, which potentially regulate c-Jun and Fra-1, could not be reduced.

A

classification of predicted miRNAs targeting c-Jun

4/4	3/4 + double	3/4	2/4 + double	2/4	1/4 + double
	hsa-miR-139-5p	hsa-miR-200b	hsa-miR-32	hsa-miR-92a	hsa-miR-362-5p
	hsa-miR-340		hsa-miR-522	hsa-miR-92b	hsa-miR-501-5p
	hsa-miR-495			hsa-miR-141	hsa-miR-637
				hsa-miR-200a	
				hsa-miR-200c	
				hsa-miR-429	
				hsa-miR-517c	
				hsa-miR-520d-5p	
				hsa-miR-524-5p	
				hsa-miR-612	
				hsa-miR-642	
				hsa-miR-891b	

B

classification of predicted miRNAs targeting Fra-1

4/4	3/4 + double	3/4	2/4 + double	2/4	1/4 + double
	hsa-miR-34a	hsa-miR-19a	hsa-miR-22	hsa-miR-15a	hsa-miR-449b
	hsa-miR-449a		hsa-miR-34c-5p	hsa-miR-15b	
			hsa-miR-138	hsa-miR-16	
			hsa-miR-149	hsa-miR-19b	
			hsa-miR-593	hsa-miR-130a	
				hsa-miR-195	
				hsa-miR-296-3p	
				hsa-miR-299-3p	
				hsa-miR-338-5p	
				hsa-miR-513a-5p	
				hsa-miR-520a-5p	
				hsa-miR-525-5p	
				hsa-miR-566	
				hsa-miR-568	
				hsa-miR-571	
				hsa-miR-646	

Table 4-2: Bioinformatics analysis of c-Jun and Fra-1 for putative, regulatory miRNAs

The prediction engines miRBase, TargetScan, PicTar and DIANA microT were searched for miRNAs that potentially regulate (**A**) c-Jun and (**B**) Fra-1. Predicted miRNAs were clustered according to the frequency of citation: (4/4) predicted by 4 out of 4 search engines, (3/4 + double) predicted by 3 out of 4 search engines with at least two binding sites, (3/4) predicted by 3 out of 4 search engines, (2/4 + double) predicted by 2 out of 4 search engines with at least two binding sites, (2/4) predicted by 2 out of 4 search engines, (1/4 + double) predicted by 1 out of 4 search engines with at least two binding sites. hsa-miR, *homo sapiens* miRNA

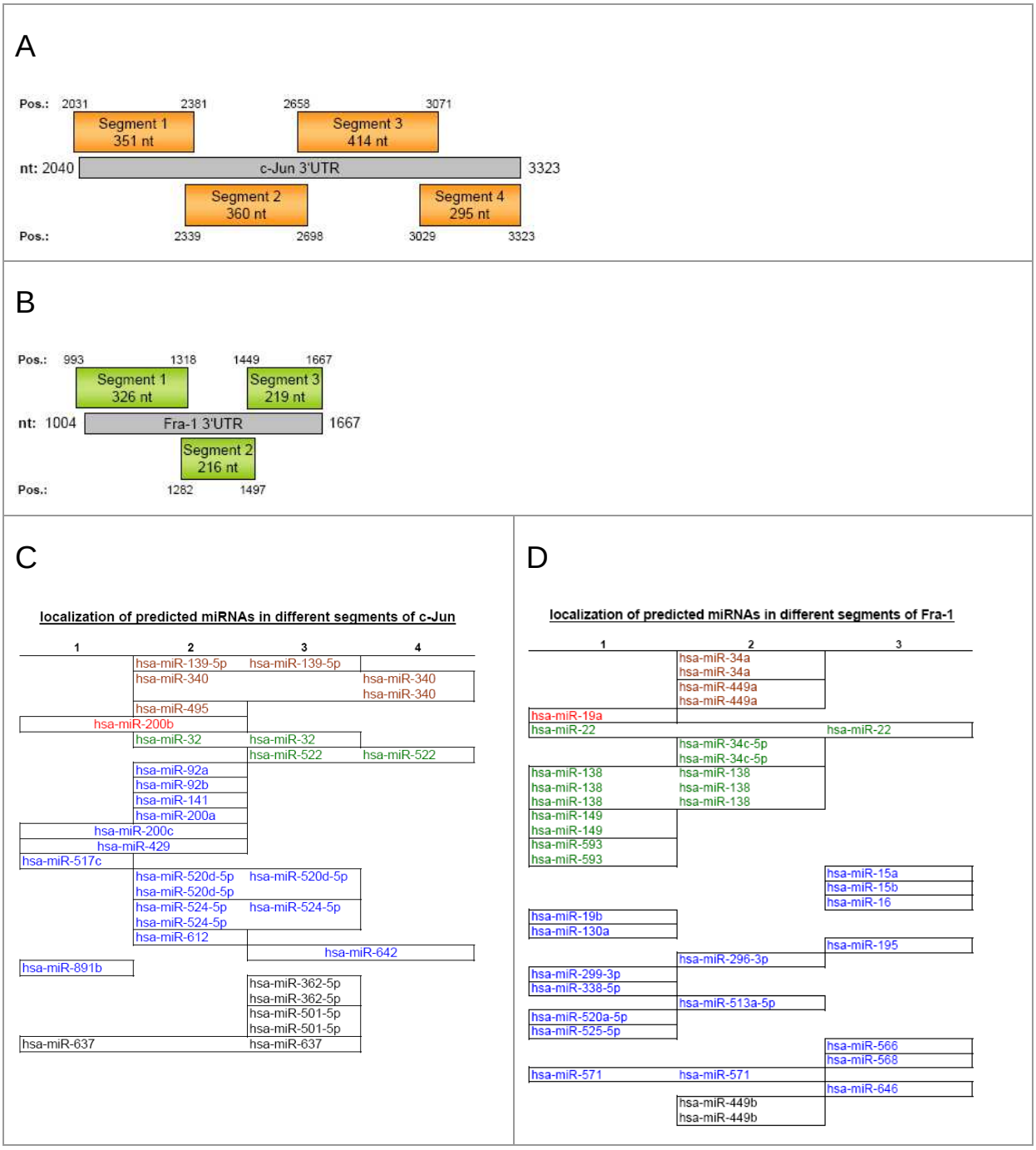

Table 4-3: Location of predicted miRNAs within the 3'UTRs of c-Jun and Fra-1

c-Jun and Fra-1 3'UTRs were divided into (**A**) four segments for c-Jun and (**B**) three segments for Fra-1. Positions (Pos.) indicate start and end of each segment; total length of each segment is displayed. All segments were overlapping with neighboring segments with ~40bp. First segments started within CDS. For detailed sequence alignments see chapter **7.2**.

Predicted miRNAs from table 4-2 were localized within (**C**) the four segments of c-Jun 3'UTR and within (**D**) the three segments of Fra-1 3'UTR.

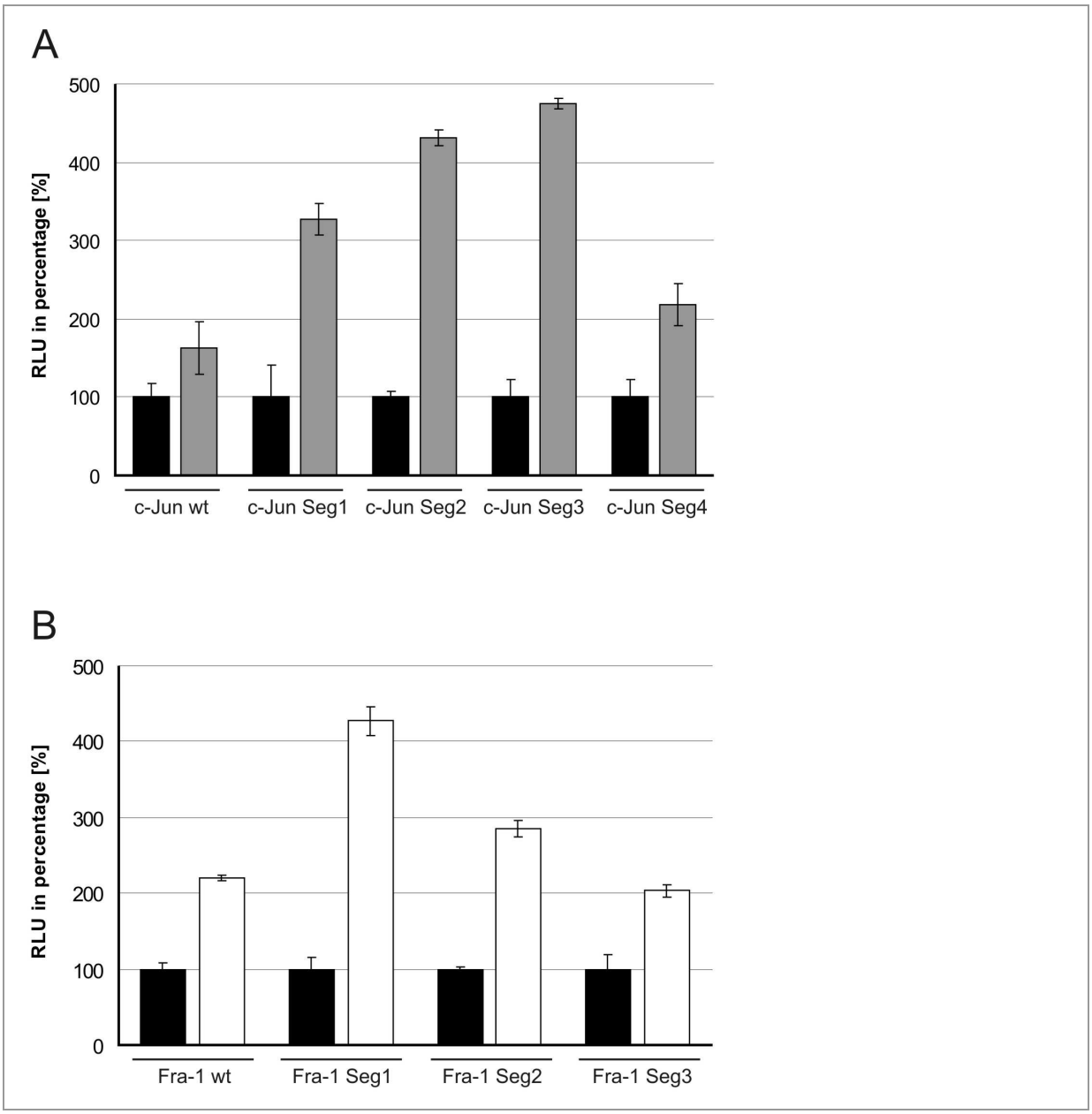

Figure 4-8: All 3'UTR segments of c-Jun and Fra-1 are responsive to miRNA-mediated regulation

Full-length 3'UTRs of c-Jun and Fra-1 were dissected and cloned into psiCHECK2 to give rise to a fusion transcript of *Renilla*-3'UTR segment; the internal *Firefly*-luciferase gene served as a normalization control. c-Jun 3'UTR was divided into 4 segments, Fra-1 3'UTR into 3 segments.

444 cells were transfected for 72h with siControl (black bars), siDrosha (white bars) or siDicer (grey bars) RNA. 24h prior to harvest, the respective psiCHECK2-3'UTR plasmid was transfected. Values were normalized against the empty plasmid. Relative increases in signal intensities compared to siControl for (**A**) c-Jun 3'UTR segments and (**B**) Fra-1 3'UTR segments were plotted in percentage. Error bars represent s.d. from 4 replicates.

4.7. miRNA expression array of 444 and CGL3 cells

Previous analysis revealed a comprehensive list of candidate miRNAs presumably regulating c-Jun and Fra-1. In order to minimize the number of candidates, miRNAs that were not expressed in the cell system were not considered for further analysis.

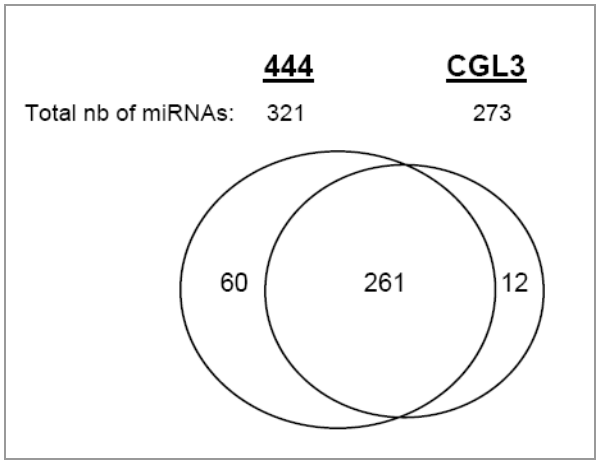

Figure 4-9: The miRNome of 444 and CGL3 cells partially overlaps

An "Illumina" miRNA expression array for 444 and CGL3 cells reveals the number of totally expressed miRNAs that are partial equally or partial uniquely expressed in each cell hybride. A miRNA was considered to be expressed, if p-value ≤ 0.01 and signal intensity ≥ 400, and considered to be differentially expressed, when changes were at least +/- 1.5 fold.

A miRNA expression profile with 470 miRNAs was performed using 444 and CGL3 cells. The threshold for a reliable miRNA expression was defined as p-value ≤ 0.01 and signal intensity ≥ 400, which was not a strict criterion, since signal intensities ranged from 200 to 35,000. A miRNA was considered to be differentially expressed, when there were at least +/- 1.5 fold changes of signal intensities of CGL3 compared to 444 cells. The array displayed general differences between the two cell hybrids, with 275 expressed miRNAs in 444 and 252 expressed miRNAs in CGL3 cells, of which 229 miRNAs were commonly expressed in both cell hybrids (**Fig. 4-9**). From the 229 commonly expressed miRNAs, in CGL3 cells, 99 miRNAs were up-regulated and 15 miRNAs were down-regulated compared to 444 cells, whereas 115 miRNAs were expressed in comparable amounts.

With respect to c-Jun that is regulated by miRNAs in 444 cells, only a miRNA, which is expressed in 444, but not in CGL3 cells, might be responsible for the regulation, since it was shown that c-Jun remained unaltered upon disruption of the miRNA pathway in CGL3 cells (**Fig. 4-3**). In this study, miR-495 was the only miRNA that was not expressed in the tumorigenic cell line CGL3 (**Tbl. 4-4**). Fra-1 was equally up-regulated in both cell lines after knockdown of the miRNA biogenesis pathway (**Fig. 4-3**); therefore, the reasoning is different. A single miRNA that is expressed in both cell lines could repress Fra-1. Furthermore, if a set of miRNAs target Fra-1, the combination of miRNAs might differ in number and in contribution, respectively. For Fra-1, these criteria are fulfilled by a subgroup of candidate miRNAs that is still numerous (**Tbl. 4-4**). On the basis of these assumptions, further experiments focused on c-Jun, in order to identify a regulatory miRNA.

A

	candidate miRNAs	444 signal	444 p-value	CGL3 signal	CGL3 p-value
c-Jun	miR-32	2893	0,0000	5629	0,0000
	miR-92a	20510	0,0000	23450	0,0000
	miR-92b	4505	0,0000	6500	0,0000
	miR-139-5p	298	0,0057	454	0,0000
	miR-141	1535	0,0000	5344	0,0000
	miR-200a	316	0,0003	265	0,3475
	miR-200b	426	0,0000	430	0,0000
	miR-200c	1624	0,0000	7211	0,0000
	miR-340	1247	0,0000	1427	0,0000
	miR-362-5p	1172	0,0000	2319	0,0000
	miR-429	30981	0,0000	31763	0,0000
	miR-495	4945	0,0000	327	0,0193
	miR-501-5p	486	0,0000	1022	0,0000
	miR-517c	628	0,0000	1083	0,0000
	miR-520d-5p	249	0,3064	241	0,5913
	miR-522	284	0,0268	414	0,0000
	miR-524-5p	227	0,7194	238	0,6487
	miR-612	390	0,0000	359	0,0018
	miR-637	214	0,8784	223	0,7922
	miR-642	258	0,2212	277	0,2287
	miR-891b	not anal.		not anal.	
Fra-1	miR-15a	26434	0,0000	26466	0,0000
	miR-15b	21446	0,0000	22358	0,0000
	miR-16	27678	0,0000	26276	0,0000
	miR-19a	13897	0,0000	19194	0,0000
	miR-19b	27824	0,0000	29666	0,0000
	miR-22	16810	0,0000	18287	0,0000
	miR-34a	3066	0,0000	3511	0,0000
	miR-34c-5p	307	0,0020	370	0,0010
	miR-130a	31547	0,0000	30008	0,0000
	miR-138	2158	0,0000	1544	0,0000
	miR-149	1504	0,0000	2067	0,0000
	miR-195	1223	0,0000	629	0,0000
	miR-296-3p	not anal.		not anal.	
	miR-299-3p	1791	0,0000	250	0,5249
	miR-338-5p	not anal.		not anal.	
	miR-449a	2329	0,0000	5426	0,0000
	miR-513a-5p	212	0,8906	215	0,8490
	miR-593	256	0,2409	263	0,3824
	miR-520a-5p	267	0,0952	281	0,2465
	miR-525-5p	571	0,0000	880	0,0000
	miR-566	454	0,0000	693	0,0000
	miR-568	331	0,0000	353	0,0028
	miR-571	311	0,0009	341	0,0080
	miR-646	283	0,0300	301	0,0902
	let-7a	32452	0,0000	31763	0,0000
	miR-7	7071	0,0000	12830	0,0000
	miR-101	27087	0,0000	27908	0,0000

B

	candidate miRNAs	444 signal	444 p-value	CGL3 signal	CGL3 p-value
c-Jun	miR-32	2893	0,0000	5629	0,0000
	miR-92a	20510	0,0000	23450	0,0000
	miR-92b	4505	0,0000	6500	0,0000
	miR-141	1535	0,0000	5344	0,0000
	miR-200b	426	0,0000	430	0,0000
	miR-200c	1624	0,0000	7211	0,0000
	miR-340	1247	0,0000	1427	0,0000
	miR-362-5p	1172	0,0000	2319	0,0000
	miR-429	30981	0,0000	31763	0,0000
	miR-495	4945	0,0000	327	0,0193
	miR-517c	628	0,0000	1083	0,0000
	miR-891b	not anal.		not anal.	
Fra-1	miR-15a	26434	0,0000	26466	0,0000
	miR-15b	21446	0,0000	22358	0,0000
	miR-16	27678	0,0000	26276	0,0000
	miR-19a	13897	0,0000	19194	0,0000
	miR-19b	27824	0,0000	29666	0,0000
	miR-22	16810	0,0000	18287	0,0000
	miR-34a	3066	0,0000	3511	0,0000
	miR-130a	31547	0,0000	30008	0,0000
	miR-138	2158	0,0000	1544	0,0000
	miR-149	1504	0,0000	2067	0,0000
	miR-195	1223	0,0000	629	0,0000
	miR-296-3p	not anal.		not anal.	
	miR-299-3p	1791	0,0000	250	0,5249
	miR-338-5p	not anal.		not anal.	
	miR-449a	2329	0,0000	5426	0,0000
	miR-525-5p	571	0,0000	880	0,0000
	miR-566	454	0,0000	693	0,0000
	let-7a	32452	0,0000	31763	0,0000
	miR-7	7071	0,0000	12830	0,0000
	miR-101	27087	0,0000	27908	0,0000

Table 4-4: miR-495 is the only differentially expressed miRNA putatively regulating c-Jun

An “Illumina” miRNA expression array for 444 and CGL3 cells displays the signal intensities for putative, regulatory miRNAs of c-Jun and Fra-1. (**A**) Read-outs for all candidate miRNAs are shown, (**B**) read-outs for candidate miRNAs are shown that are above the threshold. The threshold was defined as p-value ≤ 0.01 and signal intensity ≥ 400; not anal. = not analyzed (not included in the array).

4.8. Detailed analysis of predicted regulatory miRNAs of c-Jun

The analysis of the miRNA expression array for the most probable candidates possibly regulating c-Jun showed that miR-495 was differentially expressed in 444 and CGL3 cells (**Tbl. 4-4**). In order to confirm the data from the miRNA profiling, the expression of mature miRNAs was indirectly confirmed by expression analysis of miRNA precursor forms, primary miRNA and precursor miRNA, by semi-quantitative RT-PCR. The absence of a precursor form excludes the presence of a mature miRNA, but not vice versa as discussed in **5.6**. Besides miR-495, other predicted miRNAs for c-Jun segment 2 were investigated: miR-32, miR-92a and miR-340. Let-7a served as a positive control. RT-PCR analysis showed that, of all analyzed miRNAs, miR-495 was the only miRNA which was selectively expressed in 444 cells (**Fig. 4-10**). This confirmed the data from the expression array indicating that let-7a, miR-32, -92a and -340 are expressed in both cell hybrids, whereas miR-495 is only expressed in the non-tumorigenic cell hybrids (**Tbl. 4-4**).

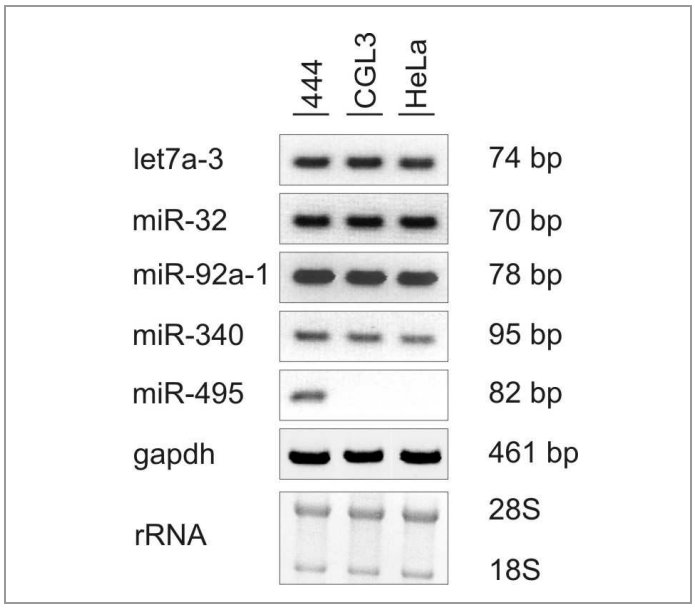

Figure 4-10: miR-495 is only expressed in 444 cells

Expression of primary- and precursor miRNAs in 444, CGL3 and HeLa cells were analyzed by semi-quantitative RT-PCR. RNA quality was monitored by agarose gel electrophoresis; gapdh served as a control. 28S and 18S ribosomal RNAs and sizes in bp are indicated.

Furthermore, the 3'UTRs of c-Jun of 444 and CGL3 cells were sequenced to exclude sequence variations that could influence miRNA binding sites. SNPs (*single nucleotide polymorphisms*) at the genomic level would be transcribed into an altered mRNA sequence and could abolish or generate miRNA binding sites (Clop *et al.*, 2006; Saunders *et al.*, 2007; Chen *et al.*, 2008). Sequences were identical apart from a point mutation (G→T) and a deletion of a G, which were both identified in segment 1 (**Fig 4-11**). However, these sequence variations do not overlap with predicted miRNA binding sites, and hence do presumably not abrogate miRNA-mediated repression. Whether these mutations generated new miRNA binding sites, was not investigated.

In conjunction with the high score of miR-495 in the bioinformatics prediction analysis and the opposing observations of the regulatory effect on c-Jun by miRNAs and the selective expression of miR-495 in 444 cells, miR-495 was a promising candidate to regulate c-Jun.

Figure 4-11: Two point mutations in c-Jun 3'UTR of CGL3 compared to 444 cells

Sequencing of the full-length 3'UTRs of c-Jun from 444 and CGL3 cells reveals one point mutation (G→T) and one deletion (G) in CGL3 compared to 444. Mutations are localized in segment 1 (**Tbl. 4-3C**). The alignment of the first 360nt of c-Jun 3'UTR (total length 1284nt) is shown.

4.9. Overexpression of miR-495 does not repress *Renilla*-cJun 3'UTR reporter gene activity

The broad analysis of several miRNAs, which were predicted to regulate c-Jun, pointed to miR-495. In order to test, whether miR-495 does repress c-Jun, "miRIDIAN Mimic" miR-495 was co-transfected with the *Renilla*-c-Jun 3'UTR reporter constructs in 444 cells. Mimic let-7a / *Renilla*-Dicer 3'UTR reporter construct served as a positive control. The luciferase assay showed a strong decrease for the Dicer 3'UTR construct, whereas miR-495

did neither repress *Renilla*-c-Jun 3'UTR full-length nor *Renilla*-c-Jun 3'UTR segment 2 (**Fig. 4-12**). This shows that miR-495 does presumably not regulate c-Jun.

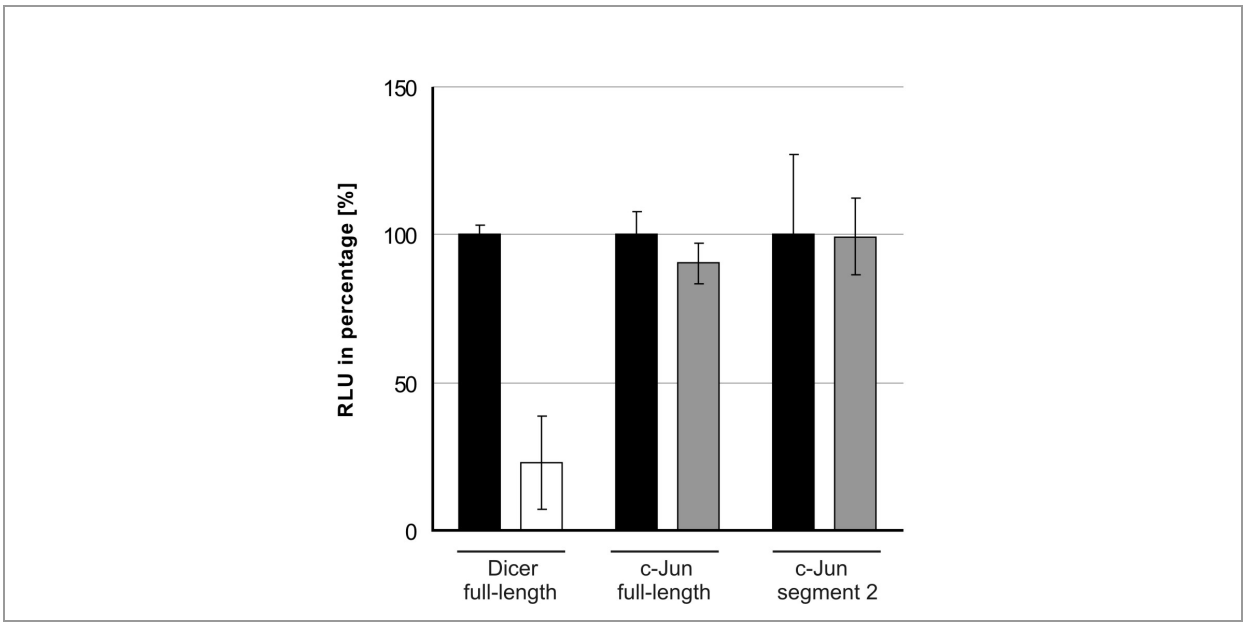

Figure 4-12: miR-495 does not repress *Renilla*-c-Jun 3'UTR reporter constructs

444 cells were co-transfected with 150nM "miRIDIAN Mimic" control RNA (black bars), mimic let-7a RNA (white bar) or mimic miR-495 RNA (grey bars) and 0.2ng of the indicated *Renilla*-3'UTR reporter plasmids. 24h after transfection, samples were analyzed with the Dual-Luciferase® Reporter Assay kit. Values for *Renilla*-luciferase were normalized against the internal *Firefly*-luciferase. Relative changes of signal intensities compared to mimic Control RNA were plotted in percentage. Error bars represent s.d. from 4 replicates.

5. Discussion

5.1. Depletion of Drosha and Dicer alters the abundance of certain AP-1 members

In the present study the question was addressed, whether miRNAs can regulate the transcription factor AP-1, a master regulator of many cellular processes like proliferation and neoplastic transformation (Angel and Karin, 1991; Eferl and Wagner, 2003). Besides studying different AP-1 subunits, the analysis also involved transcriptional regulators of AP-1 subunits. The transcriptional repressor Net, which controls *c-fos* expression (van Riggelen *et al.*, 2005), and JDP2 (*Jun dimerization protein 2*), which represses *c-jun* expression (Jin *et al.*, 2002; Heinrich *et al.*, 2004) was also investigated. Oct-1, also known as POU2F1, is a member of the POU transcription factor family (Phillips and Luisi, 2000), and was used as control.

It is a widely used strategy to detect miRNA-regulated target genes by knocking down proteins of the miRNA pathway: Drosha and Dicer (Kuehbacher *et al.*, 2007; Lee and Dutta, 2007), Dicer (Tang *et al.*, 2007), Dicer and Ago1-4 (Schmitter *et al.*, 2006), Drosha and Ago1-2 (Rehwinkel *et al.*, 2006). Disruption of the miRNA pathway by depletion of Drosha and Dicer affected significantly the abundance of miRNAs in the cell system, as exemplified by Northern blotting of let-7a in 444 cells (**Fig. 4-4**). The reduction of mature let-7a was in agreement with previous observations in HUVEC (Kuehbacher *et al.*, 2007) and HeLa cells (Lee and Dutta, 2007).

Subsequent changes in mRNA or protein levels of putative miRNA targets could arise from direct or indirect effects. A mRNA transcript that is a direct target harbors one or several miRNA binding sites in its CDS (*coding sequence*) (Tay *et al.*, 2008) and / or 3'UTR (*untranslated region*) (Krek *et al.*, 2005), to which miRNAs hybridize. Thereby, miRNAs guide the effector complexes miRISC (*miRNA induced silencing complex*) or miRNP (*miRNA ribonucleoprotein complex*) that subsequently suppress target transcripts, as already described in chapter **1.3.2**.

Besides such direct effects, also indirect effects must be considered, especially since the depletion of Drosha and Dicer leads to an impairment of the whole miRNome. Consequently, many scenarios are possible where the level of a certain protein is indirectly affected by miRNAs that directly target regulatory proteins of the protein of interest. For example, miR-29b was reported to repress the transcription factor Sp1 (Garzon *et al.*, 2009), which in turn positively regulates the transcription of IL-10 (*interleukin-10*) (Larsson *et al.*, 2009). Consequently, miR-29b might indirectly regulate IL-10 expression.

In order to monitor, whether the depletion of Drosha or Dicer led to functional effects on a known direct miRNA target, Dicer was analyzed (Forman *et al.*, 2008; Tokumaru *et al.*, 2008). The cytoplasmic RNAse III-type protein Dicer, which is a key component of the miRNA biogenesis pathway (Bernstein *et al.*, 2001; Hutvágner *et al.*, 2001), is also regulated by miRNAs, namely by let-7 through three binding sites in the CDS (Forman *et al.*, 2008) and one binding site in the 3'UTR (Tokumaru *et al.*, 2008). Genes are considered to be directly targeted by miRNAs, when mRNA levels are increased in a range of 1.5 to 2-fold upon abrogation of the miRNA biogenesis machinery (Rehwinkel *et al.*, 2006; Schmitter *et al.*, 2006). In this study, the direct target Dicer was increased in 444 and CGL3 cells upon knock-down of Drosha within this range (**Fig. 4-2, lane 2**).

	444	CGL3
Dicer	+	+
Oct-1	0	0
c-Jun	+	0
JunB	+	0
Fra-1	+	+
Fra-2	0	+
Net	+	0
JDP2	0	0
JunD	0	0
c-Fos	0	0
FosB	0	0
ATF-2	0	0

Table 5-1: Transcription factors are partially differentially regulated by miRNAs

The table gives an overview on modulated levels of AP-1 family members and of other transcription factors (except Dicer), which were found in qRT-PCR analysis, upon knock-down of Drosha and Dicer. Positive control (Dicer) and negative control (Oct-1) are highlighted in blue. +, regulated by miRNAs; 0, not regulated by miRNAs. For further details, see text.

Regarding the analyzed proteins, in 444 cells (**Fig. 4-2A**) c-Jun, JunB, Fra-1 and the transcriptional repressor Net (only siDicer treatment) showed mRNA levels within this range of 1.5- to 2-fold induction, and were therefore considered to be regulated by miRNAs. In CGL3 cells (**Fig. 4-2B**) the AP-1 members Fra-1 and Fra-2, which were only responsive to depletion of Drosha, showed increased levels, though they were moderate compared to 444 cells (**Tbl. 5-1**).

The observation that Net in 444 cells was only responsive to depletion of Dicer suggests that a transient knock-down might not be sufficiently efficient to inhibit all miRNAs. Some miRNAs might have a higher stability, which exceeds transient knock-downs. Similarly, it was found in HUVEC cells that upon transient depletion of Drosha or Dicer only a subset of miRNAs was reduced and that these reduced miRNAs were not always similarly reduced in both knock-downs (Kuehbacher *et al.*, 2007). Another study reported similar observations in colorectal cancer cells (Cummins *et al.*, 2006). Insufficient down-regulation of Dicer in CGL3

cells might also explain why Fra-1 and Fra-2 were not up-regulated to the same extent as upon depletion of Drosha.

Concerning the other analyzed genes, they displayed no or only minor changes and were then considered not to be direct targets of miRNAs, although it is possible that regulatory miRNAs for these genes were not affected by this experimental approach, see **Tbl. 5-1**. Initial experiments also included the oncoproteins HPV18 E6 and E7 that remained unaltered indicating that they are not subject to direct or indirect regulation by miRNAs in 444 cells, data not shown.

The levels of c-Jun, Fra-1 and c-Fos in 444 and CGL3 cells upon depletion of Drosha and Dicer were further confirmed on protein levels by Western blotting (**Fig. 4-3**) and were found to reflect the observed mRNA levels. Additionally, the analysis of HeLa cells revealed elevated levels of c-Jun and unchanged levels of Fra-1, while c-Fos was reduced (**Fig. 4-3**).

Since Fra-1 is regulated by miRNAs in both hybrid cell lines, but not in parental HeLa cells, this suggests that this kind of regulation is derived from the other parental cell line, GM77. Contrarily, c-Fos is indirectly regulated in HeLa cells, whereas both hybrids did not show this regulation indicating that the fusion of HeLa with GM77 cells probably also impaired this regulation.

c-Fos is the only AP-1 subunit, for which regulating miRNAs were described up to now (Lee *et al.*, 2006; Li *et al.*, 2009). Based on the concept that direct targets of miRNAs are up-regulated following depletion of Drosha and Dicer, the observed down-regulation of c-Fos in HeLa cells (**Fig. 4-3**) suggests an indirect effect as already discussed above. Different scenarios are possible, which would explain this observation: silencing of *c-fos* promoter by up-regulated transcriptional repressors that act in *trans* or by enhanced heterochromatinization of the promoter region that acts in *cis*. Besides differential transcriptional regulation, post-transcriptionally, c-Fos mRNA could be faster degraded, mediated by AREs (*adenylate uridylate-rich elements*) and mCRDs (*major protein-coding region determinant of instability*) in the 3'UTR of c-Fos (Chen and Shyu, 1995; Grosset *et al.*, 2000; Chen *et al.*, 2002). Additionally, factors that negatively regulate c-Fos protein levels could contribute to the down-regulation.

In this study, Net, a transcriptional repressor of the *c-fos* promoter, was analyzed in 444 and CGL3 cells (Giovane *et al.*, 1997; van Riggelen *et al.*, 2005). It was shown that Net is a direct target of miRNAs (**Fig. 4-7**) in 444 cells, and that its increase (**Fig. 4-2A, lane 13**) did not result in elevated c-Fos levels (**Fig. 4-2A, lane 10**), possibly because the increase was not sufficient to repress *c-fos* transcription or that Net was phosphorylated and consequently did not act as a repressor (Ducret *et al.*, 2000). In HeLa cells, however, further analysis will be necessary to decipher the miRNA-mediated mechanism, by which c-Fos is regulated.

5.2. Depletion of Drosha and Dicer modulates AP-1 composition and activity

5.2.1. Modulation of AP-1 composition shown by EMSA and super shift-analysis

The observed changes in protein levels resulted in modulation of AP-1 composition, amount and activity. In 444 cells, the increase of c-Jun and Fra-1 proteins led to an increased formation of c-Jun:c-Jun homodimers and c-Jun:Fra-1 heterodimers, as shown by EMSA (**Fig. 4-5A**) and "super shift-" analysis (**Fig. 4-5B**).

CGL3 cells did not display any differences of AP-1 composition or formation (**Fig. 4-5A**), as expected from unchanged levels of c-Jun and c-Fos. Although Fra-1 was up-regulated on protein level, and c-Jun:Fra-1 complexes display higher binding activities to DNA than c-Jun:c-Fos complexes (Ryseck and Bravo, 1991), c-Fos was not excluded from the complex and replaced by Fra-1 (**Fig. 4-5C**). The high amounts of c-Fos compared to the still low amounts of Fra-1 most likely inhibit a shift of AP-1 composition.

In HeLa cells, the increase of c-Jun and the decrease of c-Fos proteins led to a shift from c-Jun:c-Fos heterodimers to c-Jun homodimers, as shown by "super shift"- analysis (**Fig. 4-5D**). Binding of AP-1 to its consensus sequence remained unchanged, as shown by EMSA-analysis (**Fig. 4-5A**), because the alterations of c-Jun and c-Fos led rather to a different composition, but not to different amounts of AP-1.

5.2.2. Modulation of AP-1 activity as shown by exogenous reporter assays

The results of the EMSA-analysis were further validated with an AP-1 responsive reporter gene. In this study, an exogenous reporter system was used to monitor the transcriptional activity of AP-1 instead of an endogenous AP-1 target gene. Due to the experimental approach with the global impact on miRNAs, many unknown, direct and indirect, effects might influence endogenous target genes making them inapplicable for the analysis of a single transcription factor.

The reporter system pAP-1 showed that, upon depletion of Drosha and Dicer, the increased levels of AP-1 in 444 cells led to an enhanced transcriptional activity (**Fig. 4-6**). This is most likely mediated by c-Jun homodimers, since c-Jun:Fra-1 dimers act as transcriptional attenuators (Suzuki *et al.*, 1991; Zhang *et al.*, 2004) or only as moderate transcriptional activators that are preferentially involved in initiation and maintenance of, for example, HPV-16/-18 transcription (Cripe *et al.*, 1990; Butz and Hoppe-Seyler, 1993). The different activities of c-Jun:Fra-1 complexes might rely on post-translational modifications, e.g. phosphorylation. Additionally, transcription of the luciferase reporter gene might also be driven by AP-1 complexes involving JunB that was up-regulated in 444 cells (**Fig. 4-2A, lane 5**).

As expected, CGL3 cells did not show any effect on transcriptional activity (**Fig. 4-6**). In HeLa cells, the loss of c-Jun:c-Fos dimers that act as strong transcriptional activators (Suzuki *et al.*, 1991; Zhang *et al.*, 2004) is presumably compensated with the positive regulatory effect of c-Jun homodimers. Thus, the transcriptional activity of AP-1 in HeLa cells remained unaltered (**Fig. 4-6**).

In conclusion, it was shown that miRNAs can selectively modulate AP-1 formation and activity, which potentially alters the transcriptional rate of endogenous target genes.

5.3. miRNAs directly regulate c-Jun, Fra-1 and Net

Reporter assays with fusion transcripts of *Renillla* luciferase and the 3'UTRs of c-Jun, Fra-1 and Net indicated direct miRNA interactions for all three genes (**Fig. 4-6**). Regarding c-Jun that previously showed similar increases of mRNA (**Fig. 4-2, lane 4**) and protein (**Fig. 4-3**) for both knockdowns, *Renilla* activity upon Drosha depletion was consistently low for unknown reasons. The Net construct also did not respond to the knock-down of Drosha, which, however, was in agreement with the qRT-PCR analysis and was already discussed in chapter **5.1**.

Single segments of c-Jun and Fra-1 were even more sensitive to the miRNA effect than the full-length 3'UTRs in the luciferase assays by showing more pronounced effects (**Fig. 4-8**). The shorter segments were presumably more accessible to miRNAs, possibly due to reduced formation of secondary structures (Doench and Sharp, 2004; Robins *et al.*, 2005).

Taken together, these results indicate that c-Jun and Fra-1 are regulated via multiple miRNA binding sites throughout their 3'UTRs. The finding that a target gene is repressed by one or several miRNAs via different binding sites is not unusual. For example, human HMGA2 (*high mobility group AT-hook 2*) is regulated via six let-7 binding sites in its 3'UTR (Lee and Dutta, 2007). Moreover, miR-93, -98 and -197 synergistically target the tumor suppressor FUS1, also termed "TUSC2" (*tumor suppressor candidate 2*) (Du *et al.*, 2009). It has been proposed that regulation via multiple binding sites allows a more efficient inhibition (Doench *et al.*, 2003).

c-Jun and Fra-1 are transcription factors involved in a broad range of physiological and pathological processes modulating different cellular responses through selective gene transcription. AP-1 activating stimuli encompass cytokines, growth factors, stress signals and infections, which can lead to cellular proliferation, differentiation, apoptosis or neoplastic transformation (Angel and Karin, 1991; Eferl and Wagner, 2003; Hess *et al.*, 2004). miRNA-mediated regulation of such complex pathways can be easier coordinated, when different pro-

teins of the same pathway are targeted simultaneously. For example, the miR-16 family members miR-15a, miR-16 and miR-103 regulate directly and indirectly genes that cooperatively control cell cycle progression (Linsley *et al.*, 2007). Secondly, miR-34a induces G1 cell cycle arrest by targeting CCND1 (*cyclin D1*) and CDK6 (*cyclin-dependent kinase 6*) (Sun *et al.*, 2008) and thereby preventing phosphorylation of pRb (*protein retinoblastoma 1*), which, in the hypophosphorylated state, inhibits the E2F family of cell cycle transcription factors. Additionally, it seems that miR-34a also directly targets E2F-1 and -3 (Tazawa *et al.*, 2007). In conclusion, this illustrates that proteins participating in the same regulatory pathway can be simultaneously inhibited by miRNAs in order to achieve a functional effect.

Consequently, a protein that is involved in various miRNA-regulated pathways can be targeted by several miRNAs in response to different stimuli. This might be the case for c-Jun and Fra-1, for which many regulatory miRNAs are predicted.

5.4. Bioinformatics and expression analysis

5.4.1. Prediction analysis

Prediction software tools, such as miRBase, TargetScan, PicTar and DIANA microT, are useful tools to decipher miRNA target genes (Bartel, 2009). The combined application of these programs led to a list of putative miRNAs that were sorted according to the frequency of citations and to the number of predicted binding sites. This list, however, is biased by several factors.

- The search engines and the underlying algorithms do not work with the same set of annotated miRNAs. Consequently, a true prediction might not receive a high score, since it is not considered by all search engines.
- The algorithms use the criterion of seed pairing between miRNA and mRNA as one important parameter, although stringent seed pairing is not a completely reliable predictor for miRNA binding (Didiano and Hobert, 2006).
- Seed pairing is not uniformly defined, and shorter seed pairing is partially allowed when it is compensated by additional 3’ end pairing of the miRNA, e.g. DIANA microT (Maragkakis *et al.*, 2009).
- Sequence conservation among different species is an important criterion that, however, does not exclude functional miRNA:mRNA interactions that only exist in humans.
- Unknown, functional miRNAs are, of course, not considered by the analysis.

Though the bioinformatics approach faces some difficulties, it is still a valid and widely used strategy (Gabriely *et al.*, 2008; Tokumaru *et al.*, 2008; Du *et al.*, 2009).

5.4.2. miRNA expression analysis in 444 and CGL3 cells

Besides applying prediction engines in order to find eligible candidate miRNAs, the analysis of the miRNome of 444 and CGL3 cells revealed the expression status of 470 annotated miRNAs. This data was used to decipher the high-ranking candidate miR-495 for c-Jun regulation. Additionally, the data provides the basis for the question, why c-Fos is not modulated by two miRNAs as it was previously published (Lee *et al.*, 2006; Li *et al.*, 2009).

It was reported that c-Fos was repressed in the brain of mice by mmu-miR-7b (Lee *et al.*, 2006) and in human liver cells by hsa-miR-101 (Li *et al.*, 2009). Since miRNA-mediated regulation is highly conserved, both miRNAs, when expressed, were expected to repress c-Fos also in cervical carcinoma derived cell lines. However, the data, presented in the present study, did not show a direct regulation of c-Fos neither in 444, CGL3 nor HeLa cells. Despite the fact that many miRNAs are conserved across different species, mmu-miR-7b does not have a human homolog. In humans, however, there is a closely related variant, named hsa-miR-7, which differs only by one nucleotide (U→A) (**Fig. 5-1**). As shown by the miRNA expression profiling, hsa-miR-7 is strongly expressed in 444 and CGL3 cells (**Tbl. 4-4**). The detailed analysis of both predicted binding sites in the 3'UTRs of human and murine c-Fos (Lee *et al.*, 2006) reveals that the first miRNA binding site contains one mutation between *homo sapiens* and *mus musculus*, whereas the second binding site is identical (**Fig. 5-1**). The alignment of both target sites with the respective

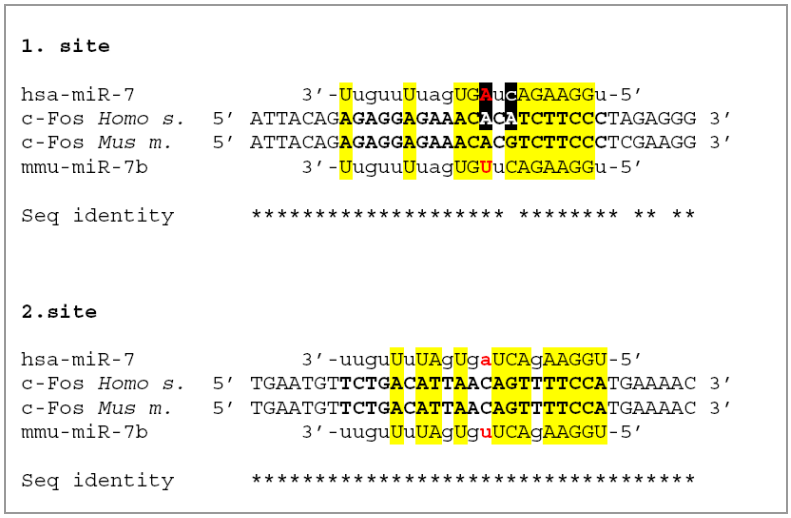

Fig. 5-1: Sequence alignment of miR-7/-7b with its predicted target sites within human and murine c-Fos 3'UTR

Alignment of the two sections of human and murine c-Fos 3'UTRs with mmu-miR-7b and hsa-miR-7. In bold: predicted miRNA target site in the mRNA; in red: sequence variations between mmu-miR-7b and hsa-miR-7; highlighted in yellow: putative base-pairing between mRNA and miRNA; highlighted in black: lost base-pairing. See text for further details.

miRNAs shows that the (U→A) conversion abolishes one base-pairing between hsa-miR-7 and human c-Fos mRNA in the first miRNA binding site. Additionally, the mutation (G→A) of human c-Fos mRNA leads to a second loss of base-pairing compared to murine c-Fos 3'UTR and mmu-miR-7b. The alignment of the second binding site with the respective miRNAs displays no difference in the number of hybridized bases, suggesting that the hsa-miR-7-mediated regulation of human c-Fos is presumably lost due to the impairment of one of two binding sites.

The other miRNA that is reported to regulate c-Fos in human liver cells is miR-101 (Li *et al.*, 2009). miR-101 is highly expressed in 444 and CGL3 cells (**Tbl. 4-4**) and no mutation was detected upon sequencing of c-Fos 3'UTR in CGL3 cells compared to the annotated sequence. This suggests that other factors inhibit miR-101-mediated degradation of c-Fos mRNA in cervical carcinoma derived cell lines, as it is discussed in chapter **5.6**. Alternatively, the possibility remains that miR-101 was not affected by the transient knock-downs of Drosha and Dicer, as discussed in chapter **5.1**. In order to exclude miR-101 regulation of c-Fos in this cell system, miR-101 would need to be selectively inhibited in further experiments.

5.5. miR-495 as a potential regulator of c-Jun

Co-transfection of miR-495 with *Renilla*-c-Jun 3'UTR full-length and *Renilla*-c-Jun 3'UTR segment 2 reporter plasmids in 444 cells did not significantly reduce *Renilla* activity (**Fig. 4-11**) indicating that miR-495 does not regulate c-Jun. However, a regulatory effect of miR-495 can not be completely ruled out because it is possible that miR-495 contributes to a cooperative regulation of c-Jun with other miRNAs. Previous studies have already shown the phenomenon of cooperative regulations by miRNAs (Tay *et al.*, 2008; Du *et al.*, 2009). Overexpression of one regulatory miRNA might then not be sufficient to repress the target mRNA.

If the amount of the mature miRNA is the key parameter, a possible regulatory effect could be elucidated by increasing the miRNA concentration. This would augment the miRNA:transcript ratio and potentially reveal an interaction, as long as cooperating partners are not titrated out.

If the amount of transfected miR-495 does not play the decisive role in 444 cells, possibly because miR-495 steady-state levels are already high enough to repress all target mRNAs, alternative approaches must be taken. Firstly, overexpression in CGL3 cells, which are devoid of miR-495, might reveal the putative interaction. Secondly, endogenous miR-495 in 444 cells could be inhibited by antagomirs (Krutzfeldt *et al.*, 2005) or a "miRNA-sponge" (Ebert *et al.*, 2007) in order to decipher a potential repressive effect.

In conclusion, although miR-495 is likely to regulate c-Jun, such an interaction was not proven in the present study.

5.6. Possible mechanisms that abolish miRNA-mediated regulation of c-Jun in CGL3 cells

It was shown that c-Jun is regulated by miRNA(s) in 444 and HeLa cells, although the specific miRNA(s) could not be identified. However, it was demonstrated that in CGL3 cells this type of regulation is lost, since c-Jun levels did not change upon depletion of Drosha and Dicer. Other reports provide examples of silenced miRNAs that could possibly explain why c-Jun is not regulated by miRNAs in CGL3 cells.

Firstly, miRNA genes can be disrupted, since they are often located in / near FRAs (*fragile sites*) and genomic regions that are prone to severe alterations (Calin *et al.*, 2004b), such as deletions or translocations. Alternatively, similar to protein-coding genes, the promoter activity of miRNA genes is regulated by many Pol II-associated transcription factors (Corcoran *et al.*, 2009; Wang *et al.*, 2009), including tumor-suppressive and oncogenic transcription factors, and can be silenced by transcriptional repressors in *trans*. Secondly, RNA-binding proteins can facilitate (Guil and Caceres, 2007) or inhibit (Newman *et al.*, 2008; Hagan *et al.*, 2009) processing of miRNA precursors leading to an enhanced or reduced activity of mature miRNAs, respectively. Thirdly, sequence variations, such as editing or point mutations, can result in impaired miRNA processing (Yang *et al.*, 2006; Kawahara *et al.*, 2007a) or target sequence specificity (Kawahara *et al.*, 2007b).

In conclusion, without knowing the specific miRNA that regulates c-Jun in 444 cells, it can only be speculated about the mechanism how this regulation is abolished in CGL3 cells. Numerous possibilities were described, of which only the most likely are mentioned here.

5.7. Conclusion

The present study describes for the first time that the AP-1 family members c-Jun, Fra-1 and c-Fos, are selectively regulated by miRNAs in HPV18-positive cervical carcinoma cell lines. Thereby, all three AP-1 members were found to be differently regulated by miRNAs in the three analyzed cell lines, which presumably attributes to the different lineages. Most importantly, miRNA-mediated regulation of c-Jun is abrogated in tumorigenic hybrid cells compared to non-tumorigenic progenitor cells. This loss of miRNA-mediated repression inhibits c-

Jun degradation and may serve as an evasive strategy for the tumorigenic hybrids in order to preserve the low basal amounts of c-Jun.

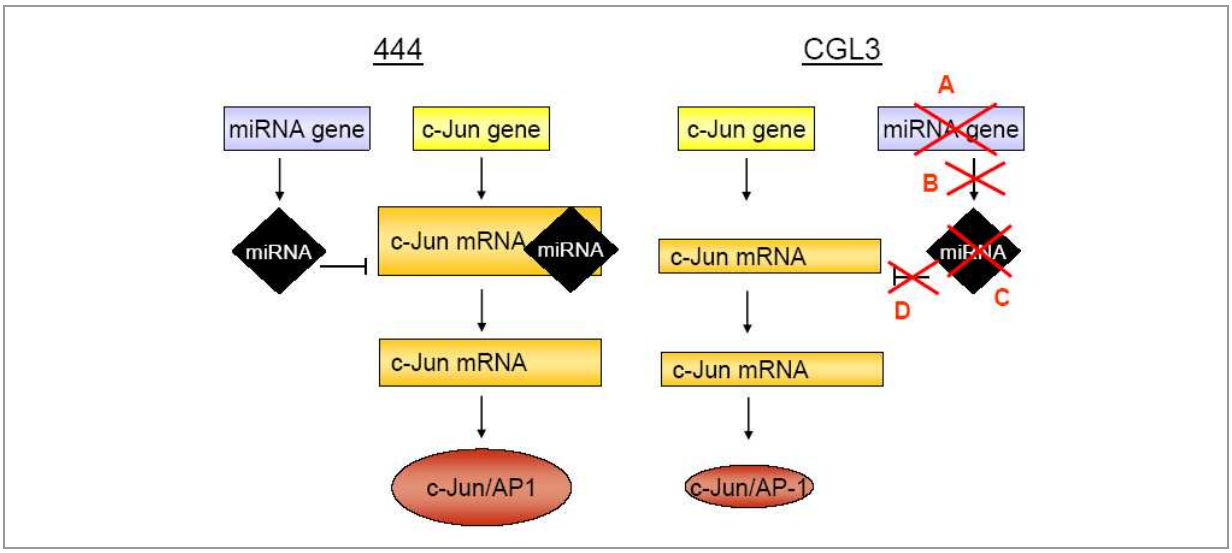

Fig. 5-2: Model of the different miRNA-mediated regulation of c-Jun in 444 and CGL3 cells

c-Jun is repressed by unknown miRNAs in 444, but not in CGL3 cells. miRNA-mediated regulation in CGL3 cells is abolished potentially through alterations at (**A**) the genomic levels, (**B**) the maturation step, (**C**) the steady-state level, or (**D**) the target repression step, as discussed in chapter **5.6**. For further details see text.
c-Jun mRNA levels are lower in CGL3 than in 444 cells (as indicated by the size of the boxes), possibly due to different transcriptional rates and / or different turn-over of the mRNA.

Furthermore, a miRNA expression array illustrates different miRNA expression profiles for the non-malignant and malignant hybrid cells. In combination with bioinformatics prediction analysis, these data reveal putative regulatory miRNAs for c-Jun and Fra-1, although no regulatory miRNA could be identified in the present study.

Besides influencing protein levels, it is also shown for the first time that miRNAs modulate AP-1 composition and transcriptional activity, thereby providing further examples of miRNA-regulated transcription factors that in turn differentially regulate target genes. By modulating only one miRNA-responsive AP-1 member, cells might be able to regulate via miRNAs various target genes of one specific AP-1 dimer composition. Since AP-1 is a master regulator of many cellular processes like proliferation and differentiation, this study underlines the complexity of many networks involving the transcription factor AP-1, and it describes how miRNAs can contribute to this regulation in cervical carcinoma cells and maybe also in other tissues.

6. Literature

Aagaard L, Amarzguioui M, Sun G, Santos LC, Ehsani A, Prydz H *et al* (2007). A facile lentiviral vector system for expression of doxycycline-inducible shRNAs: knockdown of the pre-miRNA processing enzyme Drosha. *Mol Ther* **15:** 938-45.

Abbott AL, Alvarez-Saavedra E, Miska EA, Lau NC, Bartel DP, Horvitz HR *et al* (2005). The let-7 MicroRNA family members mir-48, mir-84, and mir-241 function together to regulate developmental timing in Caenorhabditis elegans. *Dev Cell* **9:** 403-14.

Aharon T, Schneider RJ (1993). Selective destabilization of short-lived mRNAs with the granulocyte-macrophage colony-stimulating factor AU-rich 3' noncoding region is mediated by a cotranslational mechanism. *Mol Cell Biol* **13:** 1971-80.

Andersson MG, Haasnoot PC, Xu N, Berenjian S, Berkhout B, Akusjarvi G (2005). Suppression of RNA interference by adenovirus virus-associated RNA. *J Virol* **79:** 9556-65.

Angel P, Karin M (1991). The role of Jun, Fos and the AP-1 complex in cell-proliferation and transformation. *Biochim Biophys Acta* **1072:** 129-57.

Aparicio O, Razquin N, Zaratiegui M, Narvaiza I, Fortes P (2006). Adenovirus virus-associated RNA is processed to functional interfering RNAs involved in virus production. *J Virol* **80:** 1376-84.

Aravin AA, Lagos-Quintana M, Yalcin A, Zavolan M, Marks D, Snyder B *et al* (2003). The small RNA profile during Drosophila melanogaster development. *Dev Cell* **5:** 337-50.

Azuma-Mukai A, Oguri H, Mituyama T, Qian ZR, Asai K, Siomi H *et al* (2008). Characterization of endogenous human Argonautes and their miRNA partners in RNA silencing. *Proc Natl Acad Sci U S A* **105:** 7964-9.

Bagchi S, Raychaudhuri P, Nevins JR (1990). Adenovirus E1A proteins can dissociate heteromeric complexes involving the E2F transcription factor: a novel mechanism for E1A transactivation. *Cell* **62:** 659-69.

Bartel DP (2004). MicroRNAs: genomics, biogenesis, mechanism, and function. *Cell* **116:** 281-97.

Bartel DP (2009). MicroRNAs: target recognition and regulatory functions. *Cell* **136:** 215-33.

Behm-Ansmant I, Rehwinkel J, Doerks T, Stark A, Bork P, Izaurralde E (2006). mRNA degradation by miRNAs and GW182 requires both CCR4:NOT deadenylase and DCP1:DCP2 decapping complexes. *Genes Dev* **20:** 1885-98.

Bentwich I, Avniel A, Karov Y, Aharonov R, Gilad S, Barad O *et al* (2005). Identification of hundreds of conserved and nonconserved human microRNAs. *Nat Genet* **37:** 766-70.

Berezikov E, Guryev V, van de Belt J, Wienholds E, Plasterk RH, Cuppen E (2005). Phylogenetic shadowing and computational identification of human microRNA genes. *Cell* **120:** 21-4.

Bernstein E, Caudy AA, Hammond SM, Hannon GJ (2001). Role for a bidentate ribonuclease in the initiation step of RNA interference. *Nature* **409:** 363-6.

Bernstein E, Kim SY, Carmell MA, Murchison EP, Alcorn H, Li MZ *et al* (2003). Dicer is essential for mouse development. *Nat Genet* **35:** 215-7.

Berry A, Goodwin M, Moran CL, Chambers TC (2001). AP-1 activation and altered AP-1 composition in association with increased phosphorylation and expression of specific Jun and Fos family proteins induced by vinblastine in KB-3 cells. *Biochem Pharmacol* **62:** 581-91.

Bohnsack MT, Czaplinski K, Gorlich D (2004). Exportin 5 is a RanGTP-dependent dsRNA-binding protein that mediates nuclear export of pre-miRNAs. *RNA* **10:** 185-91.

Borchert GM, Lanier W, Davidson BL (2006). RNA polymerase III transcribes human microRNAs. *Nat Struct Mol Biol* **13:** 1097-101.

Bos JL (1989). ras oncogenes in human cancer: a review. *Cancer Res* **49:** 4682-9.

Bosch FX, de Sanjose S (2003). Chapter 1: Human papillomavirus and cervical cancer--burden and assessment of causality. *J Natl Cancer Inst Monogr***:** 3-13.

Boshart M, Gissmann L, Ikenberg H, Kleinheinz A, Scheurlen W, zur Hausen H (1984). A new type of papillomavirus DNA, its presence in genital cancer biopsies and in cell lines derived from cervical cancer. *EMBO J* **3:** 1151-7.

Bouvard V, Storey A, Pim D, Banks L (1994). Characterization of the human papillomavirus E2 protein: evidence of trans-activation and trans-repression in cervical keratinocytes. *EMBO J* **13:** 5451-9.

Boyle WJ, Smeal T, Defize LH, Angel P, Woodgett JR, Karin M *et al* (1991). Activation of protein kinase C decreases phosphorylation of c-Jun at sites that negatively regulate its DNA-binding activity. *Cell* **64:** 573-84.

Bradford MM (1976). A rapid and sensitive method for the quantitation of microgram quantities of protein utilizing the principle of protein-dye binding. *Anal Biochem* **72:** 248-54.

Brennecke J, Stark A, Russell RB, Cohen SM (2005). Principles of microRNA-target recognition. *PLoS Biol* **3:** e85.

Butz K, Hoppe-Seyler F (1993). Transcriptional control of human papillomavirus (HPV) oncogene expression: composition of the HPV type 18 upstream regulatory region. *J Virol* **67:** 6476-86.

Cai X, Hagedorn CH, Cullen BR (2004). Human microRNAs are processed from capped, polyadenylated transcripts that can also function as mRNAs. *RNA* **10:** 1957-66.

Cai X, Li G, Laimins LA, Cullen BR (2006). Human papillomavirus genotype 31 does not express detectable microRNA levels during latent or productive virus replication. *J Virol* **80:** 10890-3.

Calaluce R, Bearss DJ, Barrera J, Zhao Y, Han H, Beck SK *et al* (2004). Laminin-5 beta3A expression in LNCaP human prostate carcinoma cells increases cell migration and tumorigenicity. *Neoplasia* **6:** 468-79.

Calin GA, Dumitru CD, Shimizu M, Bichi R, Zupo S, Noch E *et al* (2002). Frequent deletions and down-regulation of micro- RNA genes miR15 and miR16 at 13q14 in chronic lymphocytic leukemia. *Proc Natl Acad Sci U S A* **99:** 15524-9.

Calin GA, Ferracin M, Cimmino A, Di Leva G, Shimizu M, Wojcik SE *et al* (2005). A MicroRNA signature associated with prognosis and progression in chronic lymphocytic leukemia. *N Engl J Med* **353:** 1793-801.

Calin GA, Liu CG, Sevignani C, Ferracin M, Felli N, Dumitru CD *et al* (2004a). MicroRNA profiling reveals distinct signatures in B cell chronic lymphocytic leukemias. *Proc Natl Acad Sci U S A* **101:** 11755-60.

Calin GA, Sevignani C, Dumitru CD, Hyslop T, Noch E, Yendamuri S *et al* (2004b). Human microRNA genes are frequently located at fragile sites and genomic regions involved in cancers. *Proc Natl Acad Sci U S A* **101:** 2999-3004.

Casalino L, De Cesare D, Verde P (2003). Accumulation of Fra-1 in ras-transformed cells depends on both transcriptional autoregulation and MEK-dependent posttranslational stabilization. *Mol Cell Biol* **23:** 4401-15.

Chan JA, Krichevsky AM, Kosik KS (2005). MicroRNA-21 is an antiapoptotic factor in human glioblastoma cells. *Cancer Res* **65:** 6029-33.

Chen CY, Shyu AB (1995). AU-rich elements: characterization and importance in mRNA degradation. *Trends Biochem Sci* **20:** 465-70.

Chen CY, Shyu AB (2003). Rapid deadenylation triggered by a nonsense codon precedes decay of the RNA body in a mammalian cytoplasmic nonsense-mediated decay pathway. *Mol Cell Biol* **23:** 4805-13.

Chen CY, Xu N, Shyu AB (1995). mRNA decay mediated by two distinct AU-rich elements from c-fos and granulocyte-macrophage colony-stimulating factor transcripts: different deadenylation kinetics and uncoupling from translation. *Mol Cell Biol* **15:** 5777-88.

Chen CY, Xu N, Shyu AB (2002). Highly selective actions of HuR in antagonizing AU-rich element-mediated mRNA destabilization. *Mol Cell Biol* **22:** 7268-78.

Chen K, Song F, Calin GA, Wei Q, Hao X, Zhang W (2008). Polymorphisms in microRNA targets: a gold mine for molecular epidemiology. *Carcinogenesis* **29:** 1306-11.

Chinenov Y, Kerppola TK (2001). Close encounters of many kinds: Fos-Jun interactions that mediate transcription regulatory specificity. *Oncogene* **20:** 2438-52.

Chudin E, Kruglyak S, Baker SC, Oeser S, Barker D, McDaniel TK (2006). A model of technical variation of microarray signals. *J Comput Biol* **13:** 996-1003.

Cimmino A, Calin GA, Fabbri M, Iorio MV, Ferracin M, Shimizu M *et al* (2005). miR-15 and miR-16 induce apoptosis by targeting BCL2. *Proc Natl Acad Sci U S A* **102:** 13944-9.

Clop A, Marcq F, Takeda H, Pirottin D, Tordoir X, Bibe B *et al* (2006). A mutation creating a potential illegitimate microRNA target site in the myostatin gene affects muscularity in sheep. *Nat Genet* **38:** 813-8.

Cole ST, Streeck RE (1986). Genome organization and nucleotide sequence of human papillomavirus type 33, which is associated with cervical cancer. *J Virol* **58:** 991-5.

Corcoran DL, Pandit KV, Gordon B, Bhattacharjee A, Kaminski N, Benos PV (2009). Features of mammalian microRNA promoters emerge from polymerase II chromatin immunoprecipitation data. *PLoS One* **4:** e5279.

Cordes KR, Sheehy NT, White MP, Berry EC, Morton SU, Muth AN *et al* (2009). miR-145 and miR-143 regulate smooth muscle cell fate and plasticity. *Nature* **460:** 705-10.

Cripe TP, Alderborn A, Anderson RD, Parkkinen S, Bergman P, Haugen TH *et al* (1990). Transcriptional activation of the human papillomavirus-16 P97 promoter by an 88-nucleotide enhancer containing distinct cell-dependent and AP-1-responsive modules. *New Biol* **2:** 450-63.

Cripe TP, Haugen TH, Turk JP, Tabatabai F, Schmid PG, 3rd, Durst M *et al* (1987). Transcriptional regulation of the human papillomavirus-16 E6-E7 promoter by a keratinocyte-dependent enhancer, and by viral E2 trans-activator and repressor gene products: implications for cervical carcinogenesis. *EMBO J* **6:** 3745-53.

Cronje HS (2004). Screening for cervical cancer in developing countries. *Int J Gynaecol Obstet* **84:** 101-8.

Cummins JM, He Y, Leary RJ, Pagliarini R, Diaz LA, Jr., Sjoblom T *et al* (2006). The colorectal microRNAome. *Proc Natl Acad Sci U S A* **103:** 3687-92.

Curatola AM, Nadal MS, Schneider RJ (1995). Rapid degradation of AU-rich element (ARE) mRNAs is activated by ribosome transit and blocked by secondary structure at any position 5' to the ARE. *Mol Cell Biol* **15:** 6331-40.

Dajee M, Lazarov M, Zhang JY, Cai T, Green CL, Russell AJ *et al* (2003). NF-kappaB blockade and oncogenic Ras trigger invasive human epidermal neoplasia. *Nature* **421:** 639-43.

Danos O, Katinka M, Yaniv M (1982). Human papillomavirus 1a complete DNA sequence: a novel type of genome organization among papovaviridae. *EMBO J* **1:** 231-6.

Das S (2009). Evolutionary origin and genomic organization of micro-RNA genes in immunoglobulin lambda variable region gene family. *Mol Biol Evol* **26:** 1179-89.

De-Castro Arce J (2003). RARb trans-repression of AP-1 transcription factor in HeLa cervical cancer cells: Consequences on transcription of viral and cellular AP-1 controlled genes. *PhD thesis*.

De-Castro Arce J, Soto U, van Riggelen J, Schwarz E, Hausen HZ, Rosl F (2004). Ectopic expression of nonliganded retinoic acid receptor beta abrogates AP-1 activity by selective degradation of c-Jun in cervical carcinoma cells. *J Biol Chem* **279:** 45408-16.

de Villiers EM, Fauquet C, Broker TR, Bernard HU, zur Hausen H (2004). Classification of papillomaviruses. *Virology* **324:** 17-27.

de Wet JR, Wood KV, DeLuca M, Helinski DR, Subramani S (1987). Firefly luciferase gene: structure and expression in mammalian cells. *Mol Cell Biol* **7:** 725-37.

de Wilde J, De-Castro Arce J, Snijders PJ, Meijer CJ, Rosl F, Steenbergen RD (2008). Alterations in AP-1 and AP-1 regulatory genes during HPV-induced carcinogenesis. *Cell Oncol* **30:** 77-87.

Del Vecchio AM, Romanczuk H, Howley PM, Baker CC (1992). Transient replication of human papillomavirus DNAs. *J Virol* **66:** 5949-58.

Didiano D, Hobert O (2006). Perfect seed pairing is not a generally reliable predictor for miRNA-target interactions. *Nat Struct Mol Biol* **13:** 849-51.

Distel RJ, Spiegelman BM (1990). Protooncogene c-fos as a transcription factor. *Adv Cancer Res* **55:** 37-55.

Doench JG, Petersen CP, Sharp PA (2003). siRNAs can function as miRNAs. *Genes Dev* **17:** 438-42.

Doench JG, Sharp PA (2004). Specificity of microRNA target selection in translational repression. *Genes Dev* **18:** 504-11.

Dong JT, Boyd JC, Frierson HF, Jr. (2001). Loss of heterozygosity at 13q14 and 13q21 in high grade, high stage prostate cancer. *Prostate* **49:** 166-71.

Doorbar J, Ely S, Sterling J, McLean C, Crawford L (1991). Specific interaction between HPV-16 E1-E4 and cytokeratins results in collapse of the epithelial cell intermediate filament network. *Nature* **352:** 824-7.

Du L, Schageman JJ, Subauste MC, Saber B, Hammond SM, Prudkin L *et al* (2009). miR-93, miR-98, and miR-197 regulate expression of tumor suppressor gene FUS1. *Mol Cancer Res* **7:** 1234-43.

Ducret C, Maira SM, Lutz Y, Wasylyk B (2000). The ternary complex factor Net contains two distinct elements that mediate different responses to MAP kinase signalling cascades. *Oncogene* **19:** 5063-72.

Duensing S, Münger K (2003). Centrosomes, genomic instability, and cervical carcinogenesis. *Crit Rev Eukaryot Gene Expr* **13:** 9-23.

Dürst M, Gissmann L, Ikenberg H, zur Hausen H (1983). A papillomavirus DNA from a cervical carcinoma and its prevalence in cancer biopsy samples from different geographic regions. *Proc Natl Acad Sci U S A* **80:** 3812-5.

Duursma AM, Kedde M, Schrier M, le Sage C, Agami R (2008). miR-148 targets human DNMT3b protein coding region. *RNA* **14:** 872-7.

Dyson N, Howley PM, Munger K, Harlow E (1989). The human papilloma virus-16 E7 oncoprotein is able to bind to the retinoblastoma gene product. *Science* **243:** 934-7.

Ebert MS, Neilson JR, Sharp PA (2007). MicroRNA sponges: competitive inhibitors of small RNAs in mammalian cells. *Nat Methods* **4:** 721-6.

Eferl R, Wagner EF (2003). AP-1: a double-edged sword in tumorigenesis. *Nat Rev Cancer* **3:** 859-68.

Eis PS, Tam W, Sun L, Chadburn A, Li Z, Gomez MF *et al* (2005). Accumulation of miR-155 and BIC RNA in human B cell lymphomas. *Proc Natl Acad Sci U S A* **102:** 3627-32.

Elbashir SM, Harborth J, Lendeckel W, Yalcin A, Weber K, Tuschl T (2001). Duplexes of 21-nucleotide RNAs mediate RNA interference in cultured mammalian cells. *Nature* **411:** 494-8.

Enright AJ, John B, Gaul U, Tuschl T, Sander C, Marks DS (2003). MicroRNA targets in Drosophila. *Genome Biol* **5:** R1.

Fan JB, Gunderson KL, Bibikova M, Yeakley JM, Chen J, Wickham Garcia E *et al* (2006). Illumina universal bead arrays. *Methods Enzymol* **410:** 57-73.

Fan JB, Yeakley JM, Bibikova M, Chudin E, Wickham E, Chen J *et al* (2004). A versatile assay for high-throughput gene expression profiling on universal array matrices. *Genome Res* **14:** 878-85.

Favre M, Orth G, Croissant O, Yaniv M (1975). Human papillomavirus DNA: physical map. *Proc Natl Acad Sci U S A* **72:** 4810-4.

Fehrmann F, Laimins LA (2003). Human papillomaviruses: targeting differentiating epithelial cells for malignant transformation. *Oncogene* **22:** 5201-7.

Filipowicz W, Bhattacharyya SN, Sonenberg N (2008). Mechanisms of post-transcriptional regulation by microRNAs: are the answers in sight? *Nat Rev Genet* **9:** 102-14.

Forman JJ, Legesse-Miller A, Coller HA (2008). A search for conserved sequences in coding regions reveals that the let-7 microRNA targets Dicer within its coding sequence. *Proc Natl Acad Sci U S A* **105:** 14879-84.

Franklin CC, Sanchez V, Wagner F, Woodgett JR, Kraft AS (1992). Phorbol ester-induced amino-terminal phosphorylation of human JUN but not JUNB regulates transcriptional activation. *Proc Natl Acad Sci U S A* **89:** 7247-51.

Friedman RC, Farh KK, Burge CB, Bartel DP (2009). Most mammalian mRNAs are conserved targets of microRNAs. *Genome Res* **19:** 92-105.

Fujita S, Ito T, Mizutani T, Minoguchi S, Yamamichi N, Sakurai K *et al* (2008). miR-21 Gene expression triggered by AP-1 is sustained through a double-negative feedback mechanism. *J Mol Biol* **378:** 492-504.

Gabriely G, Wurdinger T, Kesari S, Esau CC, Burchard J, Linsley PS *et al* (2008). MicroRNA 21 promotes glioma invasion by targeting matrix metalloproteinase regulators. *Mol Cell Biol* **28:** 5369-80.

Galinsky VL (2003). Automatic registration of microarray images. II. Hexagonal grid. *Bioinformatics* **19:** 1832-6.

Gallagher S, Winston S, Fuller S, Hurrell J (1997). Immunoblotting and Immunodetection In: Current Protocols in Molecular Biology (Ed.) Asube F, Brendt R, Kingston RE, Moore DD, Seidman JG, Smith JA and Struhl K. 10.8.1-10.8.21, JohnWiley & Sons, Inc.

Garzon R, Liu S, Fabbri M, Liu Z, Heaphy CE, Callegari E *et al* (2009). MicroRNA-29b induces global DNA hypomethylation and tumor suppressor gene reexpression in acute myeloid leukemia by targeting directly DNMT3A and 3B and indirectly DNMT1. *Blood* **113:** 6411-8.

Garzon R, Pichiorri F, Palumbo T, Iuliano R, Cimmino A, Aqeilan R *et al* (2006). MicroRNA fingerprints during human megakaryocytopoiesis. *Proc Natl Acad Sci U S A* **103:** 5078-83.

Giovane A, Sobieszczuk P, Ayadi A, Maira SM, Wasylyk B (1997). Net-b, a Ras-insensitive factor that forms ternary complexes with serum response factor on the serum response element of the fos promoter. *Mol Cell Biol* **17:** 5667-78.

Goldsborough MD, DiSilvestre D, Temple GF, Lorincz AT (1989). Nucleotide sequence of human papillomavirus type 31: a cervical neoplasia-associated virus. *Virology* **171:** 306-11.

Goodrich DW, Lee WH (1993). Molecular characterization of the retinoblastoma susceptibility gene. *Biochim Biophys Acta* **1155:** 43-61.

Gregory RI, Yan KP, Amuthan G, Chendrimada T, Doratotaj B, Cooch N *et al* (2004). The Microprocessor complex mediates the genesis of microRNAs. *Nature* **432:** 235-40.

Grey F, Antoniewicz A, Allen E, Saugstad J, McShea A, Carrington JC *et al* (2005). Identification and characterization of human cytomegalovirus-encoded microRNAs. *J Virol* **79:** 12095-9.

Griffiths-Jones S (2004). The microRNA Registry. *Nucleic Acids Res* **32:** D109-11.

Griffiths-Jones S, Grocock RJ, van Dongen S, Bateman A, Enright AJ (2006). miRBase: microRNA sequences, targets and gene nomenclature. *Nucleic Acids Res* **34:** D140-4.

Griffiths-Jones S, Saini HK, van Dongen S, Enright AJ (2008). miRBase: tools for microRNA genomics. *Nucleic Acids Res* **36:** D154-8.

Griffiths DJ, Venables PJ, Weiss RA, Boyd MT (1997). A novel exogenous retrovirus sequence identified in humans. *J Virol* **71:** 2866-72.

Grimson A, Farh KK, Johnston WK, Garrett-Engele P, Lim LP, Bartel DP (2007). MicroRNA targeting specificity in mammals: determinants beyond seed pairing. *Mol Cell* **27:** 91-105.

Grosset C, Chen CY, Xu N, Sonenberg N, Jacquemin-Sablon H, Shyu AB (2000). A mechanism for translationally coupled mRNA turnover: interaction between the poly(A) tail and a c-fos RNA coding determinant via a protein complex. *Cell* **103:** 29-40.

Guil S, Caceres JF (2007). The multifunctional RNA-binding protein hnRNP A1 is required for processing of miR-18a. *Nat Struct Mol Biol* **14:** 591-6.

Hagan JP, Piskounova E, Gregory RI (2009). Lin28 recruits the TUTase Zcchc11 to inhibit let-7 maturation in mouse embryonic stem cells. *Nat Struct Mol Biol*.

Hahn WC, Weinberg RA (2002). Rules for making human tumor cells. *N Engl J Med* **347:** 1593-603.

Hames B, Rickwood D (1990). Gel electrophoresis of proteins: A practical approach. *Oxford Univ. Press*.

Han J, Lee Y, Yeom KH, Kim YK, Jin H, Kim VN (2004). The Drosha-DGCR8 complex in primary microRNA processing. *Genes Dev* **18:** 3016-27.

Han J, Lee Y, Yeom KH, Nam JW, Heo I, Rhee JK *et al* (2006). Molecular basis for the recognition of primary microRNAs by the Drosha-DGCR8 complex. *Cell* **125:** 887-901.

Hanahan D, Weinberg RA (2000). The hallmarks of cancer. *Cell* **100:** 57-70.

Hayashita Y, Osada H, Tatematsu Y, Yamada H, Yanagisawa K, Tomida S *et al* (2005). A polycistronic microRNA cluster, miR-17-92, is overexpressed in human lung cancers and enhances cell proliferation. *Cancer Res* **65:** 9628-32.

He H, Jazdzewski K, Li W, Liyanarachchi S, Nagy R, Volinia S *et al* (2005a). The role of microRNA genes in papillary thyroid carcinoma. *Proc Natl Acad Sci U S A* **102:** 19075-80.

He L, Thomson JM, Hemann MT, Hernando-Monge E, Mu D, Goodson S *et al* (2005b). A microRNA polycistron as a potential human oncogene. *Nature* **435:** 828-33.

Heinrich R, Livne E, Ben-Izhak O, Aronheim A (2004). The c-Jun dimerization protein 2 inhibits cell transformation and acts as a tumor suppressor gene. *J Biol Chem* **279:** 5708-15.

Helton ES, Chen X (2007). p53 modulation of the DNA damage response. *J Cell Biochem* **100:** 883-96.

Herdegen T, Waetzig V (2001). AP-1 proteins in the adult brain: facts and fiction about effectors of neuroprotection and neurodegeneration. *Oncogene* **20:** 2424-37.

Hess J, Angel P, Schorpp-Kistner M (2004). AP-1 subunits: quarrel and harmony among siblings. *J Cell Sci* **117:** 5965-73.

Hitschler A (2007). Use of Chromatin Immunoprecipitation to target transcription factor controlled promoters. *University of Bielefeld*.

Hoppe-Seyler F, Butz K (1994). Cellular control of human papillomavirus oncogene transcription. *Mol Carcinog* **10:** 134-41.

Hutvágner G, McLachlan J, Pasquinelli AE, Balint E, Tuschl T, Zamore PD (2001). A cellular function for the RNA-interference enzyme Dicer in the maturation of the let-7 small temporal RNA. *Science* **293:** 834-8.

Iftner T, Oft M, Bohm S, Wilczynski SP, Pfister H (1992). Transcription of the E6 and E7 genes of human papillomavirus type 6 in anogenital condylomata is restricted to undifferentiated cell layers of the epithelium. *J Virol* **66:** 4639-46.

Iorio MV, Ferracin M, Liu CG, Veronese A, Spizzo R, Sabbioni S *et al* (2005). MicroRNA gene expression deregulation in human breast cancer. *Cancer Res* **65:** 7065-70.

Jakymiw A, Lian S, Eystathioy T, Li S, Satoh M, Hamel JC *et al* (2005). Disruption of GW bodies impairs mammalian RNA interference. *Nat Cell Biol* **7:** 1267-74.

Jin C, Li H, Murata T, Sun K, Horikoshi M, Chiu R *et al* (2002). JDP2, a repressor of AP-1, recruits a histone deacetylase 3 complex to inhibit the retinoic acid-induced differentiation of F9 cells. *Mol Cell Biol* **22:** 4815-26.

Jochum W, Passegue E, Wagner EF (2001). AP-1 in mouse development and tumorigenesis. *Oncogene* **20:** 2401-12.

Johnson SM, Grosshans H, Shingara J, Byrom M, Jarvis R, Cheng A *et al* (2005). RAS is regulated by the let-7 microRNA family. *Cell* **120:** 635-47.

Karin M, Liu Z, Zandi E (1997). AP-1 function and regulation. *Curr Opin Cell Biol* **9:** 240-6.

Katase K, Teshima H, Hirai Y, Hasumi K (1995). Natural history of cervical human papillomavirus lesions. *Intervirology* **38:** 192-4.

Kawahara Y, Zinshteyn B, Chendrimada TP, Shiekhattar R, Nishikura K (2007a). RNA editing of the microRNA-151 precursor blocks cleavage by the Dicer-TRBP complex. *EMBO Rep* **8:** 763-9.

Kawahara Y, Zinshteyn B, Sethupathy P, Iizasa H, Hatzigeorgiou AG, Nishikura K (2007b). Redirection of silencing targets by adenosine-to-inosine editing of miRNAs. *Science* **315:** 1137-40.

Kent OA, Mendell JT (2006). A small piece in the cancer puzzle: microRNAs as tumor suppressors and oncogenes. *Oncogene* **25:** 6188-96.

Khvorova A, Reynolds A, Jayasena SD (2003). Functional siRNAs and miRNAs exhibit strand bias. *Cell* **115:** 209-16.

Kiriakidou M, Tan GS, Lamprinaki S, De Planell-Saguer M, Nelson PT, Mourelatos Z (2007). An mRNA m7G cap binding-like motif within human Ago2 represses translation. *Cell* **129:** 1141-51.

Klingelhutz AJ, Foster SA, McDougall JK (1996). Telomerase activation by the E6 gene product of human papillomavirus type 16. *Nature* **380:** 79-82.

Klotz LO, Pellieux C, Briviba K, Pierlot C, Aubry JM, Sies H (1999). Mitogen-activated protein kinase (p38-, JNK-, ERK-) activation pattern induced by extracellular and intracellular singlet oxygen and UVA. *Eur J Biochem* **260:** 917-22.

Kozak M (1989). Circumstances and mechanisms of inhibition of translation by secondary structure in eucaryotic mRNAs. *Mol Cell Biol* **9:** 5134-42.

Kozak M (1991). An analysis of vertebrate mRNA sequences: intimations of translational control. *J Cell Biol* **115:** 887-903.

Krek A, Grun D, Poy MN, Wolf R, Rosenberg L, Epstein EJ *et al* (2005). Combinatorial microRNA target predictions. *Nat Genet* **37:** 495-500.

Krutzfeldt J, Rajewsky N, Braich R, Rajeev KG, Tuschl T, Manoharan M *et al* (2005). Silencing of microRNAs in vivo with 'antagomirs'. *Nature* **438:** 685-9.

Kuehbacher A, Urbich C, Zeiher AM, Dimmeler S (2007). Role of Dicer and Drosha for endothelial microRNA expression and angiogenesis. *Circ Res* **101:** 59-68.

Laemmli UK (1970). Cleavage of structural proteins during the assembly of the head of bacteriophage T4. *Nature* **227:** 680-5.

Lall S, Grun D, Krek A, Chen K, Wang YL, Dewey CN *et al* (2006). A genome-wide map of conserved microRNA targets in C. elegans. *Curr Biol* **16:** 460-71.

Lallemand D, Spyrou G, Yaniv M, Pfarr CM (1997). Variations in Jun and Fos protein expression and AP-1 activity in cycling, resting and stimulated fibroblasts. *Oncogene* **14:** 819-30.

Lamph WW, Wamsley P, Sassone-Corsi P, Verma IM (1988). Induction of proto-oncogene JUN/AP-1 by serum and TPA. *Nature* **334:** 629-31.

Larsson L, Johansson P, Jansson A, Donati M, Rymo L, Berglundh T (2009). The Sp1 transcription factor binds to the G-allele of the -1087 IL-10 gene polymorphism and enhances transcriptional activation. *Genes Immun* **10:** 280-4.

Lee HJ, Palkovits M, Young WS, 3rd (2006). miR-7b, a microRNA up-regulated in the hypothalamus after chronic hyperosmolar stimulation, inhibits Fos translation. *Proc Natl Acad Sci U S A* **103:** 15669-74.

Lee JW, Choi CH, Choi JJ, Park YA, Kim SJ, Hwang SY *et al* (2008). Altered MicroRNA expression in cervical carcinomas. *Clin Cancer Res* **14:** 2535-42.

Lee RC, Feinbaum RL, Ambros V (1993). The C. elegans heterochronic gene lin-4 encodes small RNAs with antisense complementarity to lin-14. *Cell* **75:** 843-54.

Lee W, Mitchell P, Tjian R (1987). Purified transcription factor AP-1 interacts with TPA-inducible enhancer elements. *Cell* **49:** 741-52.

Lee Y, Jeon K, Lee JT, Kim S, Kim VN (2002). MicroRNA maturation: stepwise processing and subcellular localization. *EMBO J* **21:** 4663-70.

Lee Y, Kim M, Han J, Yeom KH, Lee S, Baek SH *et al* (2004). MicroRNA genes are transcribed by RNA polymerase II. *EMBO J* **23:** 4051-60.

Lee YS, Dutta A (2007). The tumor suppressor microRNA let-7 represses the HMGA2 oncogene. *Genes Dev* **21:** 1025-30.

Lewis BP, Burge CB, Bartel DP (2005). Conserved seed pairing, often flanked by adenosines, indicates that thousands of human genes are microRNA targets. *Cell* **120:** 15-20.

Lewis BP, Shih IH, Jones-Rhoades MW, Bartel DP, Burge CB (2003). Prediction of mammalian microRNA targets. *Cell* **115:** 787-98.

Li S, Fu H, Wang Y, Tie Y, Xing R, Zhu J *et al* (2009). MicroRNA-101 regulates expression of the v-fos FBJ murine osteosarcoma viral oncogene homolog (FOS) oncogene in human hepatocellular carcinoma. *Hepatology* **49:** 1194-202.

Lim LP, Burge CB (2001). A computational analysis of sequence features involved in recognition of short introns. *Proc Natl Acad Sci U S A* **98:** 11193-8.

Lin Y, Liu X, Cheng Y, Yang J, Huo Y, Zhang C (2009). Involvement of MicroRNAs in hydrogen peroxide-mediated gene regulation and cellular injury response in vascular smooth muscle cells. *J Biol Chem* **284:** 7903-13.

Linsley PS, Schelter J, Burchard J, Kibukawa M, Martin MM, Bartz SR *et al* (2007). Transcripts targeted by the microRNA-16 family cooperatively regulate cell cycle progression. *Mol Cell Biol* **27:** 2240-52.

Liu J, Rivas FV, Wohlschlegel J, Yates JR, 3rd, Parker R, Hannon GJ (2005). A role for the P-body component GW182 in microRNA function. *Nat Cell Biol* **7:** 1261-6.

Lorincz AT, Quinn AP, Lancaster WD, Temple GF (1987). A new type of papillomavirus associated with cancer of the uterine cervix. *Virology* **159:** 187-90.

Lu J, Getz G, Miska EA, Alvarez-Saavedra E, Lamb J, Peck D *et al* (2005). MicroRNA expression profiles classify human cancers. *Nature* **435:** 834-8.

Lui WO, Pourmand N, Patterson BK, Fire A (2007). Patterns of known and novel small RNAs in human cervical cancer. *Cancer Res* **67:** 6031-43.

Lund E, Guttinger S, Calado A, Dahlberg JE, Kutay U (2004). Nuclear export of microRNA precursors. *Science* **303:** 95-8.

Lykke-Andersen J (2002). Identification of a human decapping complex associated with hUpf proteins in nonsense-mediated decay. *Mol Cell Biol* **22:** 8114-21.

Maragkakis M, Reczko M, Simossis VA, Alexiou P, Papadopoulos GL, Dalamagas T *et al* (2009). DIANA-microT web server: elucidating microRNA functions through target prediction. *Nucleic Acids Res* **37:** W273-6.

Martin MM, Lee EJ, Buckenberger JA, Schmittgen TD, Elton TS (2006). MicroRNA-155 regulates human angiotensin II type 1 receptor expression in fibroblasts. *J Biol Chem* **281:** 18277-84.

Martinez I, Gardiner AS, Board KF, Monzon FA, Edwards RP, Khan SA (2008). Human papillomavirus type 16 reduces the expression of microRNA-218 in cervical carcinoma cells. *Oncogene* **27:** 2575-82.

Mechta-Grigoriou F, Gerald D, Yaniv M (2001). The mammalian Jun proteins: redundancy and specificity. *Oncogene* **20:** 2378-89.

Mechta F, Lallemand D, Pfarr CM, Yaniv M (1997). Transformation by ras modifies AP1 composition and activity. *Oncogene* **14:** 837-47.

Meister G, Landthaler M, Patkaniowska A, Dorsett Y, Teng G, Tuschl T (2004). Human Argonaute2 mediates RNA cleavage targeted by miRNAs and siRNAs. *Mol Cell* **15:** 185-97.

Meister G, Tuschl T (2004). Mechanisms of gene silencing by double-stranded RNA. *Nature* **431:** 343-9.

Michael MZ, SM OC, van Holst Pellekaan NG, Young GP, James RJ (2003). Reduced accumulation of specific microRNAs in colorectal neoplasia. *Mol Cancer Res* **1:** 882-91.

Munger K, Howley PM (2002). Human papillomavirus immortalization and transformation functions. *Virus Res* **89:** 213-28.

Muralidhar B, Goldstein LD, Ng G, Winder DM, Palmer RD, Gooding EL *et al* (2007). Global microRNA profiles in cervical squamous cell carcinoma depend on Drosha expression levels. *J Pathol* **212:** 368-77.

Musti AM, Treier M, Bohmann D (1997). Reduced ubiquitin-dependent degradation of c-Jun after phosphorylation by MAP kinases. *Science* **275:** 400-2.

Newman MA, Thomson JM, Hammond SM (2008). Lin-28 interaction with the Let-7 precursor loop mediates regulated microRNA processing. *RNA* **14:** 1539-49.

O'Donnell KA, Wentzel EA, Zeller KI, Dang CV, Mendell JT (2005). c-Myc-regulated microRNAs modulate E2F1 expression. *Nature* **435:** 839-43.

O'Hara BM, Klinger HP, Curran T, Zhang YD, Blair DG (1987). Levels of fos, ets2, and myb proto-oncogene RNAs correlate with segregation of chromosome 11 of normal cells and with suppression of tumorigenicity in human cell hybrids. *Mol Cell Biol* **7:** 2941-6.

Orom UA, Nielsen FC, Lund AH (2008). MicroRNA-10a binds the 5'UTR of ribosomal protein mRNAs and enhances their translation. *Mol Cell* **30:** 460-71.

Ota A, Tagawa H, Karnan S, Tsuzuki S, Karpas A, Kira S *et al* (2004). Identification and characterization of a novel gene, C13orf25, as a target for 13q31-q32 amplification in malignant lymphoma. *Cancer Res* **64:** 3087-95.

Parker R, Song H (2004). The enzymes and control of eukaryotic mRNA turnover. *Nat Struct Mol Biol* **11:** 121-7.

Parkin DM, Bray FI, Devesa SS (2001). Cancer burden in the year 2000. The global picture. *Eur J Cancer* **37 Suppl 8:** S4-66.

Pavlidis N, Fizazi K (2005). Cancer of unknown primary (CUP). *Crit Rev Oncol Hematol* **54:** 243-50.

Pecorelli S, Favalli G, Zigliani L, Odicino F (2003). Cancer in women. *Int J Gynaecol Obstet* **82:** 369-79.

Pfeffer S, Sewer A, Lagos-Quintana M, Sheridan R, Sander C, Grasser FA *et al* (2005). Identification of microRNAs of the herpesvirus family. *Nat Methods* **2:** 269-76.

Pfister H, zur Hausen H (1978). Characterization of proteins of human papilloma viruses (HPV) and antibody response to HPV 1. *Med Microbiol Immunol* **166:** 13-9.

Phillips K, Luisi B (2000). The virtuoso of versatility: POU proteins that flex to fit. *J Mol Biol* **302:** 1023-39.

Pulverer BJ, Kyriakis JM, Avruch J, Nikolakaki E, Woodgett JR (1991). Phosphorylation of c-jun mediated by MAP kinases. *Nature* **353:** 670-4.

Ramaswamy S, Tamayo P, Rifkin R, Mukherjee S, Yeang CH, Angelo M *et al* (2001). Multiclass cancer diagnosis using tumor gene expression signatures. *Proc Natl Acad Sci U S A* **98:** 15149-54.

Rehwinkel J, Natalin P, Stark A, Brennecke J, Cohen SM, Izaurralde E (2006). Genome-wide analysis of mRNAs regulated by Drosha and Argonaute proteins in Drosophila melanogaster. *Mol Cell Biol* **26:** 2965-75.

Robins H, Li Y, Padgett RW (2005). Incorporating structure to predict microRNA targets. *Proc Natl Acad Sci U S A* **102:** 4006-9.

Rodriguez A, Griffiths-Jones S, Ashurst JL, Bradley A (2004). Identification of mammalian microRNA host genes and transcription units. *Genome Res* **14:** 1902-10.

Rösl F, Das BC, Lengert M, Geletneky K, zur Hausen H (1997). Antioxidant-induced changes of the AP-1 transcription complex are paralleled by a selective suppression of human papillomavirus transcription. *J Virol* **71:** 362-70.

Rösl F, Schwarz E (1997). Regulation of E6 and E7 oncogene transcription. *In: Tommasino M (ed.), Papilloma viruses in human cancer***:** 25-70.

Ruby JG, Jan CH, Bartel DP (2007). Intronic microRNA precursors that bypass Drosha processing. *Nature* **448:** 83-6.

Ryder K, Nathans D (1988). Induction of protooncogene c-jun by serum growth factors. *Proc Natl Acad Sci U S A* **85:** 8464-7.

Ryseck RP, Bravo R (1991). c-JUN, JUN B, and JUN D differ in their binding affinities to AP-1 and CRE consensus sequences: effect of FOS proteins. *Oncogene* **6:** 533-42.

Saunders MA, Liang H, Li WH (2007). Human polymorphism at microRNAs and microRNA target sites. *Proc Natl Acad Sci U S A* **104:** 3300-5.

Scheffner M, Huibregtse JM, Vierstra RD, Howley PM (1993). The HPV-16 E6 and E6-AP complex functions as a ubiquitin-protein ligase in the ubiquitination of p53. *Cell* **75:** 495-505.

Scheidereit C, Cromlish JA, Gerster T, Kawakami K, Balmaceda CG, Currie RA *et al* (1988). A human lymphoid-specific transcription factor that activates immunoglobulin genes is a homoeobox protein. *Nature* **336:** 551-7.

Schmitter D, Filkowski J, Sewer A, Pillai RS, Oakeley EJ, Zavolan M *et al* (2006). Effects of Dicer and Argonaute down-regulation on mRNA levels in human HEK293 cells. *Nucleic Acids Res* **34:** 4801-15.

Schneider G, Saur D, Siveke JT, Fritsch R, Greten FR, Schmid RM (2006). IKKalpha controls p52/RelB at the skp2 gene promoter to regulate G1- to S-phase progression. *EMBO J* **25:** 3801-12.

Schneppenheim R, Budde U, Dahlmann N, Rautenberg P (1991). Luminography--a new, highly sensitive visualization method for electrophoresis. *Electrophoresis* **12:** 367-72.

Schreiber E, Matthias P, Muller MM, Schaffner W (1989). Rapid detection of octamer binding proteins with 'mini-extracts', prepared from a small number of cells. *Nucleic Acids Res* **17:** 6419.

Schultz J, Lorenz P, Gross G, Ibrahim S, Kunz M (2008). MicroRNA let-7b targets important cell cycle molecules in malignant melanoma cells and interferes with anchorage-independent growth. *Cell Res* **18:** 549-57.

Schwarz DS, Hutvagner G, Du T, Xu Z, Aronin N, Zamore PD (2003). Asymmetry in the assembly of the RNAi enzyme complex. *Cell* **115:** 199-208.

Schwarz E, Freese UK, Gissmann L, Mayer W, Roggenbuck B, Stremlau A *et al* (1985). Structure and transcription of human papillomavirus sequences in cervical carcinoma cells. *Nature* **314:** 111-4.

Sehgal A, Briggs J, Rinehart-Kim J, Basso J, Bos TJ (2000). The chicken c-Jun 5' untranslated region directs translation by internal initiation. *Oncogene* **19:** 2836-45.

Shaulian E, Karin M (2002). AP-1 as a regulator of cell life and death. *Nat Cell Biol* **4:** E131-6.

Short JD, Pfarr CM (2002). Translational regulation of the JunD messenger RNA. *J Biol Chem* **277:** 32697-705.

Skinner M, Qu S, Moore C, Wisdom R (1997). Transcriptional activation and transformation by FosB protein require phosphorylation of the carboxyl-terminal activation domain. *Mol Cell Biol* **17:** 2372-80.

Soto U, Das BC, Lengert M, Finzer P, zur Hausen H, Rosl F (1999). Conversion of HPV 18 positive non-tumorigenic HeLa-fibroblast hybrids to invasive growth involves loss of TNF-alpha mediated repression of viral transcription and modification of the AP-1 transcription complex. *Oncogene* **18:** 3187-98.

Soto U, Denk C, Finzer P, Hutter KJ, zur Hausen H, Rosl F (2000). Genetic complementation to non-tumorigenicity in cervical-carcinoma cells correlates with alterations in AP-1 composition. *Int J Cancer* **86:** 811-7.

Southern EM (1975). Detection of specific sequences among DNA fragments separated by gel electrophoresis. *J Mol Biol* **98:** 503-17.

Stanbridge E (1984). Genetic analysis of tumorigenicity in human cell hybrids. *Cancer Surv*. pp 335-350.

Steinmüller L, Cibelli G, Moll JR, Vinson C, Thiel G (2001). Regulation and composition of activator protein 1 (AP-1) transcription factors controlling collagenase and c-Jun promoter activities. *Biochem J* **360:** 599-607.

Stern-Ginossar N, Elefant N, Zimmermann A, Wolf DG, Saleh N, Biton M *et al* (2007). Host immune system gene targeting by a viral miRNA. *Science* **317:** 376-81.

Su AI, Welsh JB, Sapinoso LM, Kern SG, Dimitrov P, Lapp H *et al* (2001). Molecular classification of human carcinomas by use of gene expression signatures. *Cancer Res* **61:** 7388-93.

Sullivan CS, Grundhoff AT, Tevethia S, Pipas JM, Ganem D (2005). SV40-encoded microRNAs regulate viral gene expression and reduce susceptibility to cytotoxic T cells. *Nature* **435:** 682-6.

Sun F, Fu H, Liu Q, Tie Y, Zhu J, Xing R *et al* (2008). Downregulation of CCND1 and CDK6 by miR-34a induces cell cycle arrest. *FEBS Lett* **582:** 1564-8.

Suzuki T, Okuno H, Yoshida T, Endo T, Nishina H, Iba H (1991). Difference in transcriptional regulatory function between c-Fos and Fra-2. *Nucleic Acids Res* **19:** 5537-42.

Takamizawa J, Konishi H, Yanagisawa K, Tomida S, Osada H, Endoh H *et al* (2004). Reduced expression of the let-7 microRNAs in human lung cancers in association with shortened postoperative survival. *Cancer Res* **64:** 3753-6.

Talotta F, Cimmino A, Matarazzo MR, Casalino L, De Vita G, D'Esposito M *et al* (2009). An autoregulatory loop mediated by miR-21 and PDCD4 controls the AP-1 activity in RAS transformation. *Oncogene* **28:** 73-84.

Tam W (2001). Identification and characterization of human BIC, a gene on chromosome 21 that encodes a noncoding RNA. *Gene* **274:** 157-67.

Tam W, Hughes SH, Hayward WS, Besmer P (2002). Avian bic, a gene isolated from a common retroviral site in avian leukosis virus-induced lymphomas that encodes a noncoding RNA, cooperates with c-myc in lymphomagenesis and erythroleukemogenesis. *J Virol* **76:** 4275-86.

Tang KF, Wang Y, Wang P, Chen M, Chen Y, Hu HD *et al* (2007). Upregulation of PHLDA2 in Dicer knockdown HEK293 cells. *Biochim Biophys Acta* **1770:** 820-5.

Tay Y, Zhang J, Thomson AM, Lim B, Rigoutsos I (2008). MicroRNAs to Nanog, Oct4 and Sox2 coding regions modulate embryonic stem cell differentiation. *Nature* **455:** 1124-8.

Tazawa H, Tsuchiya N, Izumiya M, Nakagama H (2007). Tumor-suppressive miR-34a induces senescence-like growth arrest through modulation of the E2F pathway in human colon cancer cells. *Proc Natl Acad Sci U S A* **104:** 15472-7.

Tokumaru S, Suzuki M, Yamada H, Nagino M, Takahashi T (2008). let-7 regulates Dicer expression and constitutes a negative feedback loop. *Carcinogenesis* **29:** 2073-7.

Towbin H, Staehelin T, Gordon J (1979). Electrophoretic transfer of proteins from polyacrylamide gels to nitrocellulose sheets: procedure and some applications. *Proc Natl Acad Sci U S A* **76:** 4350-4.

Tseng CP, Verma AK (1995). Lack of 12-O-tetradecanoylphorbol-13-acetate responsiveness of ornithine decarboxylase introns which have AP-1 consensus sequences. *Mol Cell Biochem* **146:** 7-12.

Tulchinsky E (2000). Fos family members: regulation, structure and role in oncogenic transformation. *Histol Histopathol* **15:** 921-8.

van Dam H, Castellazzi M (2001). Distinct roles of Jun : Fos and Jun : ATF dimers in oncogenesis. *Oncogene* **20:** 2453-64.

van Dijk E, Cougot N, Meyer S, Babajko S, Wahle E, Seraphin B (2002). Human Dcp2: a catalytically active mRNA decapping enzyme located in specific cytoplasmic structures. *EMBO J* **21:** 6915-24.

van Riggelen J, Buchwalter G, Soto U, De-Castro Arce J, Hausen HZ, Wasylyk B *et al* (2005). Loss of net as repressor leads to constitutive increased c-fos transcription in cervical cancer cells. *J Biol Chem* **280:** 3286-94.

Vogt PK, Bos TJ (1990). jun: oncogene and transcription factor. *Adv Cancer Res* **55:** 1-35.

Volinia S, Calin GA, Liu CG, Ambs S, Cimmino A, Petrocca F *et al* (2006). A microRNA expression signature of human solid tumors defines cancer gene targets. *Proc Natl Acad Sci U S A* **103:** 2257-61.

von Knebel Doeberitz M, Bauknecht T, Bartsch D, zur Hausen H (1991). Influence of chromosomal integration on glucocorticoid-regulated transcription of growth-stimulating papillomavirus genes E6 and E7 in cervical carcinoma cells. *Proc Natl Acad Sci U S A* **88:** 1411-5.

Wang J, Lu M, Qiu C, Cui Q (2009). TransmiR: a transcription factor-microRNA regulation database. *Nucleic Acids Res*.

Wang Q, Sun Z, Yang HS (2008a). Downregulation of tumor suppressor Pdcd4 promotes invasion and activates both beta-catenin/Tcf and AP-1-dependent transcription in colon carcinoma cells. *Oncogene* **27:** 1527-35.

Wang X, Tang S, Le SY, Lu R, Rader JS, Meyers C *et al* (2008b). Aberrant expression of oncogenic and tumor-suppressive microRNAs in cervical cancer is required for cancer cell growth. *PLoS One* **3:** e2557.

Wei W, Jin J, Schlisio S, Harper JW, Kaelin WG, Jr. (2005). The v-Jun point mutation allows c-Jun to escape GSK3-dependent recognition and destruction by the Fbw7 ubiquitin ligase. *Cancer Cell* **8:** 25-33.

Werness BA, Levine AJ, Howley PM (1990). Association of human papillomavirus types 16 and 18 E6 proteins with p53. *Science* **248:** 76-9.

Wienholds E, Kloosterman WP, Miska E, Alvarez-Saavedra E, Berezikov E, de Bruijn E *et al* (2005). MicroRNA expression in zebrafish embryonic development. *Science* **309:** 310-1.

Wightman B, Ha I, Ruvkun G (1993). Posttranscriptional regulation of the heterochronic gene lin-14 by lin-4 mediates temporal pattern formation in C. elegans. *Cell* **75:** 855-62.

Wu L, Fan J, Belasco JG (2006). MicroRNAs direct rapid deadenylation of mRNA. *Proc Natl Acad Sci U S A* **103:** 4034-9.

Yamashita A, Chang TC, Yamashita Y, Zhu W, Zhong Z, Chen CY *et al* (2005). Concerted action of poly(A) nucleases and decapping enzyme in mammalian mRNA turnover. *Nat Struct Mol Biol* **12:** 1054-63.

Yanaihara N, Caplen N, Bowman E, Seike M, Kumamoto K, Yi M *et al* (2006). Unique microRNA molecular profiles in lung cancer diagnosis and prognosis. *Cancer Cell* **9:** 189-98.

Yandell M, Mungall CJ, Smith C, Prochnik S, Kaminker J, Hartzell G *et al* (2006). Large-scale trends in the evolution of gene structures within 11 animal genomes. *PLoS Comput Biol* **2:** e15.

Yang HS, Knies JL, Stark C, Colburn NH (2003). Pdcd4 suppresses tumor phenotype in JB6 cells by inhibiting AP-1 transactivation. *Oncogene* **22:** 3712-20.

Yang W, Chendrimada TP, Wang Q, Higuchi M, Seeburg PH, Shiekhattar R *et al* (2006). Modulation of microRNA processing and expression through RNA editing by ADAR deaminases. *Nat Struct Mol Biol* **13:** 13-21.

Yi R, Doehle BP, Qin Y, Macara IG, Cullen BR (2005). Overexpression of exportin 5 enhances RNA interference mediated by short hairpin RNAs and microRNAs. *RNA* **11:** 220-6.

Yi R, Qin Y, Macara IG, Cullen BR (2003). Exportin-5 mediates the nuclear export of pre-microRNAs and short hairpin RNAs. *Genes Dev* **17:** 3011-6.

Yin Q, Wang X, McBride J, Fewell C, Flemington E (2008). B-cell receptor activation induces BIC/miR-155 expression through a conserved AP-1 element. *J Biol Chem* **283:** 2654-62.

Zhang Q, Kleeberger SR, Reddy SP (2004). DEP-induced fra-1 expression correlates with a distinct activation of AP-1-dependent gene transcription in the lung. *Am J Physiol Lung Cell Mol Physiol* **286:** L427-36.

Zheng D, Ezzeddine N, Chen CY, Zhu W, He X, Shyu AB (2008). Deadenylation is prerequisite for P-body formation and mRNA decay in mammalian cells. *J Cell Biol* **182:** 89-101.

Zhou J, Sun XY, Stenzel DJ, Frazer IH (1991). Expression of vaccinia recombinant HPV 16 L1 and L2 ORF proteins in epithelial cells is sufficient for assembly of HPV virion-like particles. *Virology* **185:** 251-7.

zur Hausen H (1996). Papillomavirus infections--a major cause of human cancers. *Biochim Biophys Acta* **1288:** F55-78.

zur Hausen H (2002). Papillomaviruses and cancer: from basic studies to clinical application. *Nat Rev Cancer* **2:** 342-50.

7. Appendix

7.1. Abbreviations

A	Ampere
AP-1	Activating protein 1
ATF-2	Activating transcription factor 2
ATP	Adenosin 5’-triphosphate
bp	Basepair
BSA	Bovine serum albumin
cDNA	Complementary DNA (from mRNA)
c-Fos	Cellular FBJ murine osteosarcoma viral oncogene homolog
c-Jun	Jun oncogene
℃	Degree Celsius
Ci	Curie
CIA	Chloroform-Isoamyl alcohol 49:1
CIAP	Calf Intestine Alkaline Phosphatase
cpm	Counts per minute
DEPC	Diethyl pyrocarbonat
DNA	Deoxyribonucleic acid
dNTP	2’ Deoxynucleosite-5’-triphosphate
DMEM	Dulbecco’s modified Eagle’s medium
DMSO	Dimethyl sulfoxide
ds	Double-stranded
DTT	Dithiothreitol
E-64	N-N-(L-3-trans-carboxyoxirane-2-carbonyl)-L-leucyl-agmatine
ECL-Reagent	Enhanced Chemiluminescence Reagent
EDTA	Ethylenediaminetetraacetic acid
EGTA	Ethylene glycol-bis[β-aminoethylether]-N,N,N’,N’-tetraacetic acid

EMSA	Electrophoresis mobility shift assay
F	Forward
FBS	FCS Fetal Calf Bovine Serum
FosB	FBJ murine osteosarcoma viral oncogene homolog B
Fra-1	FOS-like antigen 1
Fra-2	FOS-like antigen 2
GAPDH	Glyceraldehyde-3-phosphate dehydrogenase
h	Hour
HEPES	4-(2-hydroxyethyl)-1-piperazineethanesulfonic acid
HRP	Horseradish peroxidase
IgG	Immunoglubuline G
JDP2	Jun dimerization protein 2
JunB	Jun B proto-oncogene
JunD	Jun D proto-oncogene
kbp	Kilobasepair
kDa	Kilodalton
LB-Medium	Luria-Bertani medium
M	Molar
min	Minute
ml	Milliliter
MOPS	3-[N-Morpholino]-propanesulfonic acid
mRNA	Messenger RNA
miRNA	MicroRNA
Net	New ETS transcription factor (also known as ELK3)
Oct-1	Octamer-binding transcription factor 1
OD	Optical density
PAGE	Polyacrylamide gel electrophoresis
PBS	Phosphate buffered saline

PCR	Polymerase chain reaction
pDNA	Plasmid DNA
Pefabloc SC	4-(2-Aminoethyl)-benzensulfonylfluoride
Pen	Penicillin
PMSF	Phenylmethanesulphonylfluoride
pre-miRNA	Precursor miRNA
pri-miRNA	Primary miRNA
PVDF	Polyvinylidene fluoride
qRT-PCR	quantitative reverse transcription-PCR
R	Reverse
RNA	Ribonucleic acid
RNase	Ribonuclase
rpm	Revolutions per minute
RT	Reverse transcription
sd	Single-stranded
s.d.	Standard deviation
sec	Second
SDS	Sodium dodecyl sulphate
SDS-PAGE	Denaturing polyacrylamid gel electrophoresis
S.O.C.	SOB medium (Super Optimal Growth) with 20mM Glucose
SSC	Standard saline-citrate
Strep	Streptomycin
T_A	Annealing temperature
TAE	TRIS-acetate-EDTA
TBS	TRIS-buffered saline
TBST	TRIS-buffered saline with Tween
TE	TRIS-EDTA
TEMED	N,N,N',N'-Tetramethylethylenediamine

TRIS	Tris(hydroxymethyl)-aminomethan
U	Unit (enzymativ activity)
V	Volt
v/v	Volume precentage
w/v	Weight percentage

7.2. Alignment of putative regulatory miRNAs with c-Jun and Fra-1 3'UTRs

7.2.1. Alignment of predicted miRNAs with c-Jun 3'UTR

Nt	Search engine	Pred. miRNA	
			Linker **stop codon**
2040			AGGGCGATCGCCTCGAGACATTT**TGA**AGAGAGACCGTCGGGGGCTGAGGGGCAACGAAGA
	2,3	891b	AGTTACTGAGTCCATTCAACGT
2074			AAAAAAATAACACAGAGAGACAGACTTGAGAACTTGACAAGTTGCGACGGAGAGAAAAAA
	3	637	UGCGUCUCGGGCUUU
	2,3	517c	UGUG
2134			GAAGTGTCCGAGAACTAAAGCCAAGGGTATCCAAGTTGGACTGGGTTGCGTCCTGACGGC
			CGGGGGUCA
			AGAUUUUCCUACGUGCUA
2194			GCCCCCAGTGTGCACGAGTGGGAAGGACTTGGCGCGCCCTCCCTTGGCGTGGAGCCAGGG
2254			AGCGGCCGCCTGCGGGCTGCCCCGCTTTGCGGACGGGCTGTCCCCGCGCGAACGGAACGT
	3,4	429	UGCCAAAAUGGUCUGUCA
	2,3,4	200b	aguAGUAAUGGUCCGUCA
	3,4	200c	GGUAGUAAUGGGCCGUCA
2314			TGGACTTTTCGTTAACATTGACCAAGAACTGCATGGACCTAACATTCGATCTCATTCAGT
	1,3	92a	GUCCGGCCCUGUUCACGUUAU
	3,4	92b	UAAU CCUCCGGCCCUGCUCACGUUAU
	1,3	32	UAAU CGUUGAAUCAUUACACGUUAU
	1,3,4	139-5p	UAAU UCUGUGCACGUGACAUCU
2374			ATTAAAGGGGGGAGGGGGAGGGGGTTACAAACTGCAATAGAGACTGTAGATTGCTTCTGT
2434			AGTACTCCTTAAGAACACAAAGCGGGGGGAGGGTTGGGGAGGGGCGGCAGGAGGGAGGTT
2494			TGTGAGAGCGAGGCTGAGCCTACAGATGAACTCTTTCTGGCCTGCCTTCGTTAACTGTGT
	3,4	524-5p	CUCUUUCACGA
	3,4	520d-5p	CUUUCCCGA
	2	340	TTAGTCAGAGT
2554			ATGTACATATATATTTTTTAATTTGATGAAAGCTGATTACTGTCAATAAACAGCTTCA
	3	524-5p	AGGGAAACAUC CUCUUUCACGAAGGGAAACAUC
	3	520d-5p	AGGGAAACAUC CUUUCCCGAAGGGAAACAUC
	1,3	200a	UGUAGCAAUGGUCUGUCACAAU
	1,3	141	GGUAGAAAUGGUCUGUCACAAU
	2	340	AACGAAATATT
	2,3	612	uuccuCGAGUCUUCGGGACGGGUCG
	2,3,4	495	uucUUCACGUGGUACAAACAAA
2614			TGCCTTTGTAAGTTATTTCTTGTTTGTTTGTTTGGGTATCCTGCCCAGTGTTGTTTGTAA

	1	32	CGUUGAAUCAUUACACGUUAU
	3	524-5p	CUCUUUCACGAAGGGAAACAUC
	3	520d-5p	CUUUCCCGAAGGGAAACAUC
	2,3	522	UGUGAGAUUUCCCUUGGUAAAA
2674			ATAAGAGATTTGGAGCACTCTGAGTTTACCATTTGTAATAAAGTATATAATTTTTTTATG
	3	501-5p	AGAGUGGGUCCCUGUUUCCUAA
	3	362-5p	UGAGUGUGGAUCCAAGGUUCCUAA
2734			TTTTGTTTCTGAAAATTCCAGAAAGGATATTTAAGAAAATACAATAAACTATTGGAAAGT
	1,3,4	139-5p	UCUGUGCACGUGACAUCU
2794			ACTCCCCTAACCTCTTTTCTGCATCATCTGTAGATACTAGCTATCTAGGTGGAGTTGAAA
2854			GAGTTAAGAATGTCGATTAAAATCACTCTCAGTGCTTCTTACTATTAAGCAGTAAAAACT
	3	637	UGCGUC
2914			GTTCTCTATTAGACTTTAGAAATAAATGTACCTGATGTACCTGATGCTATGGTCAGGTTA
			UCGGGCUUUCGGGGGUCA
	3	501-5p	AGAGUGGGUCCCUGUUUCCUAA
	3	362-5p	UGAGUGUGGAUCCAAGGUUCCUAA
2974			TACTCCTCCTCCCCCAGCTATCTATATGGAATTGCTTACCAAAGGATAGTGCGATGTTTC
	2,3	642	GUUCUGUGUAAACCUCUCCCUG
3034			AGGAGGCTGGAGGAAGGGGGGTTGCAGTGGAGAGGGACAGCCCACTGAGAAGTCAAACAT
	3	522	UUGUGAGAUUUCCCUUGGUAAAA
	3,4	340	TTAGTCAGAGTAACGAAATATT
3094			TTCAAAGTTTGGATTGTATCAAGTGGCATGTGCTGTGACCATTTATAATGTTAGTAGAAA
3154			TTTTACAATAGGTGCTTATTCTCAAAGCAGGAATTGGTGGCAGATTTTACAAAAGATGTA
			TTAGTCAGA
3214			TCCTTCCAATTTGGAATCTTCTCTTTGACAATTCCTAGATAAAAAGATGGCCTTTGCTTA
	3,4	340	GTAACGAAATATT Linker
3274			TGAATATTTATAACAGCATTCTTGTCACAATAAATGTATTCAAATACCAAGTTTAAACGC
			GGCCGCACG

miRNAs that are predicted to align with c-Jun 3'UTR are displayed. Nucleotides (Nt) indicate the position within the 3'UTR starting counting with the first nucleotide after the stop codon TGA. miRNAs are predicted by (1) PicTar, (2) miRBase, (3) TargetScan, (4) DIANA microT. Nucleotides of miRNAs that presumably base-pair with the 3'UTR are highlighted in yellow. Nucleotides of the 3'UTR that belong to anterior and posterior segments are highlighted in turquoise. Nucleotides of the 3'UTR that are underlined are part of the Linker for cloning purposes.
miR-495 is predicted to have two overlapping binding sites, of which only one is indicated in the figure.

7.2.2. Alignment of predicted miRNAs with Fra-1 3'UTR

Nt	Search engine	Pred. miRNA	
			Linker **stop codon**
1004			TCGAGTCGCTTTG**TGA**GGCGCCTGAGCCCTACTCCCTGCAGATGCCACCCTAGCCAATGT
	3	571	GAGUGAGUCUACCGGUUGAGU
	2,3	299-3p	UUCGCCAAAUGGUAGGGUGUAU
	1	138	CUAAGUGUUGUGGUCGA
	1	138	CUAAGUGUUGUGGUCG
1048			CTCCTCCCCTTCCCCCACCGGTCCAGCTGGCCTGGACAGTATCCCACATCCAACTCCAGC
	2,3	338-5p	GUGAGUCGUGGUCCUAUAACAA
	1,3	149	CCUCACUUCUGUGCCUCGGUCU
	1	138	A CUAAGUGUUGUGGUCGA
1108			AACTTCTTCTCCATCCCTCTAATGAGACTGACCATATTGTGCTTCACAGTAGAGCCAGCT
	2,3	130a	UACGGGAAAAUUGUAACGUG
	2,3,4	19a	AGUCAAAACGUAUCUAAACGUGU
	3,4	19b	AGUCAAAACGUACCUAAACGUGU
		593	UCUUUG
1168			TGGGGCCACCAAAGCTGCCCACTGTTTCTCTTGAGCTGGCCTCTCTAGCACAATTTGCAC
		130a	AC
	3	593	UCUUUGGGGUCGUCUCUGU
	2,3	593	GGGUCGUCUCUGU
	1	149	CCUCACUUCUGUGCCUCGGUCU
1228	1	22	UGUCAAGAAGUUGACCGUCGAA
			TAAATCAGAGACAAAATATTTCCCATTTGTGCCAGAGGAATCCTGGCAGCCCAGAGACTT
	3	449b	CGGUCGAUUGUUAUGUGACGGA
	3	34c-5p	UUGUUGGUCGAUUCUGUGACGGU
	2,3	525-5p	UCUUUCACGUAGGGAGACCUC
	2,3	520a-5p	UCUUUCAUGAAGGGAGACCUC
	2,3,4		UGGUCGAUUGUUAUGUGACGGU
1288	2,3,4	449a	UGUUGGUCGAUUCUGUGACGGU
		34a	TGTAGATCCTTAGAGGTCCTCTGGAGCCCTAACCCCTTCCAGATCACTGCCACACTCTCC
	2,3		UACUGUGGAGGGACACUU
		513a-5p	GAG
1348	2,3		CCUCUCGGAGGUGGGUUGGGAG
		571	ATCACCCTCTTCCTGTGATCCACCCAACCCTATCTCCTGACAGAAGGTGCCACTTTACCC
		296-3p	
	3		CGGUCGAUUGUUAUGUGACGGA
	2		UGAGUCUACCGGUUGAGU
	2,3,4	449b	UGGUCGAUUGUUAUGUGACGGU
	2,3	571	CGUUAGUCGAUUGAUGUGACGGA
	2,3,4	449a	UGUUGGUCGAUUCUGUGACGGU
	1	34c-5p	CUAAGUGUUGUGGUCGA
	1	34a	CUAAGUGUUGUGGUCGA
1408	1,3	138	CUAAGUGUUGUGGUCGA
		138	ACCTAGAACACTAACTCACCAGCCCCACTGCCAGCAGCAGCAGGTGATTGGACCAGGCCA
		138	
1468	2,3		CAACCCUAGUGUCCGCGGG
			TTCTGCCGCCCCCTCCTGAACCGCACAGCTCAGGAGGCGCCCTTGGCTTCTGTGATGAGC
		566	CGGAG
			ACAUUUGG
		646	GUGUUUGG
		15b	GCGGUUAU
		15a	CGGUUAU
1528		16	UGUCAAGAAGU
		195	TGATCTGCGGATCTCAGCTTTGAGAAGCCTTCAGCTCCAGGGAATCCAAGCCTCCACAGC
		22	

	2,3		UCUCCGUCGACGAA
	2,3		CACACAUAUGUAAAUAUGUA
	1,3	646	UACUACACGACGAU
	1,3	568	UAAUACACGACGAU
	1,3	15b	AAAUGCACGACGAU
	1,3	15a	AAAGACACGACGAU
	1,3	16	UGACCGUCGAA
1588		195	GAGGGCAGCTGCTATTTATTTTCCTAAAGAGAGTATTTTTATACAAACCTACCAAAATGG
		22	Linker
1648			AATAAAAGGCTTGAAGCTGTGGTTTAAACGC

miRNAs that are predicted to align with c-Jun 3'UTR are displayed. Nucleotides (Nt) indicate the position within the 3'UTR starting counting with the first nucleotide after the stop codon TGA. miRNAs are predicted by (1) PicTar, (2) miRBase, (3) TargetScan, (4) DIANA microT. Nucleotides of miRNAs that presumably base-pair with the 3'UTR are highlighted in yellow. Nucleotides of the 3'UTR that belong to anterior and posterior segments are highlighted in turquoise. Nucleotides of the 3'UTR that are underlined are part of the Linker for cloning purposes.

Acknowledgements

I would like to thank *Prof. Dr. Frank Rösl* for the opportunity to join his laboratory, for the freedom to work on this project and for the many discussions letting me reflect about experimental approaches, results and scientific writing. I could learn much about good scientific work and also much for my personal and professional life in general.

I would like to thank *Dr. Johanna de Castro Arce* for her great interest in my project that could only start because she came up with the idea. Her continuous support and advice in difficult and more thriving times made this work possible.

Many thanks go to *Elke Göckel-Krzikalla* for her excellent support in the laboratory.

I would like to thank current and past members of our research group, who were always willing to discuss my project and to support me with ideas and materials: *Prof. Dr. Rainer Zawatzky, Dr. Katalin Darvas, Dr. Lars Krüger, Dr. Bladimiro Rincon-Orozco, Anna, Dorothea, Kai, Nicolas, Simone, Steffi* and *Vlada*. Equally important was the friendly atmosphere at work and also outside, to which all of them contributed.

I would like to thank *Prof. Dr. Elisabeth Schwarz* for her willingness to be the first referee of my Ph.D. thesis, and *Prof. Dr. Gert Fricker*, *Prof. Dr. Frank Rösl* and *Prof. Dr. Rainer Zawatzky* for their participation on my examination committee.

Thanks go to *Dr. Sven Diederichs*, DKFZ, *Dr. Gunter Meister*, Max Planck Institute of Biochemistry, and *Dr. Ramesh Pillai*, EMBL, who were willing to discuss my results and experimental approaches.

I would like to thank *Dr. Bernhard Korn* for the miRNA expression profiling and *Julia Winter* who taught me how to do miRNA Northern blots.

Last, but not least, I am grateful to *Katrin* for her understanding and moral support. I am looking forward to more opportunities to share a lot more time!